KRAS-dependent Regulation of Extracellular RNAs in Colorectal Cancer

By
Diana Jean Cha

Dissertation
Submitted to the Faculty of the
Graduate School of Vanderbilt University
in partial fulfillment of the requirements
for the degree of

DOCTOR OF PHILOSOPHY
in

Biological Sciences

May, 2017
Nashville, Tennessee

Approved:

Todd R. Graham, Ph.D.

James G. Patton, Ph.D.

Antonis Rokas, Ph.D.

Robert Coffey, M.D.

Kasey C. Vickers, Ph.D.

DEDICATION

To my family, Mom and Dad, for teaching me the value of hard work and always believing in me. To my sister and best friend, Hana, for always being my rock. Thank you all for your endless love and infinite support.

To my friends that have become my second family during graduate school. From late nights in the lab, to late nights in the bars, my sanity has been left intact.

ACKNOWLEDGMENTS

This work would not have been possible without the financial support of Vanderbilt University Department of Biological Sciences and the Vanderbilt University Medical Center. I am grateful to all of those whom I have had the pleasure to work with and their numerous contributions and guidance during my graduate school career.

I am especially indebted to my adviser, Dr. James Patton, for all his support and guidance throughout my doctoral training. My development as a scientist has been deeply influenced by his insight and confidence in my abilities to conduct research independently. As my mentor, he has shown me, by his example, what a good scientist and person should be.

I am grateful to my dissertation committee members, who have been incredibly patient and supportive of my research goals. Each of the members of my committee has provided me extensive personal and professional guidance to prepare me for the next stages in my career. This has made my experiences in graduate school both intellectually stimulating and enjoyable.

This work was supported by grants from the National Institutes of Health, U19CA179514.

Page

LIST OF TABLES

LIST OF FIGURES

Chapter 1

Introduction

The traditional role of RNA has been that it serves only as an intermediary between the DNA and encoded proteins. Non-coding RNAs (ncRNA) were thought to fulfill relatively generic functions in the process of decoding DNA and generating proteins, such as the roles played by ribosomal RNA (rRNA) and transfer RNA (tRNA) in mRNA translation. More recently, analyses comparing transcriptomes and genomes have established that in humans, approximately two-thirds of genomic DNA is pervasively transcribed, while less than 2-3% endodes proteins (Djebali et al. 2012). It is now increasingly evident that RNAs participate in a wide repertoire of biological functions, and as first predicted by Jacob and Monod 55 years ago (Jacob and Monod 1961), play important roles in gene regulation, both in *cis* and in *trans.* The most recent addition to the expanding view of the role of RNA, both regulatory noncoding transcripts and transcripts encoding proteins, is the finding that RNA can be released into the extracellular milieu, suggesting a function beyond the cell of origin.

The first report of extracellular RNA (exRNA) was described in 2007 where mRNAs from mouse mast cells were transferred and translated into proteins in human recipient mast cells (Valadi et al. 2007). Since this initial discovery, various types of endogenous RNAs have been detected in the circulation, including messenger RNAs (mRNAs), microRNAs (miRNAs), and a variety of other non-coding RNAs (ncRNAs), such as circular RNAs (circRNAs), transfer RNAs (tRNAs), and ribosomal RNAs (rRNAs) (Valadi et al. 2007; Bellingham, Coleman, and Hill 2012; Cha et al. 2015; Dou et al. 2016; Freedman et al. 2016). Although a wide range of exRNA have been unambiguously identified, many of these sequences align to incomplete or unannotated regions (Vickers et al. 2015). Thus, it is likely that novel exRNAs are yet to be discovered. Nonetheless, specific RNAs are secreted into the extracellular milieu, and exhibit differences in processing and expression patterns dependent on their source (Bellingham, Coleman, and Hill 2012**).** RNA export appears to be evolutionarily well-conserved, as it has been documented in bacteria (Deng et al. 2015), plants (Brosnan and Voinnet 2011), fungi (Silva et al. 2015), nematodes (Jose, Garcia, and Hunter 2011), flies (Lefebvre et al. 2016), and mammals (Valadi et al. 2007). Additionally, recent studies have found the presence of exogenous exRNAs

derived from diet or from the microbiome in human plasma and serum (H. Liang et al. 2015; Beatty et al. 2014), suggesting trans-species transfer of extracellular RNAs.

Because extracellular fluids display abundant ribonuclease (RNAse) activity, exRNAs must be protected from degradation. ExRNAs in circulation are stabilized and protected from RNAses either in protein complexes (Arroyo et al. 2011; Andrey Turchinovich et al. 2011), lipid complexes (Vickers et al. 2011; Tabet et al. 2014; Wagner et al. 2013), or extracellular vesicles (EVs) (Bellingham, Coleman, and Hill 2012; Mittelbrunn et al. 2011; Skog et al. 2008). EVs represent a novel vehicle for intercellular communication in that they allow exchange of lipid, protein, RNA, and more recently, DNA cargo (Colombo, Raposo, and Théry 2014; Fischer et al. 2016), and they are released by all cell types (Colombo, Raposo, and Théry 2014). Studies have also shown that cancer cells secrete many more EVs than healthy cells (reviewed in (D'Souza-Schorey and Clancy 2012)). Thus, in the context of cancer, EVs can serve as vehicles for transport of exRNA from cancer cells to normal cells, both locally and systemically. From the perspective of a cancer cell, this potentially allows secretion of RNAs that could inhibit growth while simultaneously transferring oncogenic RNAs to healthy cells, contributing to overall cancer progression and drug resistance (Melo et al. 2014; Boelens et al. 2014). Interestingly, circulating RNAs encased in vesicles or protein complexesare often altered in cancer and bear tumor type-specific 'signatures', making them attractive candidates as clinical biomarkers for disease diagnosis and prognosis (Lawrie et al. 2008; Xi Chen et al. 2008; Mitchell et al. 2008; N. Kosaka et al. 2010).

Although there is accumulating evidence to suggest that RNAs can function as extracellular signaling molecules, the origin, secretory mechanism(s), and physiological functions remain largely unknown. This review will focus on some of the different classes of exRNAs, particularly those found in EVs, and their roles in cancer. The mechanisms for exRNA loading into EVs and functional transfer into target cells will also be discussed.

1.1 Composition of extracellular RNA

The seminal finding that mRNAs and miRNAs can exist outside the cell and be transferred to recipient cells through extracellular vesicles (EVs) (Valadi et al. 2007) challenged the traditional view of RNA and led to the hypothesis that exRNAs can function in cell-to-cell

communication. Apart from coding RNA (mRNA), advances in next generation sequencing (NGS) technology have revealed a broad spectrum of ncRNAs in plasma, serum, biological fluids, and conditioned media from cell culture (Table 1). It is becoming more evident that the classes of RNAs enriched in EVs largely depend on the source cell. These profiles can be dynamically regulated in response to different stimuli and activation states (Montecalvo et al. 2012; Y. Zhang et al. 2010).

Table 1. Summary of different classes of exRNAs

Name (abbreviation)	**Size range (nt)**	**Function(s) (reference)**
microRNA (miRNA, miR)	19-22	Inhibits protein translation and/or facilitates degradation of mRNA (Eulalio, Tritschler, and Izaurralde 2009); activation of immune response (Fabbri et al. 2012)
Small nucleolar RNA (snoRNA)	60-300	Guides the methylation or pseudouridylation of rRNAs and other RNAs (Matera, Terns, and Terns 2007)
Small nuclear RNA (snRNA)	~150	Modulation of RNA polymerase II activity; splicing (Matera, Terns, and Terns 2007).
Piwi-interacting RNA (piRNA)	20-30	Chromatin modification and transposon silencing (Iwasaki, Siomi, and Siomi 2015)
yRNA fragment (yRF)	27-33	Cell proliferation (C. P. Christov, Trivier, and Krude 2008); apoptosis (Chakrabortty et al. 2015).
tRNA-derived fragment (tRF)	19-22	Translational repression, analogous to miRNAs (Haussecker et al. 2010; Y. S. Lee et al. 2009)
tRNA-derived half (tRH, tiRNA)	30-40	Stress-induced translation repression (Yamasaki et al. 2009; P. Ivanov et al. 2011)
Vault RNA fragments	~23	Translation repression, analogous to miRNAs (Persson et al. 2009)
Long ncRNA (lncRNA)	>200	Chromatin remodeling (Meller, Joshi, and Deshpande 2015); translational regulation; mRNA stability (reviewed in (Fatica and Bozzoni 2014))
Circular RNA (circRNA)	>80 nt	miRNA sponges (Hansen et al. 2013); transcriptional regulation (Z. Li et al. 2015)

mRNAs

Intact mammalian mRNAs vary in length from 400 nucleotides (nt) up to >100,000 nt, with the average transcript being ~2,100 nt in size (Lander et al. 2001). Despite initial reports indicating the presence of mRNAs in EVs (Valadi et al. 2007), the majority of EV-associated RNAs fall within a size distribution of 25-700 nt from a variety of biofluids (Pegtel et al. 2010; Noerholm et al. 2012). Thus, it remains controversial whether these mRNAs are full-length or fragmented transcripts, though this may depend on the exact size and origin of the EV (see below). Nonetheless, transfer of mRNAs has been described for several tumor types, including colon and gastric cancer (Hong et al. 2009), glioblastoma (GBM) (Skog et al. 2008), leukemia (Milani et al. 2017), breast cancer (Conley et al. 2016), and prostate cancer (Lázaro-Ibáñez et al. 2017). The mRNAs appear to have tumor-specific signatures. In GBM cells, secreted EVs are enriched in mRNAs associated with cell proliferation, migration, angiogenesis, histone modification and immune repression (Skog et al. 2008). Additionally, mutant *EGFRvIII* transcripts can be detected in EVs isolated from the serum of GBM patients whose tumors expressed mutant *EGFRvIII* (Skog et al. 2008). Furthermore, colorectal cancer (CRC) cell EVs are enriched for mRNAs related to cell cycle pathways, specifically associated with M-phase activities (Hong et al. 2009). These M-phase-related mRNAs are differentially expressed across CRC patients, suggesting a potential role in tumor progression. Thus, tumor-specific RNAs in serum EVs could provide a cell-free 'biopsy' of the tumor cell to identify somatic mutations and changes in gene expression.

In addition to coding sequences, other reports demonstrate that EV-associated mRNAs are largely enriched for 3'-UTR fragments (Batagov and Kurochkin 2013). Although the precise mechanisms for how 3'UTRs are selected for secretion are unknown, one possibility is that mRNAs undergo post-transcriptional cleavage to produce 3'UTR fragments, as reported by Mercer et al. (Mercer et al. 2011). Another possibility is that exosome-associated mRNAs undergo degradation after secretion via extracellular RNases. This seems unlikely, however, as we and others observe sequencing reads spanning both full-length transcripts as well as smaller/fragmented transcripts, suggesting that these fragments are generated within the cell before sorting into exosomes.

microRNAs (miRNAs)

The most well studied exRNAs are miRNAs, one of the most abundant classes of small RNA found in plasma (Huang et al. 2013). miRNAs are single-stranded RNAs ~22 nt in length that bind to target mRNAs to inhibit their expression (For review, see (Bartel 2004)). With more than 24,000 identified vertebrate and invertebrate miRNAs (www.mirbase.org), they represent one of the largest gene families and are predicted to target 30-60% of protein coding genes (Griffiths-Jones et al. 2006; Bartel 2004). Since their initial discovery in *C. elegans* (R. C. Lee, Feinbaum, and Ambros 1993), miRNAs have proven fundamental to nearly every biological process.

Canonical miRNA biogenesis occurs through a series of coordinated cropping and dicing steps to yield the ~22nt mature miRNA (Figure 2). This process begins with transcription of the miRNA-containing locus by RNA polymerase II (Pol II) in the nucleus to produce long, hairpin-shaped transcripts that are subsequently processed to precursor-miRNAs (pre-miRNAs) by the microprocessor, which minimally contains the RNAse III enzyme Drosha in complex with the DiGeorge Critical Region 8 (DGCR8/Pasha) (Y. Lee et al. 2003; Gregory et al. 2004). Pre-miRNAs are recognized by the nuclear export protein, Exportin-5, and are transported out of the nucleus into the cytoplasm (Lund et al. 2004; Yi et al. 2003). After export into the cytoplasm, the pre-miRNA is bound and further processed by a second RNase-III-like enzyme, Dicer, which cleaves the stem loop structure to generate a mature miRNA:miRNA* duplex ~21-23 bp in length (Bernstein et al. 2001; Ketting et al. 2001; Pasquinelli et al. 2000). One strand of the miRNA duplex is then loaded onto Argonaute (Ago) bound to GW182 (glycine and tryptophan repeats protein molecular weight of 182kD) to form an RNA-induced silencing complex (RISC) and usually, the strand that is less stably paired at the 5' end is retained (Hammond et al. 2000; Schwarz et al. 2003). The mature miRNA then base-pairs imperfectly with cognate mRNA targets leading to translation repression, deadenylation and eventual target degradation (Krol, Loedige, and Filipowicz 2010).

miRNAs have been detected in virtually every body fluid, including serum (Xi Chen et al. 2008), plasma (Freedman et al. 2016), breast milk (Nobuyoshi Kosaka et al. 2010), semen (Vojtech et al. 2014) and cerebrospinal fluid (CSF) (Lehmann et al. 2012). Specific sets of miRNAs have been found inside EVs, as well as in protein and lipid complexes. For example, *miR-223* is enriched in HDL isolated from plasma of familial hypercholesterolemia patients

compared to healthy patients (Vickers et al. 2011). Additionally, miRNAs found in human plasma and serum can be bound to proteins, such as Ago2, that are not associated with EVs (Arroyo et al. 2011). Several studies have shown that in cancer, tumor-released EVs contain distinct miRNA profiles representative of the source tumor cell, with specific miRNAs enriched in EVs compared to their cell of origin. For example, *let-7* family members are abundant in EVs secreted by metastatic gastric cancer cells, but not other cancer cells (Ohshima et al. 2010). In breast cancer cells, >99% of *miR-451* is secreted by malignant cells, but preferentially retained in benign cancer cells (Pigati et al. 2010). Interestingly, *miR-451* has been shown to act as tumor suppressor in certain cancers (Nan et al. 2010; Bitarte et al. 2011). Furthermore, we have previously shown *miR-100* is preferentially secreted in EVs from mutant *KRAS* CRC cells (Cha et al. 2015) in a process that is dependent on *KRAS* status since *miR-100* is not enriched in EVs released by wild-type *KRAS* CRC cells (Cha et al. 2015; H. Ji et al. 2014). These data suggest that miRNA packaging into EVs and other carriers occurs by a selective sorting process that can be differentially regulated in different cancers.

Long non-coding RNAs (lncRNAs)

lncRNAs are classically defined as RNA transcripts >200 nucleotides in length that lack significant open reading frames. They are often 5' capped and polyadenylated, consistent with transcription by RNA Polymerase II (Fatica and Bozzoni 2014). According to GENCODE (www.gencodegenes.org), the current Ensembl human genome annotation (CRch38, v23) identifies more than 27,800 transcripts from ~16,000 genes as lncRNAs. Expression of lncRNAs is typically cell- and tissue-specific and often implicated in the control of various homeostatic processes (Fatica and Bozzoni 2014). The deregulation of lncRNA expression has been associated with the development and progression of certain cancers, and has been linked to modulating oncogenic and tumor-suppressive pathways (Berrondo et al. 2016; Q. Ji et al. 2014).

Although the majority of studies profiling various biofluids and conditioned media have focused on small RNAs (<200 nt) (Andrey Turchinovich et al. 2011), in certain contexts, lncRNAs are preferentially enriched in EVs. For instance, Prostate Cancer Antigen 3 (PCA3), or DD3, is a well-known lncRNA that is overexpressed in more than 95% of primary prostate cancers (PCa). Furthermore, PCA3 is readily identified in urine and has been implemented as the first urine-based molecular diagnostic test approved by the Food and Drug Administration (G. L.

Lee, Dobi, and Srivastava 2011). As its levels correlate with the tumor Gleason score, circulating PCA3 can also reflect the aggressiveness of prostate cancer (Merola et al. 2015).

Circular RNAs (circRNAs)

In Eukaryotes, circRNAs are covalently closed, single-stranded transcripts produced from back-splicing of genes, catalyzed by the spliceosomal machinery (Ashwal-Fluss et al. 2014). Discovered more than 30 years ago, they were traditionally thought to be by-products of aberrant splicing, with no known function (Capel et al. 1993; Cocquerelle et al. 1993). Recent advances in NGS of non-polyadenylated transcripts have found that circRNA expression is widespread (Jeck et al. 2013; Memczak et al. 2013; A. Ivanov et al. 2015; Dou et al. 2016). CircRNAs have cell- and tissue-specific expression patterns and can function as miRNA sponges (Hansen et al. 2013), competitors for complexes involved in normal splicing (Ashwal-Fluss et al. 2014), or as regulators of the local concentration of RNA-binding proteins (RBPs) (Memczak et al. 2013). We previously showed that circRNAs are globally down-regulated in mutant *KRAS* CRC cells, while specific circRNAs are enriched in their secreted exosomes (Dou et al. 2016). Expression levels of certain circRNAs, specifically circ-KLDHC10, were also shown to be significantly increased in serum EVs of CRC patients (Y. Li et al. 2015). In both cases, circRNAs in EVs were highly enriched compared to the levels of the corresponding linear RNAs, indicating that some circRNAs are more efficiently incorporated into EVs.

tRNA-derived fragments (tRFs)

One major class of RNA observed in circulation is tRNA fragments. tRNA undergoes several steps of processing and modification before becoming competent for translation (H. Li 2007). tRNA fragments result from normal processing of tRNAs (constitutive) to produce tRNA-derived fragments (tRFs)(Y. S. Lee et al. 2009), or in response to cell stress to produce tRNA-derived half transcripts (tRH), also known as tiRNAs(Yamasaki et al. 2009). Constitutive tRFs are comprised of three general types: one produced by cleavage at the 3'-end of the pre-tRNA transcript by RNase Z (3'-U tRF), and two produced by cleavage of the mature tRNA at the 3'- (3'-CCA tRF) and 5'-ends (5'-tRF) by Dicer (Haussecker et al. 2010). Similar to miRNAs, these tRFs are approximately 19-22 nt in length. 3'-tRFs have been shown to preferentially associate with AGO3-4, and 3'-CCA tRFs can function to silence specific targets analogous to miRNAs

(Haussecker et al. 2010).

In addition to constitutive tRFs, cell stress can induce tRNA cleavage into half-tRNA molecules by the ribonuclease angiogenin (ANG) (RNY1 in yeast (Thompson and Parker 2009)). ANG cleaves within the anticodon loops of mature tRNAs to produce 5'- and 3'-tRH that are ~30 and ~40 nt, respectively (Yamasaki et al. 2009). 5'-tRH RNAs have been reported to bind eukaryotic initiation factor (eIF) 4G to relocate the preinitiation complex away from mRNA, subsequently causing translational repression and stress granule assembly (P. Ivanov et al. 2011). 5'-tRH RNAs are abundant in blood plasma where they are hypothesized to associate with vesicle-free protein complexes such as HDL (Dhahbi, Spindler, Atamna, Yamakawa, et al. 2013). In contrast to blood plasma, 5'-tRH RNAs are also abundantly found within seminal fluid EVs from healthy male donors (Vojtech et al. 2014). In addition to 5'-tRH, 5'-tRNA fragments represent the most abundant type of RNA found in EVs secreted by immune cells, with a unique size distribution of ~40-50 nt (E. N. M. N.-'t Hoen et al. 2012). It is unknown whether these fragments are produced through angiogenin-mediated cleavage or represent byproducts of normal tRNA processing.

Although tRNA fragments make up a large percentage of exRNA, the functional consequences of their transfer to recipient cells are largely unknown. Considering that tRFs can be robustly induced upon cellular stress, it is likely that their expression patterns are altered in cancer. It was recently shown that a novel class of tRFs are induced in breast cancer cells, directly bind to Y-Box protein I (YBX1), and act to suppress the stability of multiple oncogenic transcripts by displacing YBX1 from the 3'-UTR (Goodarzi et al. 2015). Interestingly, YBX1 is required for the sorting of *miR-223* to EVs in HEK293T cells (Shurtleff et al. 2016), and possibly other RNAs in different contexts.

yRNA-derived fragments

yRNAs are a largely unexplored class of noncoding RNA species that have poorly characterized functions, but are best known as components of Ro and La ribonucleoproteins (RNPs), clinically significant autoantigens recognized by antibodies in patients with autoimmune disease (Sim and Wolin 2011; Lerner et al. 1981). Since their initial discovery, yRNAs have been shown to have additional functions, including formation of the DNA replication complex (Christo P. Christov et al. 2006) and chaperoning of misfolded RNAs (Kowalski and Krude

2015). In humans, the four yRNA genes are clustered together at a single chromosomal locus on chromosome 7q36 (Maraia et al. 1994). Individual yRNA genes are transcribed by RNA polymerase III from distinct promotors to produce transcripts of ~84-112 nt (Perreault et al. 2005). The 5' and 3' RNA ends hybridize to fold into characteristic secondary stem-loop structures containing at least 3 stems (Teunissen et al. 2000). The nucleotide sequences within the stem regions are highly conserved, whereas the internal loop sequence is varied between individual yRNAs and across different organisms (Teunissen et al. 2000).

In addition to the four annotated human yRNAs, yRNA fragments (yRFs) have been detected both intra- and extracellularly. Although some reports have shown that specific yRFs are a result of caspase-dependent cleavage and subsequent truncation during apoptosis (Rutjes et al. 1999), it is unclear whether all yRFs represent degradation products. Sequencing of small RNAs from tumor samples revealed yRFs ~25 nt in length, similar to miRNAs, are highly expressed in multiple cancer tissues (Meiri et al. 2010). Additionally, yRFs have been shown to associate with Ago2 in breast cancer cells (Thomson et al. 2015). These small yRFs reportedly do not possess miRNA-like activity (Meiri et al. 2010; Thomson et al. 2015) and are processed independent of the miRNA biogenesis pathway (Nicolas et al. 2012). In addition to yRFs found within cancer cells and tumor samples, specific 5'-yRFs, approximately 27 nt and 30-33 nt, represent a large fraction of the total small RNAs present in human serum (Dhahbi, Spindler, Atamna, Boffelli, et al. 2013). Similarly, yRFs represent the most abundant class of RNA in EVs from endothelial cells, and are highly expressed in EVs from seminal fluid. Enrichment of specific yRFs are likely cell-type specific, since endothelial EVs are preferentially enriched for RNY5 fragments (Balkom et al. 2015), while RNY4 fragments appear to be the dominant yRF moieties in seminal fluid EVs (Vojtech et al. 2014). In both cases, however, the majority of sequences mapped to the 5' ends of yRNA, suggesting selective sorting of yRFs into EVs may be regulated by common processing pathways that are presently unknown.

Vault RNA fragments (vRFs)

In addition to yRNA and tRNA fragments, an abundant class of exRNA preferentially enriched in EVs compared to the cell is vault RNA (vRNA) fragments (vRFs). vRNAs are a family of cytoplasmic non-coding RNAs associated with vault RNP complexes containing multiple copies of major Vault protein (MVPs) (Kedersha and Rome 1986). Despite the known

roles of MVPs in intracellular and nucleocytoplasmic transport(J.-Y. Li et al. 1999; Chugani, Rome, and Kedersha 1993; Herrmann et al. 1999), the precise cellular functions of the vault RNAs are not well understood. To date, there are three human vRNA genes arranged in a triple repeat on chromosome 5 that encode 98 nt (hvg1) or 88 nt (hvg2 and hvg3) single-exon pol III transcripts (Zon et al. 2001). A fourth vRNA-related sequence, hvg4, is located on the X-chromosome, but is presumably a silent pseudogene(Zon et al. 2001).

Expression levels of vRNA vary substantially in human tissues, with high expression observed in lung, breast and adipose tissues (Persson et al. 2009; M. A. Izquierdo et al. 1996). Additionally, vRNAs have been found to be up-regulated in various cancers and can contribute to multi-drug resistance (Persson et al. 2009). In cancer cells, it was shown that the majority of vault complexes associate with hvg1, however, consistently more hvg3 was bound to vaults isolated from multi-drug resistant cells compared to their drug-sensitive counterparts (Zon et al. 2001). Interestingly, hvg1 and hvg2 can specifically bind to mitoxantrone, a chemotherapeutic agent commonly used to treat breast cancer, myeloid leukemia and non-Hodgkin's lymphoma (Gopinath et al. 2005). This suggests the ratio in which vRNA species are associated with vaults or chemotherapeutic drugs may be of functional significance. Furthermore, levels of vRNA are not always correlated with MVP abundance (M. A. Izquierdo et al. 1996), suggesting vRNA biogenesis occurs independently of its association with MVP. This raises the possibility that the accumulation of yRNAs may be mediated via transfer of extracellular vRNA derived from exogenous sources.

It was recently demonstrated that vRNAs can be further processed into smaller ~23 nt fragments (vRFs) through a DICER-dependent and DROSHA-independent process (Persson et al. 2009). These vRFs can associate with Ago proteins to guide sequence-specific repression of target genes, similar to miRNAs (Persson et al. 2009). Interestingly, in immune cell exosomes, vRFs sequences predominantly correspond to the internal stem loop of the vRNA. In contrast, the bulk of cellular vRNAs are derived from 3' and 5' ends (E. N. M. N.-'t Hoen et al. 2012). Although it is unknown whether stem-loop derived fragments can also function as miRNAs or regulate target genes, differential accumulation in either cellular or exosomal samples suggests specific products of vRNA cleavage are preferentially incorporated into EVs .

1.2. Classes of EVs

EVs consist of a number of membrane encased cell-secreted vesicles. These include exosomes, microvesicles, apoptotic bodies, and oncosomes. As the nomenclature and exact purification strategies vary, (Gould and Raposo 2013), EVs provide a convenient term to refer to all secreted vesicles. Due to differences in their biogenesis, each class of EV likely have unique lipid composition, proteins and RNA cargo (Graça Raposo and Stoorvogel 2013), and distinct functional roles. This section will discuss some of these EV classes and what is known regarding their physical properties, composition and biogenesis.

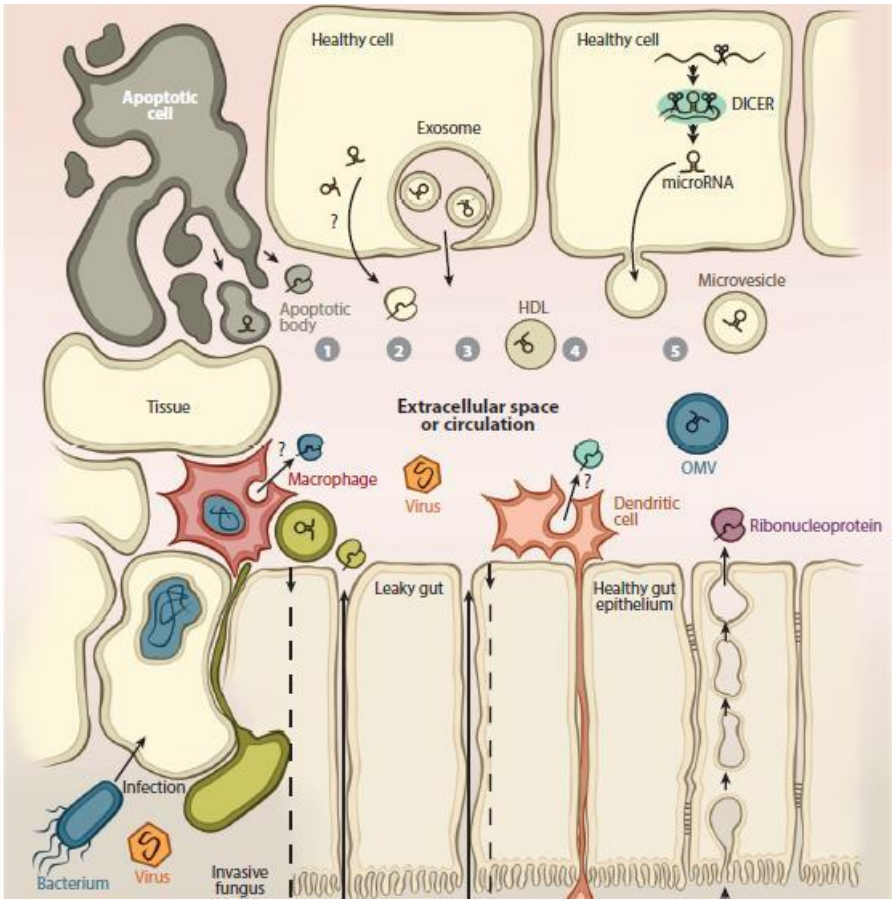

Figure 1. Origins and classes of exRNA carriers. (from Fritz et al. 2016). During cell death, apoptotic bodies containing RNA are released into extracellular space (1). RNP complexes are likely also released during cell death (1), and from healthy cells (2), although no specific mechanisms have been described. Healthy cells also secrete exosomes (3), high-density lipoproteins (HDLs) (4), and microvesicles (5) associated with RNAs. In some cases, bacteria, viruses and fungi are able to hijack the mammalian export machinery to induce infected cells to release exogenous exRNAs through various carriers into circulation.

Exosomes

Traditionally, exosomes are classified as the smallest EVs with a diameter of 50-150nm. These vesicle originate from the endosomal pathway and are secreted by fusion of late endosomes (also called multivesicular bodies; MVBs) with the plasma membrane (reviewed in (Colombo, Raposo, and Théry 2014; Maas, Breakefield, and Weaver 2016; Graça Raposo and Stoorvogel 2013)). On their way to becoming MVBs, the small membrane domains become enriched with various cargos including lipids, such as cholesterol, lysobisphosphatidid acid (LPBA), sphingomyelins and ceramide (reviewed in (Cocucci and Meldolesi 2015), which are also enriched in exosomes (Simpson, Kalra, and Mathivanan 2012). A critical component of MVB maturation and exosome formation is the accumulation and processing of ubiquitinated proteins sorted by the endosomal sorting complex required for transport (ESCRT) machinery (Colombo et al. 2013). In addition to ESCRT, exosomes can be generated through ESCRT-independent mechanisms that appears to be cell-type specific. For example, in mouse oligodendroglial cells, production of exosomes requires the hydrolysis of sphingomyelin to ceramide by neutral sphingomyelinase (nSMase) (Trajkovic et al. 2008). Ceramide can undergo catabolism to produce sphingosine and sphingosine 1-phosphate (S1P) (Perry and Hannun 1998). S1P-mediated activation of Gi-coupled S1P receptors on MVBs is required for cargo sorting in exosomes of Hela cells (Kajimoto et al. 2013). According to EV databases *ExoCarta* and *Vesiclepedia* (Simpson, Kalra, and Mathivanan 2012; Kalra et al. 2012), the proteins most frequently enriched in exosomes are the tetraspanin family members CD9, CD63 and CD81, heat shock proteins Hsp70 and Hsp90, Flotillin-1, as well as enzymes involed in cellular metabolism, including Enolase1, Aldolase A, phosphoglycerate kinase 1 (PGK1) and lactate dehydrogenase A (LDHA)(Higginbotham et al. 2011a; Welton et al. 2010).

Microvesicles

Microvesicles (MVs), also known as shedding vesicles or ectosomes, are larger than exosomes, with a diameter of 0.15-1μm, and result from direct budding from the surface of the plasma membrane (Graça Raposo and Stoorvogel 2013). Consequently, the membrane composition of MVs reflects that of the parent cell more closely than does the membrane composition of exosomes (Andaloussi et al. 2013). MV shedding can be induced by asymmetric distribution of phospholipids in the plasma membrane, resulting in the exposure of

phosphatidylserine (PS) and phosphatidylethanolamine (PE) in the outer leaflet of the MV membrane (Larson et al. 2012; Lima et al. 2009). In cancer cells, shedding can also be induced by the ADP-ribosylation factor 6 (ARF6), a GTP binding protein that is enriched in MVs (Muralidharan-Chari et al. 2009, 6). Accumulation of protein and RNA cargoes in the MV lumen occurs by various mechanisms. Although the ESCRT machinery was initially thought to be important only for MVBs, ESCRTs have also been shown to regulate processes that are specific to the plasma membrane, such as membrane sorting, budding and fission during cytokinesis and virus budding (Bissig and Gruenberg 2014). For example, Tsg101, a component of ESCRT-I, can relocate to the plasma membrane to interact with Alix and Arrestin domain-containing protein 1 (ARDDC1) at the site of MV release (Nabhan et al. 2012). Additionally, ESCRT-III is a critical component for the abscission and release of MVs (Nabhan et al. 2012). In addition to ESCRT, internalization of proteins into MVs requires the binding of cytoplasmic proteins to the inner leaflet of the plasma membrane, which is often dependent on membrane anchors, such as myristoylation and palmitoylation, and higher-order polymerization that concentrates proteins to small membrane domains of MV budding (Shen et al. 2011; Yang and Gould 2013).

Table 2. Characteristics of different extracellular vesicles

	Exosomes	**Microvesicles**	**Apoptotic Bodies**	**Large oncosomes**
Diameter	50-150 nm	150-1000 nm	>1000 nm	1-10 μm
Origin	Endosomes	Plasma membrane	Plasma membrane of cells undergoing apoptosis	Plasma membrane
Markers	Tetraspanins (CD63, CD81), Tsg101, flotillin	Integrins, selectins, CD40, ARF6	Phosphatidyl serine, annexin V, DNA	KRT18
Sedimentation	100,000 x g	10,000 x g	~2,000 x g	10,000-20,000 x g

Apoptotic Bodies (ABs)

Cells undergoing apoptosis release large vesicles 0.5-2μm in diameter, known as apoptotic bodies (ABs), that results in nuclear fragmentation, increase in membrane permeability, and externalization of PS (Taylor, Cullen, and Martin 2008). As these vesicles are rich in PS, they aid in the clearance of corpses by phagocytes (Rubartelli, Poggi, and Zocchi 1997). The generation of ABs occurs during the late stages of programmed cell death by caspase-mediated cleavage and subsequent activation of ROCK1(Mills et al. 1998). Previously, ABs were thought to form stochastically (Taylor, Cullen, and Martin 2008), but it was recently shown in T-cells the biogenesis of these vesicles occurs in a tightly regulated multi-step process that involves the formation of 'string-like' membrane protrusion (also known as apoptopodia) after the onset of membrane blebbing (Poon et al. 2014). Although not well understood mechanistically, cellular contents such as cytokines, miRNA and DNA can be packaged into ABs to regulate immunity, tissue repair and tumorigenesis (Zernecke et al. 2009; Bergsmedh et al. 2001). Because apoptosis results in nuclear fragmentation, it has been reported that ABs contain nuclear material, such as DNA (Taille et al. 1999). Whether luminal transfer of ABs occurs *in vivo* and results in functional consequences requires further investigation.

Oncosomes

Oncosomes are the largest class of EVs (1-10um diameter) that bleb from the surface of metastatic cancer cell membranes (Di Vizio et al. 2012). Although the term oncosome has been used to describe a category of tumor-derived MVs, they are enriched for cargoes that are absent from typical MVs, such as Caveolin-1 and cytokeratin 18 (KRT18) (Di Vizio et al. 2012; Minciacchi et al. 2015), suggesting they represent a separate and distinct class of EVs. The abundance of oncosomes are reportedly correlated with tumor progression (Di Vizio et al. 2012), and can be induced by repression of cytoskeletal regulator Diaphanous-related formin-3 (DIAPH3), by overexpression of certain oncogenes, or by activation of EGFR (Vizio et al. 2009; Hager et al. 2012; Kim et al. 2014). Less is known regarding the RNA cargo and functional importance of oncosomes in cell-to-cell communication compared to other classes of EVs. Nonetheless, it was shown that large oncosomes secreted by breast cancer cells are enriched for mRNAs encoding E2F transcriptional targets and histone proteins. These mRNAs are mostly expressed in S-phase of the cell cycle, suggesting their sorting into oncosomes may occur during

S-phase (Conley et al. 2016). In addition to mRNAs, certain miRNAs were selectively enriched in prostate cancer cell oncosomes to enhance migration of cancer-associated fibroblasts (CAFs) upon transfer (Morello et al. 2013). It is important to note, however, that due to limitations in isolation techniques, one cannot exclude the possible contribution of several EV populations to the reported protein and RNA profiles. Furthermore, because oncosomes, like MVs and ABs, are formed directly from the plasma membrane, it remains unclear whether these EVs are completely distinct, arise through different biogenic pathways and/or differ in their functional roles.

1.3. Mechanisms of exRNA loading into EVs

Among the different types of EVs, exosomes are perhaps the best studied and characterized. Given the lack of knowledge regarding RNA sorting into larger vesicles, this section will focus on RNA loading into exosomes. Although care must be taken when evaluating the different purification protocols and characterization between different reports, exosomes appear to carry a distinct repertoire of RNAs different from the parent cell of origin (Chiba 2012). This suggests a selective sorting process for exRNA in exosomes.

Because exosomes arise through the endosomal pathway, it appears that RNA sorting into exosomes is regulated, at least in part, by subcellular localization of the RNA and its associated binding protein(s) (Figure 2). For example, inhibition of the Endosomal Sorting Complex Required for Transport (ESCRT) results in the accumulation of GW182, a component of the RISC machinery required for miRNA-mediated silencing, on the surface of late endosomes, (Gibbings et al. 2009). This results in compromised target mRNA repression and is consistent with the idea that RISC complexes localize to the surface of late endosomes or MVBs. Also consistent with the model that RISC activity affects miRNA sorting into EVs , depletion of GW182 or AGO2 reduces miRNA secretion in exosomes (Yao et al. 2012; Guduric-Fuchs et al. 2012). In macrophages, cell-activation-dependent changes in mRNA levels can promote miRNA relocation from cytoplasmic P-Bodies (sites of miRNA repression) to the surface of MVBs (sites of RISC turnover and exosome biogenesis), thereby controlling miRNA secretion in exosomes (Squadrito et al. 2014). Furthermore, certain miRNAs can also undergo non-template directed nucleotide additions (NTAs) that alter miRNA activity, stability, and association with RISC (Wei et al. 2012; Burroughs et al. 2010; Thornton et al. 2014; Heo et al. 2012). As such, certain

miRNA isoforms that are 3'-uridylated appear to be enriched in exosomes compared to the parental cell (Koppers-Lalic et al. 2014). However, not all miRNAs undergo NTAs, suggesting additional targeting mechanisms exist.

Similar to the fact that *cis*-acting elements in an RNA can regulate subcellular localization (Jambhekar and DeRisi 2007), miRNAs may also be sorted to EVs in a sequence-dependent fashion. An exosome-sorting motif has been described for miRNAs secreted by T-lymphocyte cells (Villarroya-Beltri et al. 2013a) consisting of a GGAG sequence within the 3'-end of the miRNA (Villarroya-Beltri et al. 2013a). The hypothesis is that this sequence is recognized by a SUMOylated version of heteronuclear ribonucleoprotein (hnRNP) A2B1 which then targets the miRNA for export into exosomes.

Another mechanism that may drive sorting specificity is through lipid-mediated RNA loading into EVs, specifically the sphingolipid ceramide (N. Kosaka et al. 2010). Reduction of ceramide synthesis by inhibition of neutral sphingomyelinase 2 (nSMase2) impairs exosomal maturation and release (Trajkovic et al. 2008), and is required for exosomal miRNA secretion in HEK293 cells (N. Kosaka et al. 2010). Interestingly, ceramide depletion through nSMase2 inhibition increases transport of specific miRNAs on HDL (Vickers et al. 2011), suggesting that the secretion of miRNAs may occur through overlapping but distinct mechanisms. Similar to the bioactive role of ceramide, sphingosine-1-phosphate (S1P), a metabolite produced through acylation and phosphorylation of ceramide, is an essential component in exosomal maturation and release (Kajimoto et al. 2013). It is unknown whether S1P affects RNA secretion.

Overall, these data suggest multiple biogenic routes exist for the secretion of RNAs in exosomes and EVs that may be cell-type and cell-state dependent. Whether these pathways are distinct and reflect the heterogeneity of EVs and their cargoes remains to be determined.

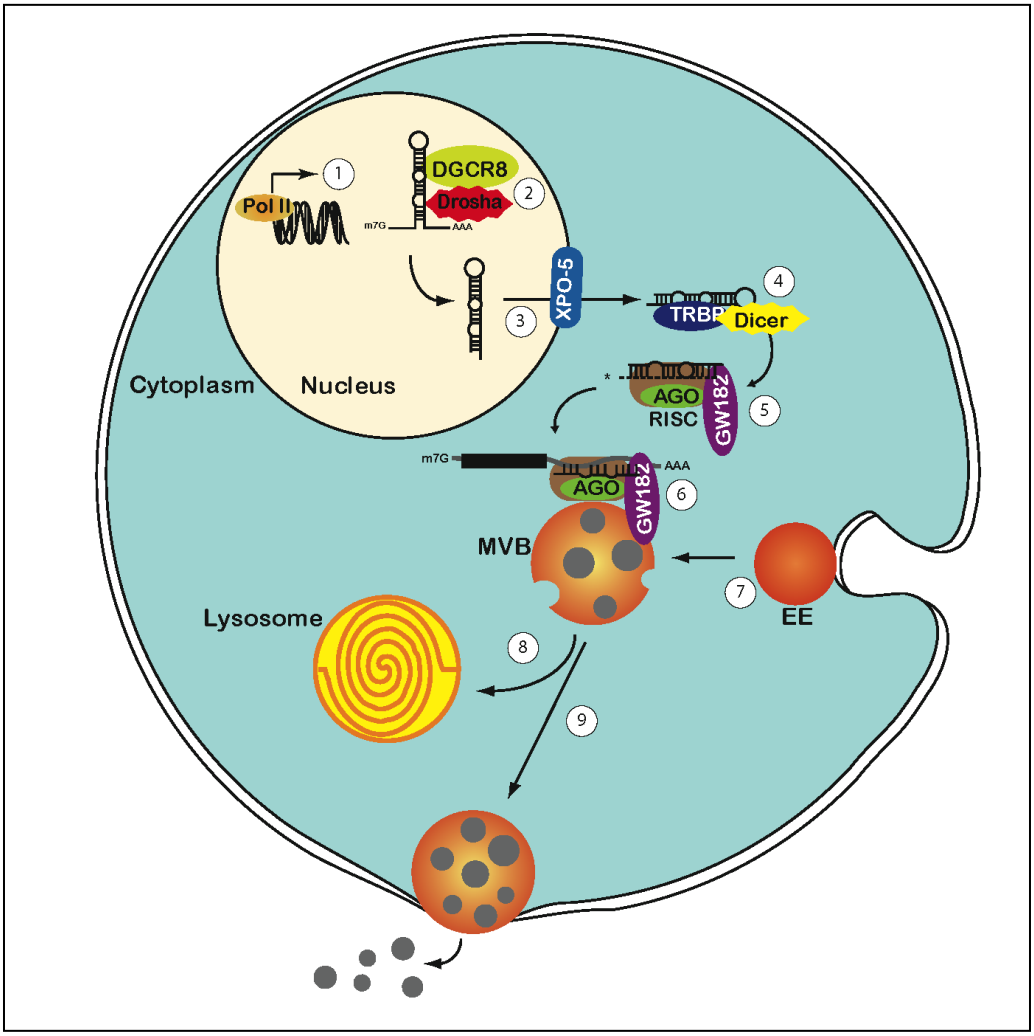

Figure 2. General model of miRNA biogenesis and export into exosomes. 1) miRNA genes are transcribed by RNA polymerase II as pri-miRNAs and 2) processed by Drosha in complex with DGCR8 to pre-miRNAs in the nucleus. 3) Pre-miRNAs are exported to the cytoplasm by Exportin-5, where they are further 4) processed into mature miRNA:miRNA* duplexes by Dicer. 5) The guide strand is bound by AGO and partner GW182, and preferentially retained in the RISC 6) where it base-pairs with target mRNAs to mediate target repression or cleavage localized to MVBs. MVBs arise from maturation of 7) early endosomes and form by inward budding into MVBs. MVBs can 8) be targeted to the lysosome, or 9) to the plasma membrane to release their intraluminal vescicles (exosomes; grey circles) into the extracellular space.

1.4. EV-mediated transfer of exRNA

The current prevailing paradigm is that EVs are tiny "packages" of information that can reach various targets, representing a novel form of communication between cells. A key component is that EVs can provide exchange of genetic information, particularly in the form of RNA, and that this information can be transferred over long distances. As such, the functional output of exRNAs ultimately depends on its uptake by recipient cells. A variety of different mechanisms addressing internalization and release of luminal contents have been described in detail (Colombo, Raposo, and Théry 2014; Mulcahy, Pink, and Carter 2014). The primary pathways that have been demonstrated include endocytosis (Morelli et al. 2004; Nanbo et al. 2013) and direct fusion to the plasma membrane (Montecalvo et al. 2012; Parolini et al. 2009). This section will review some of the modes of EV uptake as well as the functional consequences of RNA unloading in recipient cells (Figure 3).

EV Uptake

Considering the topology of EVs and the fact that they contain a variety of signaling proteins on their surface (Segura et al. 2005; Higginbotham et al. 2011a), most evidence suggests that EVs are taken up via endocytosis (Segura et al. 2005; Tian et al. 2010; E. N. M. N.-'t Hoen et al. 2009; Higginbotham et al. 2011a). This uptake can occur rapidly, with EVs being detected inside recipient cells as early as 15 minutes after incubation (Feng et al. 2010). EV endocytosis can occur through various molecular internalization pathways, including clathrin- (Escrevente et al. 2011; Tian et al. 2014) and caveolin-mediated endocytosis (Nanbo et al. 2013), macropinocytosis (Nakase et al. 2015; Fitzner et al. 2011), and phagocytosis (Montecalvo et al. 2012; Feng et al. 2010). In these cases, EV internalization requires subsequent back-fusion at the endosomal membrane for cytosolic RNA delivery, which may be facilitated by the acidic pH found in endosomes (Parolini et al. 2009).

Another possible entry mechanism is by direct fusion of the EV membrane with the cell plasma membrane. Membrane fusion requires that two phospholipid bilayers merge to form an aqueous fusion pore (Jahn and Südhof 1999), connecting cytosolic compartments of the EV to the target cell. Although EV-uptake via fusogenic routes is energetically unfavorable (Jahn and Südhof 1999), and thus, less likely to occur, it was demonstrated that in dendritic cells, cell-to-

cell transfer of miRNAs occurs through EV hemifusion with the plasma membrane of acceptor cells (Montecalvo et al. 2012). Additionally, exosomes produced by melanoma cells cultured in low pH display increased fusion and internalization by recipient cells (Parolini et al. 2009).

Whether EV uptake depends on endocytic routes or direct fusion remains unclear. As no universal mechanism has been identified, it seems likely that specific recipient cells utilize distinct mechanisms for EV uptake that is influenced by the physiological state of the donor as well as the recipient cell (Mulcahy, Pink, and Carter 2014).

Functional transfer of RNA

Although the exact mechanism of uncoating remains to be determined, transfer of EV-associated RNAs has been shown to have numerous effects in recipient cells. In cancer, these include mediating cell-to-cell transfer of oncogenic RNAs, modulation of the tumor microenvironment, and recruiting of pro-tumorigenic immune cells (Higginbotham et al. 2011a; Luga et al. 2012; Bobrie et al. 2012).

One of the first functional studies investigating transfer of mRNAs tested delivery of mouse MC/9 EVs mRNAs into human mast cells (Valadi et al. 2007). Unfortunately, follow up studies on functional protein-coding mRNAs in circulation are lacking. Nonetheless, overexpression studies revealed the possibility of delivering functional mRNAs to target cells. Glioblastoma-derived microvesicles containing *GLuc* mRNA could be transferred to and expressed in recipient human brain microvascular endothelial cells (Skog et al. 2008). Additionally, an *in vivo* model showed that transplantation of lung carcinoma tumor cells expressing Cre recombinase into reporter mice led to Cre-mediated recombination events near the tumor site, suggesting Cre mRNA can be secreted in EVs and function on nearby cells (Ridder et al. 2015).

Among the different types of exRNAs, most functional studies have focused on the consequences of miRNA transfer because reporter assays can easily be adapted (reviewed in (A. Turchinovich, Samatov, and Burwinkel 2013)). In theory, mRNA transfer should also be readily detectable but specific examples of mRNA transfer are limited (Batagov and Kurochkin 2013; Valadi et al. 2007). Besides canonical silencing of mRNAs via miRNA transfer, EV-derived miRNAs can also elicit non-canonical responses in target cells (Figure 3). Tumor-secreted *miR-21* and *miR-29a* can bind as ligands to Toll-like receptors (TLR) (murine *TLR7* and human

TLR8) in immune cells to trigger inflammatory responses (Fabbri et al. 2012) that can facilitate tumor growth and metastasis. Interestingly, extracellular yRNA fragments associated with Ro60 have also been shown to induce TLR7-dependent NF-KB activation in models of atherosclerosis (Hizir et al. 2017). Whether exRNA-mediated activation of TLRs has sequence-specific requirements or is restricted to immune cells remains to be determined.

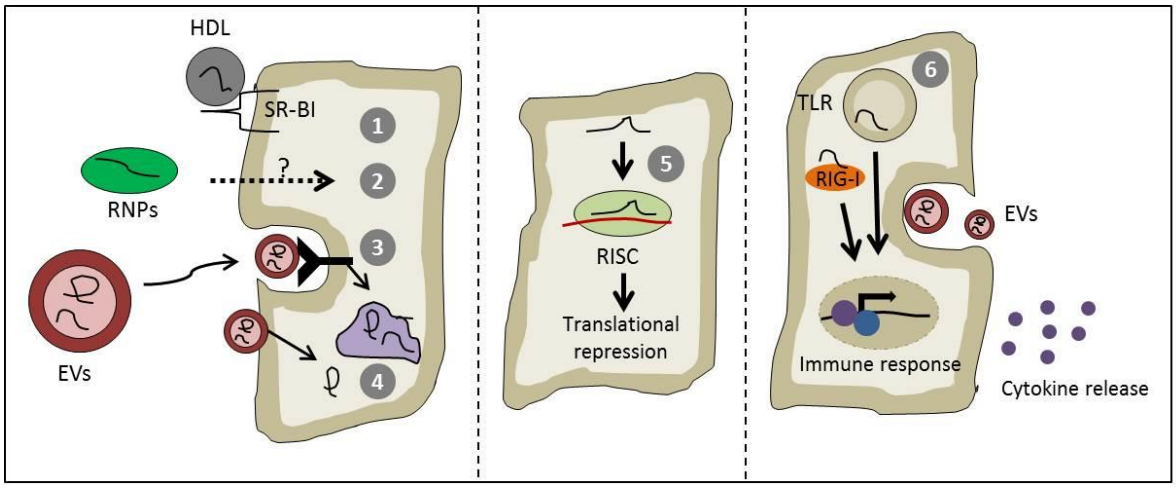

Figure 3. Uptake and functions of extracellular small RNAs in target cells. (1) The scavenger receptor class B member 1 (SR-BI) has been shown to be involved in the uptake of high-density lipoprotein (HDL)-associated miRNAs. (2) Small RNAs complexed in ribonucleoproteins (RNPs) have been found in circulation, but their uptake mechanisms remain largely unknown. RNAs encased in extracellular vesicles (EVs) can be taken up by (3) receptor-mediated endocytosis, or by (4) direct fusion with the plasma membrane of the target cell. After the RNA is released into the cytosol of acceptor cells, some exRNAs have been shown to cause (5) translational repression through the RNA-induced silencing complex (RISC), or immune activation by direct interaction with (6) Toll-like receptors (TLRs) found in late endsosomes, or trhough retinoic acid-inducible gene 1 (RIG-1).

Insight into the role of EV-mediated transfer of RNAs other than miRNAs and mRNAs is only beginning to emerge. EV-derived RNAs from stromal cells can activate the pattern recognition receptor RIG-I to activate antiviral signaling in breast cancer cells (Boelens et al. 2014). Typically, RIG-I activation occurs by viral RNA bearing 5’ triphosphate, but interestingly, stromal EVs predominantly contain transposable element RNAs, which can also have 5'-triphosphate ends (Dieci et al. 2013). Additionally, cancer cell secreted yRNA fragments, specifically yRNA5 (or RNY5), triggered rapid cell death when transferred to healthy primary cells, but not other cancer cells (Chakrabortty et al. 2015). Although the mechanisms are unclear, yRNAs are known to be significantly up-regulated in cancer tissues and can regulate cell

proliferation (C. P. Christov, Trivier, and Krude 2008). Furthermore, transfer of *CDR1as*, a circRNA known to function as a *miR-7* sponge (Hansen et al. 2013), from breast cancer cells to recipient liver cells abrogated *miR-7*-induced growth suppression (Y. Li et al. 2015). Thus, the transfer of these RNA moieties may reflect a novel strategy used by cancer cells to establish pro-metastatic microenvironments.

1.5. Quantitative analysis of exRNAs in EVs

Despite growing evidence of EV-mediated RNA transfer as a mode of intercellular communication, current models lack quantitative and physiological significance of this paradigm. Quantitative analysis of miRNAs contained within exosomes demonstrated that on average, less than one miRNA molecule is found per exosome, representing 2.5% (median) of total secreted miRNAs from a variety of biological fluids (Chevillet et al. 2014). As several reports have shown that cells secrete a heterogenous population of EVs, one possibility is that miRNAs and other RNAs are only contained within specific subclasses of EVs. Some of these EVs might contain substantially high numbers of RNA molecules, while other EVs might contain no RNA cargo at all. Theoretically, an EV with a 150 nm diameter, containing a lipid bilayer 4 nm in width, has an internal radius of approximately 71 nm, to produce a maximum internal volume of $(4/3\pi R^3)$ ~1.5×10^{-12} nm^3. Considering the calculated volume of a 100 nt RNA transcript, which is approximately 6×10^{-17} nm^3 (Voss and Gerstein 2005), one EV could thus tightly accommodate about 2.5×10^4 small RNA molecules.

Despite the reportedly low numbers of RNA cargo per EV, there can be up to 10^{12} EV particles per ml of body fluid (M. Li et al. 2014; Chevillet et al. 2014). Thus, as a population, RNAs encased within EVs can accumulate to high numbers in recipient cells. Furthermore, cellular uptake of exosomes between cells might be rapid and continuous, which would not necessarily be reflected in circulation or from conditioned media at steady state. Rapid uptake has been observed in macrophages, which can internalize an equivalent of their cell surface in pinocytic vesicles every 33 minutes (Steinman, Brodie, and Cohn 1976). In this case, low levels of circulating RNAs could accumulate to functionally sufficient quantities in target cells. Interestingly, mutant *KRAS* pancreatic adenocarcinoma cells exhibit high levels of EV uptake via macropinocytosis compared to wild type *KRAS* cells (Nakase et al. 2015), suggesting a role

in *RAS*-mediated macropinocytosis of EVs in malignant progression. In addition to bulk uptake, the exchange of EVs and their associated RNAs might occur through direct cell-to-cell connections, such as tunneling nanotubes (TNTs) or gap junctions. In support of this, EVs derived from malignant cancer cells have been shown to increase the formation of TNTs (non-adherent, actin-based cytoplasmic extensions), and that these TNTs function as conduits for intercellular transfer of EVs between connected cells (Thayanithy et al. 2014). Lastly, RNAs might function in non-canonical pathways where single copies are sufficient in eliciting a biological response.

In the case of miRNAs or other small RNAs, another possibility is that these RNAs are in complex within vesicle-free RNPs, such as Ago2 (Arroyo et al. 2011), or as part of HDL complexes (Vickers et al. 2011; Tabet et al. 2014). These complexes have been shown to co-sediment with EVs during common ultracentrifugation isolation procedures (Arroyo et al. 2011). Thus, it is possible that some of the RNAs described in EVs are perhaps not present in EVs at all, but in other co-isolating carriers. Whether these RNP-associated miRNAs are secreted by active processes in donor cells, and how these miRNAs reassemble into functional RISC in recipient cells remains to be defined.

Quantitative evaluation regarding the stoichiometric ratio of RNA transcripts per EV and in circulation outside of EVs will be essential to understanding the requirements and limits of exRNA-mediated communication. As more sequencing profiles and data sets are being generated, a comprehensive model to determine the contents of each EV and how likely those contents contribute to physiological processes will be of critical importance. Despite most studies indicating a general enrichment of small RNA species in EVs, among the RNA candidates most likely to confer changes in recipient cells are those that can be amplified, such as mRNAs, which can be translated repeatedly to produce many proteins. Thus, just a few mRNA molecules would be sufficient to illicit significant changes in acceptor cells. Alternately, the RNA product, or the RNA itself, could have regulatory functions.

1.6 Conclusions

Accumulating evidence demonstrates the importance of exRNA in normal development as well as in pathological processes. However, a caveat of the field is that most studies on EV-

mediated RNA transfer have been based primarily on *in vitro* experiments or *ex vivo* manipulations, leaving their physiological relevance unclear. It is well documented that different cell types differ in the composition of RNAs and EVs that they secrete, as well as their propensity for EV-mediated uptake. There is promising potential for EV-derived exRNAs as disease biomarkers and their applications in cancer immunotherapy. However, the mechanisms involved in EV secretion and cargo loading, as well as their interaction with target cells is only beginning to emerge. It is important to recognize that apart from mRNAs and miRNAs, other RNA classes may act as signaling molecules. It will important to determine the mechanisms that determine selective RNA export, how EVs are targeted to specific cells, and how exRNAs are released in recipient cells to alter gene expression patterns.

Chapter 2

KRAS-dependent sorting of miRNA to exosomes[1]

2.1 Abstract

Mutant *KRAS* colorectal cancer (CRC) cells release protein-laden exosomes that can alter the tumor microenvironment. To test whether exosomal RNA might also contribute to changes in gene expression in recipient cells, and to test whether mutant *KRAS* might regulate the composition of secreted miRNAs, we compared small RNAs of cells and matched exosomes from isogenic CRC cell lines differing only in *KRAS* status. We show that exosomal profiles are distinct from cellular profiles, and mutant *KRAS* exosomes cluster separately from wild type *KRAS* exosomes. *miR-10b* was selectively increased in wild type *KRAS* exosomes while *miR-100* was increased in mutant *KRAS* exosomes. Neutral sphingomyelinase inhibition caused accumulation of *miR-100* only in mutant *KRAS* cells, suggesting *KRAS*-dependent miRNA export. In Transwell co-culture experiments, mutant *KRAS* donor cells conferred *miR-100*-mediated target repression in wild type *KRAS* recipient cells. These findings suggest extracellular miRNAs can function in target cells and uncover a potential new mode of action for mutant *KRAS* in CRC.

1. *Diana J. Cha, *Jeffrey L. Franklin, Yongchao Dou, Qi Liu, James N. Higginbotham, Michelle Demory Beckler, Alissa M. Weaver, Kasey Vickers, Nripesh Prasad, Shawn Levy, Bing Zhang, Robert J. Coffey, and James G. Patton. 2015. "KRAS-Dependent Sorting of miRNA to Exosomes." *eLife* 4 (July): e07197. doi:10.7554/eLife.07197. *These authors contributed equally to this work.

2.2 Introduction

An emerging paradigm in the study of cell signaling is the potential role for post-transcriptional gene regulation by extracellular RNAs. microRNAs (miRNAs) are perhaps the best characterized class of small noncoding RNAs that have been detected in extracellular fluids (Valadi et al. 2007). Mature miRNAs are 21-23 nucleotides in length and bind to target mRNAs to inhibit their expression (Krol, Loedige, and Filipowicz 2010). Because miRNAs imperfectly pair with their mRNA targets, they can potentially regulate hundreds of transcripts within a genome(Bartel 2004). However, individual miRNAs exhibit exquisite tissue-specific patterns of expression(Wienholds 2005), control cell fate decisions(Alvarez-Garcia and Miska 2005), and are often aberrantly expressed in human cancers(Calin and Croce 2006), affording possible disease-specific signatures with diagnostic, prognostic and therapeutic potential(J. Lu et al. 2005; Volinia et al. 2006).

In addition to their intracellular roles, recent experiments have identified miRNAs outside the cell in extracellular vesicles (EVs) including exosomes or larger vesicles(Valadi et al. 2007; Graça Raposo and Stoorvogel 2013), in high density lipoprotein (HDL) particles(Vickers et al. 2011), or in smaller complexes with Argonaute 2 protein (AGO2)(Arroyo et al. 2011). Exosomes are small 40-130nm vesicles of endosomal origin that are secreted by all cells and can fuse and be internalized by recipient cells(Valadi et al. 2007; N. Kosaka et al. 2010). It has been suggested that protein cargo transfer by exosomes between cells is associated with tumor aggressiveness and metastasis(Skog et al. 2008; Higginbotham et al. 2011a; Luga et al. 2012; Hoshino et al. 2013). With the discovery that miRNAs and other RNAs can also be packaged into EVs, or exported by other extracellular mechanisms, it remains unclear the extent to which RNA cargo is sorted for export and how it is dysregulated in disease conditions, such as cancer.

Despite accumulating evidence that exosomes are biologically active, little is known regarding how oncogenic signaling affects the repertoire of miRNAs or proteins that are selected for secretion. Given the potential of cancer-derived secreted RNAs to modulate the tumor microenvironment, elucidation of the potential mechanisms for selective sorting of cargo into exosomes is critical to understanding extracellular signaling by RNA. *KRAS* mutations occur in approximately 34-45% of colon cancers(Wong and Cunningham 2008). We have previously shown that exosomes from mutant *KRAS* CRC cells can be transferred to wild type cells to induce cell growth and migration(Higginbotham et al. 2011a; Demory Beckler et al. 2012).

Compared to exosomes derived from isogenically matched wild type cells, exosomes derived from mutant *KRAS* cells contain dramatically different protein cargo(Demory Beckler et al. 2012). Here, we show that *KRAS* status also prominently affects the miRNA profile in cells and their corresponding exosomes. Exosomal miRNA profiles are distinct from cellular miRNA patterns and exosomal miRNA profiles are better predictors of *KRAS* status than cellular miRNA profiles. Furthermore, we show that cellular trafficking of miRNAs is sensitive to neutral sphingomyelinase inhibition in mutant, but not wild type, *KRAS* cells and that transfer of miRNAs between cells can functionally alter gene expression in recipient cells.

2.3. Results

Small noncoding RNAs are differentially distributed in exosomes

Because small RNAs are thought to be sorted at endosomal membranes and since *KRAS* signaling can also occur on late endosomes(A. Lu et al. 2009), we hypothesized that oncogenic KRAS signaling could alter RNA export into exosomes. We prepared small RNA libraries from both exosomes and whole cells using isogenically matched CRC cell lines that differ only in *KRAS* status (Table 2)(Senji Shirasawa et al. 1993). Exosomes were purified using differential centrifugation and consisted of vesicles ranging in size from 40-130 nm(Higginbotham et al. 2011a; Demory Beckler et al. 2012). These preparations exclude larger microvesicles but contain smaller lipoproteins and probably other small RNA-protein complexes (unpublished observation). Comprehensive sequencing analyses of both cellular and exosomal small RNAs from all three cell lines revealed that more than 85% of the reads from the cellular RNA libraries mapped to the genome, compared to only 50-71% from the exosomal libraries (Figure2A). The non-mappable reads consisted largely of sequences that contain mismatches to genomic sequences.

The global small RNA profiles identified reads from various classes of RNA, including miRNAs, with differential enrichment of specific RNAs in both the cellular and exosomal fractions. Compared to cellular RNA samples, which displayed an enrichment of miRNA sequences (~70%), miRNA reads in exosomal samples comprised a smaller percentage of the total small reads (5-18%) compared to other ncRNA classes (e.g. tRNAs, rRNAs, snRNAs) (Figure 4B,C). Most of these reads appear to be fragments of larger RNAs, both cytoplasmic and nuclear. It is not clear how these RNAs are associated with and/or deposited into exosomes.

Table 3. Colorectal cancer cell lines.

Cell line	*KRAS* allele	Growth in soft agar	Tumors in nude mice
DLD-1	WT/G13D	Yes	Yes
DKs-8	WT	No	No
DKO-1	G13D	Yes	Yes

Small RNA sequencing libraries were prepared from three isogenic colorectal cancer cell lines with the indicated alleles of KRAS. Table is based on work done in (Senji Shirasawa et al. 1993).

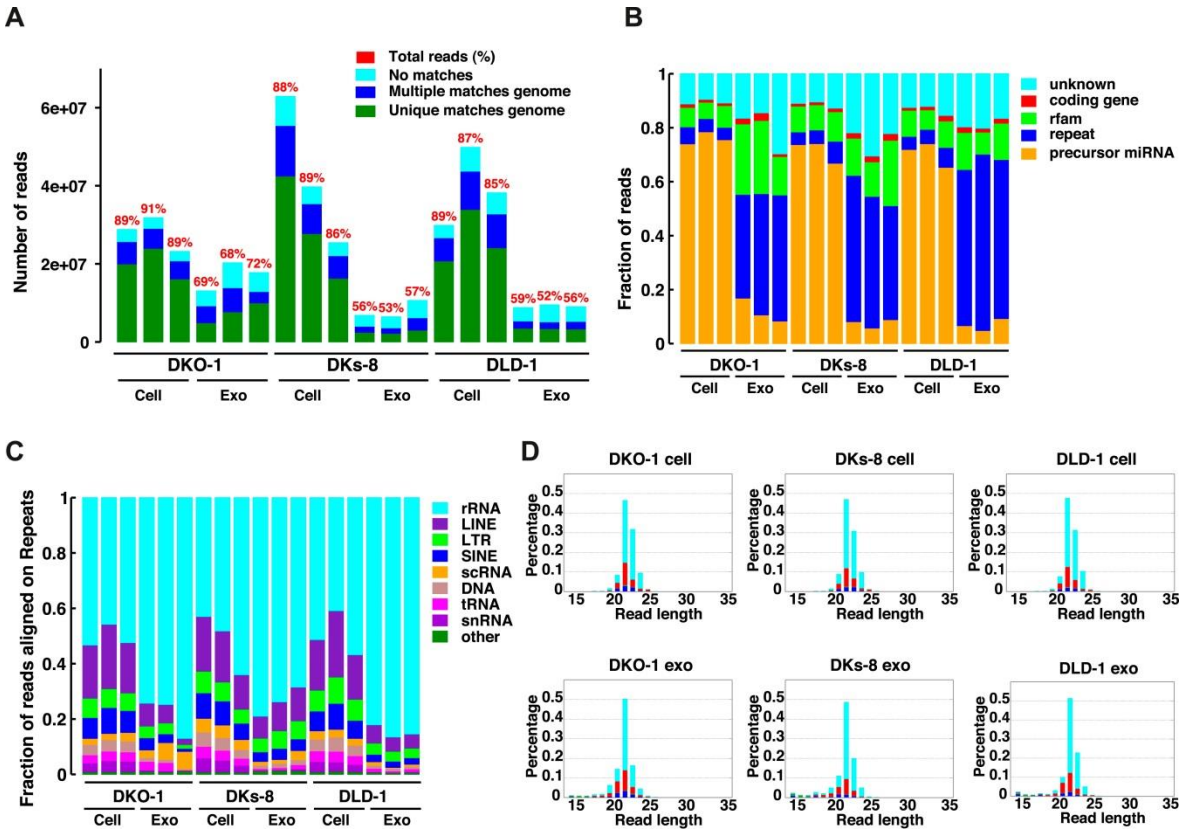

Figure 4. Small RNA sequencing analysis of cellular and exosomal RNAs from CRC cell lines. Shown are (**A**) total read numbers (y-axis) and the total percentage of mappable reads (red), percentage of unique mappable reads (green), reads that map to multiple genomic locations (dark blue), and those that could not be mapped (cyan). (**B**) The majority of mappable small RNA reads were derived from noncoding RNAs in cells and exosomes. In cells, the majority of small RNA reads mapped to microRNAs (miRNAs) (miRbase 19), whereas in exosomes, the majority of small RNA reads mapped to repetitive elements. (**C**) The origin of repetitive reads from exosomal small RNA sequencing is shown. Repeat reads were annotated based on RepeatMasker and Rfam classified into tRNAs, rRNAs, snRNAs, and others. (**D**) The length distribution of reads mapping to miRNA hairpins was determined for small RNA reads from the three CRC cell lines and their purified exosomes. Colors represent the nucleotides identified for the 5′ base, T (cyan), A (red), G (green), and C (blue)

The size distribution of cellular small RNA matched that expected from miRNA-derived reads (21-23 nucleotides). However, the small RNA read distribution from exosomes was much broader with many reads smaller than 22 nucleotides in length(A.1). Given that these reads map to RNAs other than known miRNAs, these data suggest that a large proportion of small exosomal RNA reads are derived from processing of other RNAs, in addition to post-transcriptionally modified miRNA reads that are apparently subject to editing, trimming, and/or tailing(Koppers-Lalic et al. 2014). Consistent with this, when read identity was restricted to miRNAs by mapping back to known miRNA hairpin sequences, the length distribution of mappable reads was nearly identical between cells and exosomes (Figure 4D).

miRNAs are differentially enriched in exosomes dependent on *KRAS* status

Focusing on mappable reads, we sought to ascertain whether miRNAs might be differentially represented when comparing cells to their secreted exosomes. For this, we quantified the relative abundance of individual miRNAs and made pairwise comparisons between normalized miRNA reads. Spearman correlation analyses demonstrated high correlation between replicates of individual cell lines (r=0.95-0.96) and between cellular datasets differing only in *KRAS* status (r=0.92-0.96) (A.2,A.3). In contrast, the miRNA profiles from exosomes compared to their parent cells were less correlated (DKO-1 r=0.67-0.81, DKs-8 r=0.64-0.71, DLD-1 r=0.64-0.69) (A.2, A.3).

We next utilized Principal Component (PC) analysis to determine whether the overall miRNA profiles could distinguish between cells and exosomes and/or between wild type and mutant *KRAS* status. The miRNA profiles from the three cell lines all clustered close to one another indicating that overall miRNA expression profiles are fairly similar among the different cell types (Figure 5). In marked contrast, Principal Component analysis revealed that exosomal miRNA profiles clearly segregate according to *KRAS* status (Figure 5). Relatively minor differences between cellular miRNA expression profiles become much more prominent when comparing exosomal miRNA patterns (A.3). This indicates that the presence of a mutant *KRAS* allele alters sorting of specific miRNAs to exosomes, a finding that has potentially important implications for biomarker development.

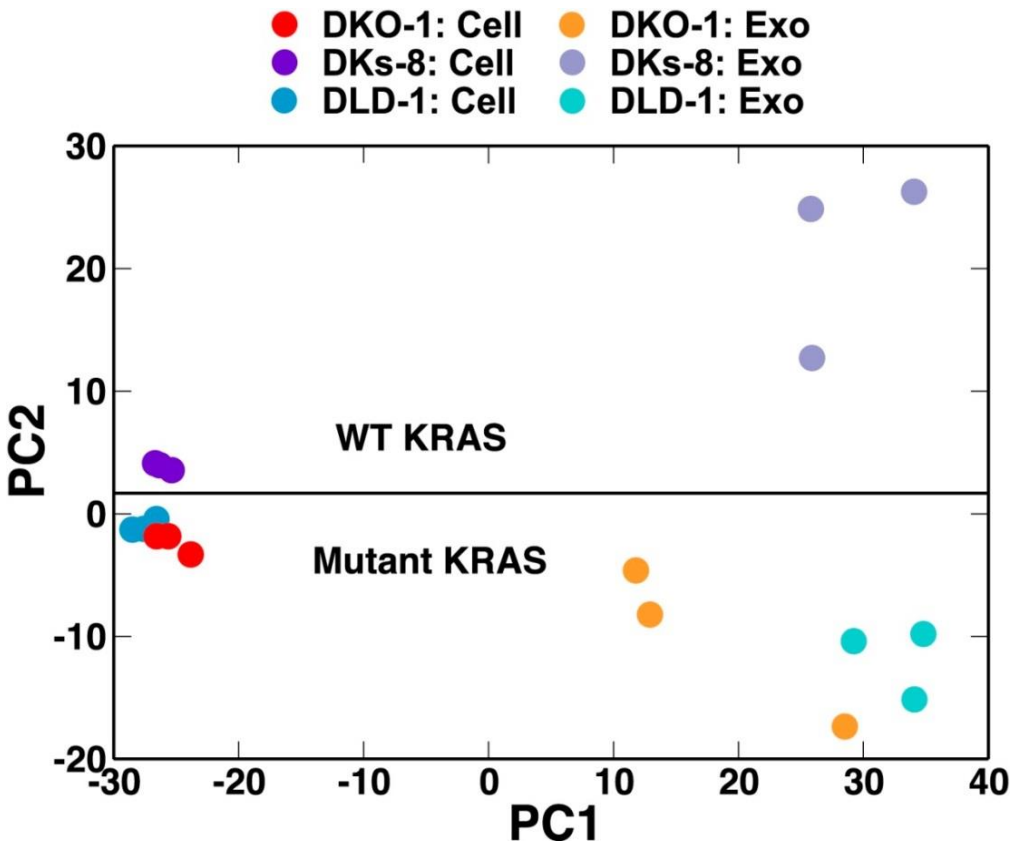

Figure 5. Small RNA composition segregates with KRAS status.
Principal component analysis was performed comparing small RNA sequencing data sets from CRC cells and exosomes. The small RNA composition from cells differed significantly from exosomes. Nevertheless, clustering showed that mutant *KRAS* status could be inferred from small RNA composition.

To gain more insight into the relative abundance of miRNAs in cells versus matched exosomes, we examined the most abundant miRNA species in the various sequencing libraries (determined by mean reads of individual miRNAs). For many miRNAs, exosomal abundance correlated with cellular abundance. However, calculation of fold-changes among the three isogenic *KRAS* cell lines, and exosomes released from these cells, showed that distinct subsets of miRNAs are enriched in either exosomes or cells (Tables 4,5). For all three cell lines, 25 miRNAs were consistently up-regulated in cells and 29 miRNAs were consistently up-regulated in exosomes (Figure 6A,B). Additionally, the diversity of miRNAs was substantially greater in mutant *KRAS* DKO-1 exosomes (94 unique miRNAs) compared to parental DLD-1 or wild type *KRAS* DKs-8 exosomes (Figure 6B). A select subset of cell and exosomally targeted miRNAs were validated separately by qRT/PCR (Figure 6C). Collectively, these data indicate that the miRNA profiles observed in exosomes are distinct from their parental cells with specific

miRNAs preferentially overrepresented or underrepresented in exosomes. We observed a mutant *KRAS*-specific pattern of secreted miRNAs, consistent with the hypothesis that dysregulation of miRNA metabolism is associated with tumorigenesis, a previously unrecognized feature of mutant *KRAS*.

***KRAS*-dependent sorting of miRNAs**

miR-100

Down regulation of *miR-100-5p* was observed in mutant *KRAS* DKO-1 and parental DLD-1 cells compared to wild type *KRAS* DKs-8 cells (Table 4). This is consistent with reports that have shown decreased *miR-100* expression in metastatic cancers(Petrelli et al. 2012; Gebeshuber and Martinez 2013). *miR-100* has also been shown to negatively regulate migration, invasion, and the epithelial-mesenchymal transition(D. Chen et al. 2014; M. Wang et al. 2014; Zhou et al. 2014). Interestingly, *miR-100* was enriched in exosomes derived from mutant *KRAS* cells (>8-fold and >3-fold enriched in DKO-1 and DLD-1 exosomes, respectively), suggesting that decrease of *miR-100* in cells is due to secretion in exosomes. This is in line with findings that circulating levels of *miR-100* are up-regulated in the plasma of mutant *KRAS*-expressing mouse pancreatic cancer models and in pancreatic cancer patients(LaConti et al. 2011). More broadly, the observation that *miR-100-5p* specifically accumulates in exosomes suggests there may be sequence-specific requirements for the sorting of certain miRNAs into exosomes.

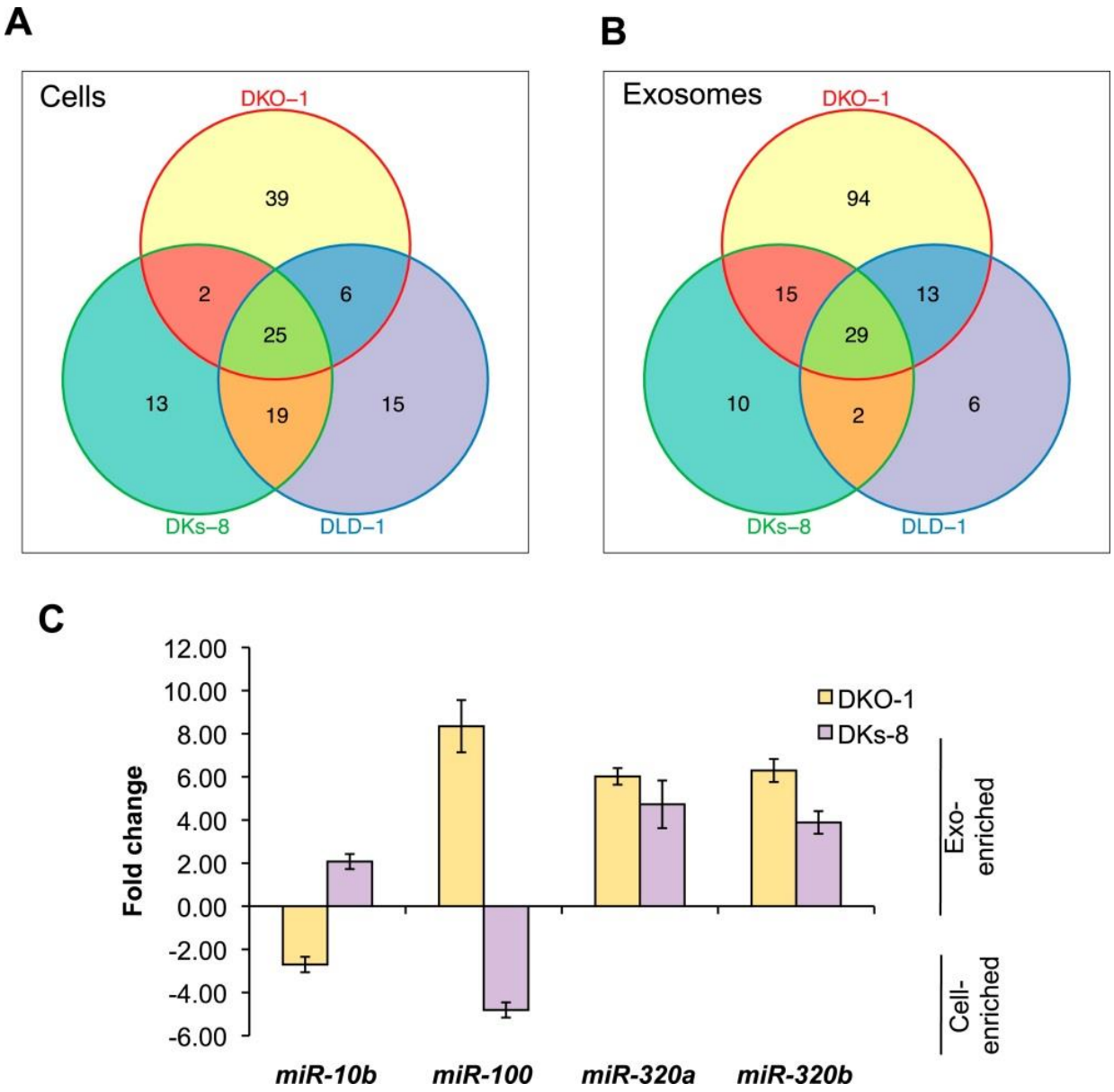

Figure 6. *KRAS*-dependent regulation of miRNAs in exosomes and cells.
Differentially distributed miRNAs in (**A**) cells and (**B**) exosomes from the three CRC cell lines differing in *KRAS* status. (**C**) qRT-PCR validation of selected miRs from DKs-8 and DKO-1 cellular and exosomal RNA samples normalized to U6 snRNA. Fold changes were calculated using the ΔΔC(t) method comparing exosomes to cells. Negative fold changes indicate greater enrichment in cells, and positive fold changes indicate greater enrichment in exosomes.

miR-10b

Our RNA sequencing data identified *miR-10b* as preferentially secreted in exosomes isolated from cells harboring a wild type *KRAS* allele (>3 fold-change and >2 fold-change enrichment in DKs-8 and DLD-1 exosomes, respectively), but retained in mutant *KRAS* DKO-1 cells (~3 fold-change cell enrichment). *miR-10b* is referred to as an oncomiR because it is frequently up-regulated during progression of various cancers, including CRC(Ma et al. 2010).

miR-320

miR-320 is aberrantly expressed in several types of cancer, including colon cancer. It is expressed in the proliferative compartment of normal colonic crypts(Schepeler et al. 2008; Hsieh et al. 2013). *miR-320* members (*miR-320b, -c, d, and -e*) were abundant in both mutant *KRAS* (DKO-1) and wild type *KRAS* (DKs-8) exosomes, but underrepresented in the matched cells, indicating that some miRNAs are transcribed and predominantly exported into exosomes, independent of *KRAS* status (Table 4). Of these family members, *miR-320a* and *-320b* were the most abundant species represented in exosomes by our RNA sequencing analyses (*miR-320a* in DKO-1 exosomes, and *miR-320b* in DKs-8 and DKO-1 exosomes). Interestingly, however, we observed the largest enrichment for *miR-320d* (fold-changes >241 in DKs-8 and >229 in DKO-1) in exosomes relative to cells, despite being ~4-fold less abundant than *miR-320b* levels. Because the 3'-terminus may be important in regulating miRNA stability and turnover, coupled to the fact that the sequences of *miR-320a-d* members differ only at their 3'-termini, enrichment of certain miRNAs in exosomes could be due to higher turnover/decay rates in cells.

Exosomal secretion and strand selection

Because we observed differential export of specific miRNAs, we investigated whether there might be miRNA sequence-specific sorting signals. Previous reports have shown differential accumulation of 5p or 3p strands in exosomes compared to parental cells(H. Ji et al. 2014). Thus, we analyzed our data sets to test whether exosomes might be preferentially enriched for one strand over the other. We were able to identify individual miRNAs where the two strands differentially sorted between cells and exosomes. For example, the -5p strands of *miR-423* were overrepresented in DKO-1 exosomes but in exosomes from DKs-8 cells, both strands were overrepresented compared to cells (data not shown). This indicates that *KRAS*

status may differentially affect selection of passenger or guide strands for sorting into exosomes for select individual miRNAs.

Individual miRNAs often exist as populations of variants (isomiRs) that differ in length and/or nucleotide composition generated by template- or non-template-directed variation(Burroughs et al. 2010; Newman, Mani, and Hammond 2011; Neilsen, Goodall, and Bracken 2012). When we analyzed our sequencing data sets, we did not detect differential accumulation of isomers with variable 5' termini (data not shown). For cellular miRNAs, most reads were full length with a slight enrichment in 3' non-template addition (NTA) of A-tailed miRNAs, regardless of *KRAS* status (Figure 7; A.6). For exosomes, we observed a slight enrichment for C residues added to the 3' ends of miRNAs from wild type *KRAS* cells. We did not observe this in mutant *KRAS* exosomes, where instead, we noticed an increase in 3' trimming of miRNAs (Figure 7, A.7). Overall, it remains to be determined whether such modifications constitute a global exosomal sorting signal in these cells.

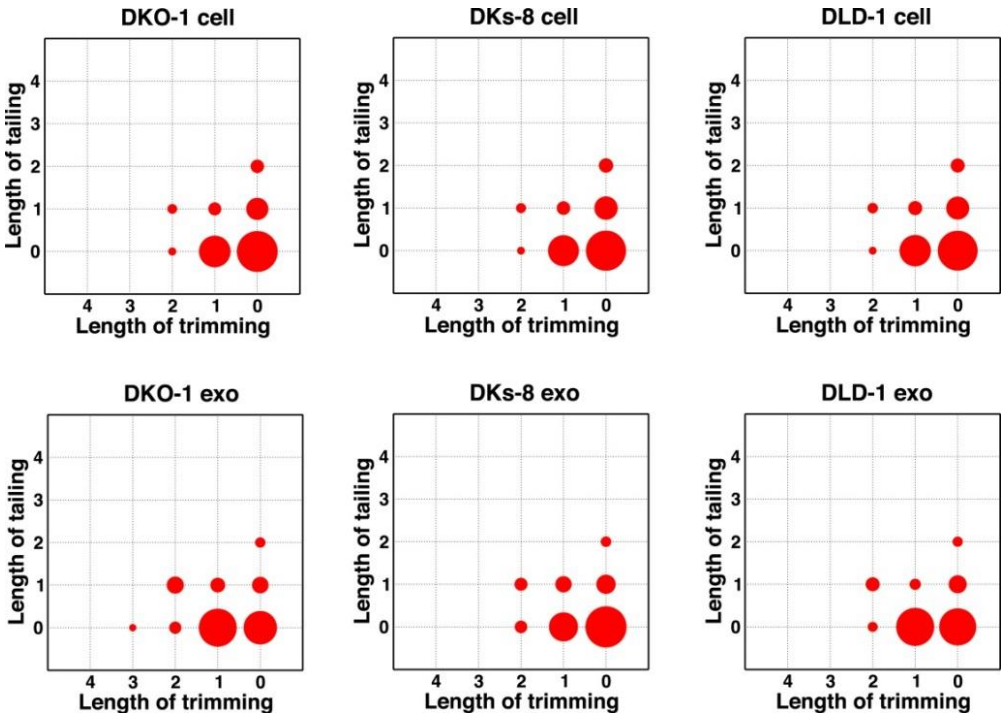

Figure 7. Comparison of miRNA 3′ trimming and tailing between cells and exosomes.
Overall changes in either 3′ nucleotide additions (tailing) or 3′ resection (trimming) compared to full length miRNA sequences (intact). Overall, the patterns between cells and between exosomes are very similar. A comparison of cells to exosomes shows that exosomes display a slight increase in trimmed miRNAs.

Consistent with published data, we have shown that miRNA expression patterns vary between parental cells and their cognate exosomes (Tables 4,5; Figure 6). Differential export suggests that specific signals must exist to sort distinct miRNAs(Batagov, Kuznetsov, and Kurochkin 2011; Villarroya-Beltri et al. 2013a). We therefore conducted MEME analysis to attempt to identify sequence motifs that might serve as targeting signals. When we examined all miRNA reads detected in exosomes, we did not find any global enrichment for specific sequences or motifs, including those reported to be bound by hnRNP A2B1 (GGAG or U/CC)(Bolukbasi et al. 2012; Villarroya-Beltri et al. 2013a) (A.8). However, when we analyzed *miR-320* because it is preferentially exported to exosomes independent of *KRAS* status, we were able to identify the GGAG sequence contained within the 3' end of the mature sequence. Additionally, upon restricting our analysis to reads from the most differentially expressed miRNAs when comparing exosomes to cells, we found a slight enrichment for C residues, possibly alternating C residues in exosomal miRNAs(A.8).

Sphingomyelinase-dependent sorting of miRNAs to exosomes

Although little is understood regarding the molecular mechanisms for packaging exosomal miRNAs, recent evidence suggests that the secretion of miRNAs in exosomes is dependent on ceramide via its production by neutral sphingomyelinase 2 (nSMase2)(Nobuyoshi Kosaka et al. 2010; Mittelbrunn et al. 2011). Inhibition of *de novo* ceramide synthesis by treatment with a neutral sphingomyelinase inhibitor impaired exosomal miRNA release, apparently due to decreased formation of miRNA-containing exosomes(Nobuyoshi Kosaka et al. 2010; Mittelbrunn et al. 2011). To test the role of neutral sphingomyelinase in miRNA secretion in our system, we treated CRC cells with the nSMase inhibitor, GW4869. We determined the effect of this inhibitor on *miR-10b* since it is preferentially found in wild type *KRAS* DKs-8 exosomes, *miR-100* since it is preferentially found in mutant *KRAS* DKO-1 and DLD-1 exosomes, and *miR-320* which sorts into exosomes regardless of *KRAS* status. For *miR-10b*, we did not observe significant changes in its cellular levels after treatment with GW4869 in either wild type *KRAS* DKs-8 or mutant *KRAS* DKO-1 cells (Figure 8C). In contrast, inhibition of neutral sphingomyelinase caused a ~3-fold increase in intracellular levels of *miR-100* in mutant *KRAS* DKO-1 cells but remained unchanged in wild type DKs-8 *KRAS* cells (Figure 8). Similarly, *miR-320* levels were found to increase (~2.5 fold) only in GW4869-treated mutant

KRAS DKO-1 cells (Figure 8C). These data are most consistent with the hypothesis that impaired ceramide synthesis alters cellular accumulation of miRNAs dependent on mutant *KRAS* and suggest that multiple biogenic routes exist for miRNA secretion.

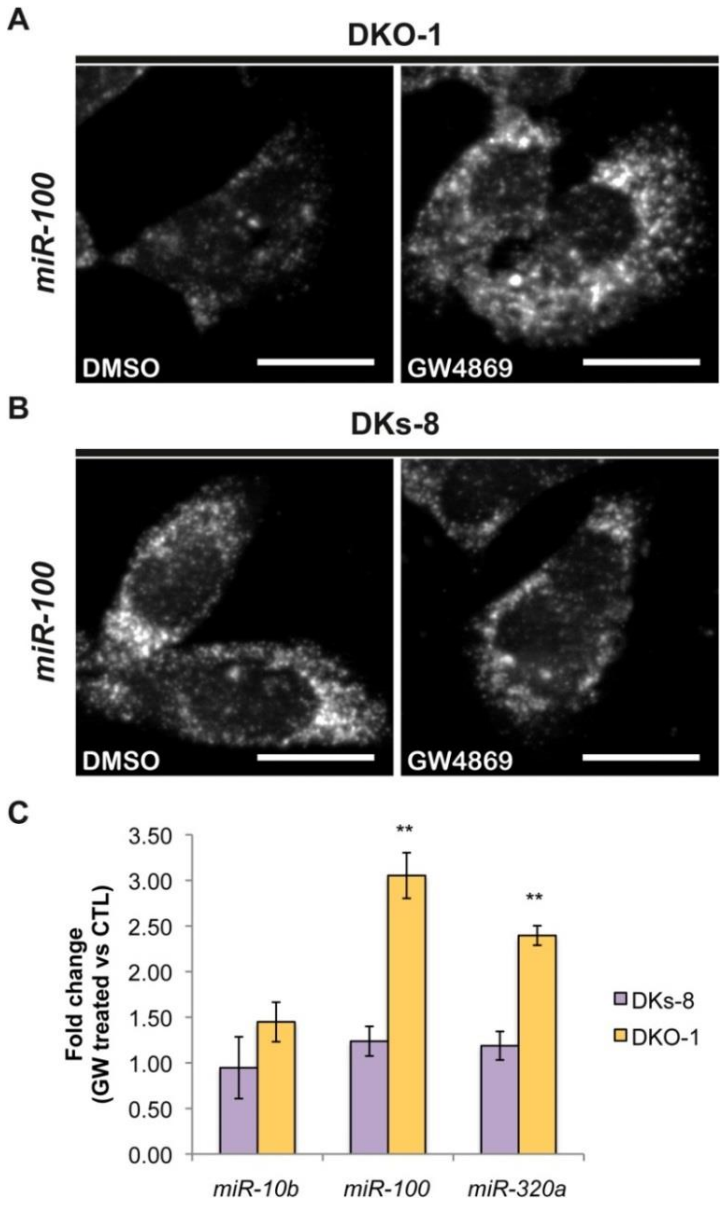

Figure 8. Ceramide-dependent miRNA export into exosomes.
DKO-1 or DKs-8 cells were treated with an inhibitor of neutral sphingomyelinase 2 (nSMase 2), GW4869. After treatment, in situ hybridization experiments were performed with probes against *miR-100* (**A**, **B**). (**C**) qRT-PCR for*miR-10b*, *miR-100*, and *miR-320a* was performed on cells treated with GW4869 or DMSO, and fold change in expression was determined in treated vs untreated cells. In wild-type *KRAS* cells (DKs-8), inhibition of nSMase 2 had little or no effect on the cellular levels of these miRNAs. In contrast, mutant *KRAS* cells (DKO-1) showed an increase in cellular miRNA levels after inhibition of nSMAse 2. Data were derived from three biological replicates and performed in technical triplicates for qRT-PCR. Significance was determined by two-tailed, paired t-tests where * are p values ≤ 0.05 and ** ≤0.01.

Extracellular transfer of *miR-100*

Several reports have found that extracellular miRNAs can be taken up by recipient cells to mediate heterotypic cell-cell interactions and facilitate target repression in neighboring cells(Mittelbrunn et al. 2011; Boelens et al. 2014; Squadrito et al. 2014). To determine whether secreted miRNAs function in recipient cells, we designed luciferase (Luc) constructs containing either 3 perfect *miR-100* recognition elements (MREs) in the 3' UTR (Luc-100-PT) or scrambled 3' UTR sequences that do not match any known miRNAs (Luc-CTL). These constructs were expressed in wild type *KRAS* DKs-8 cells (recipient cells) in the presence or absence of donor cells. Baseline repression of Luc in the absence of donor cells was first analyzed to determine the levels of repression from endogenous *miR-100* in DKs-8 cells. Compared to the scrambled control (Luc-CTL), strong Luc repression in the absence of donor cells was observed with perfect *miR-100* recognition elements (*miR-100*-PT) (Figure 9A). This supports our finding that *miR-100* is expressed and retained in DKs-8 cells.

To determine whether secretion of *miR-100* by mutant *KRAS* DKO-1 donor cells could further augment *miR-100* function in recipient wild type cells, Transwell co-culture experiments were performed with DKs-8 recipient cells expressing the luciferase reporters in the presence of DKO-1 donor cells (Figure 9). Significantly increased repression of Luc was observed when the reporter construct containing three perfect *miR-100* sites was used (*miR-100*-PT)(Figure 9A). Because exosomes released from DKO-1 cells contain abundant levels of *miR-100,* increased luciferase repression is consistent with transfer of additional copies of *miR-100.* Two control experiments were performed to test the hypothesis that additional copies of *miR-100* are transferred between donor and recipient cells. First, we treated donor cells with antagomirs that block production of *miR-100*. Luc repression was almost completely reversed upon pretreatment of DKO-1 donor cells with a *miR-100* hairpin antagomir inhibitor (AI-100) (Figure 9D). Second, we performed qRT/PCR to calculate the increase in *miR-100* levels in recipient cells. Cells grown in the presence or absence of donor cells showed an approximate 34% increase in the levels of *miR-100* (Figure 9E and A.9).

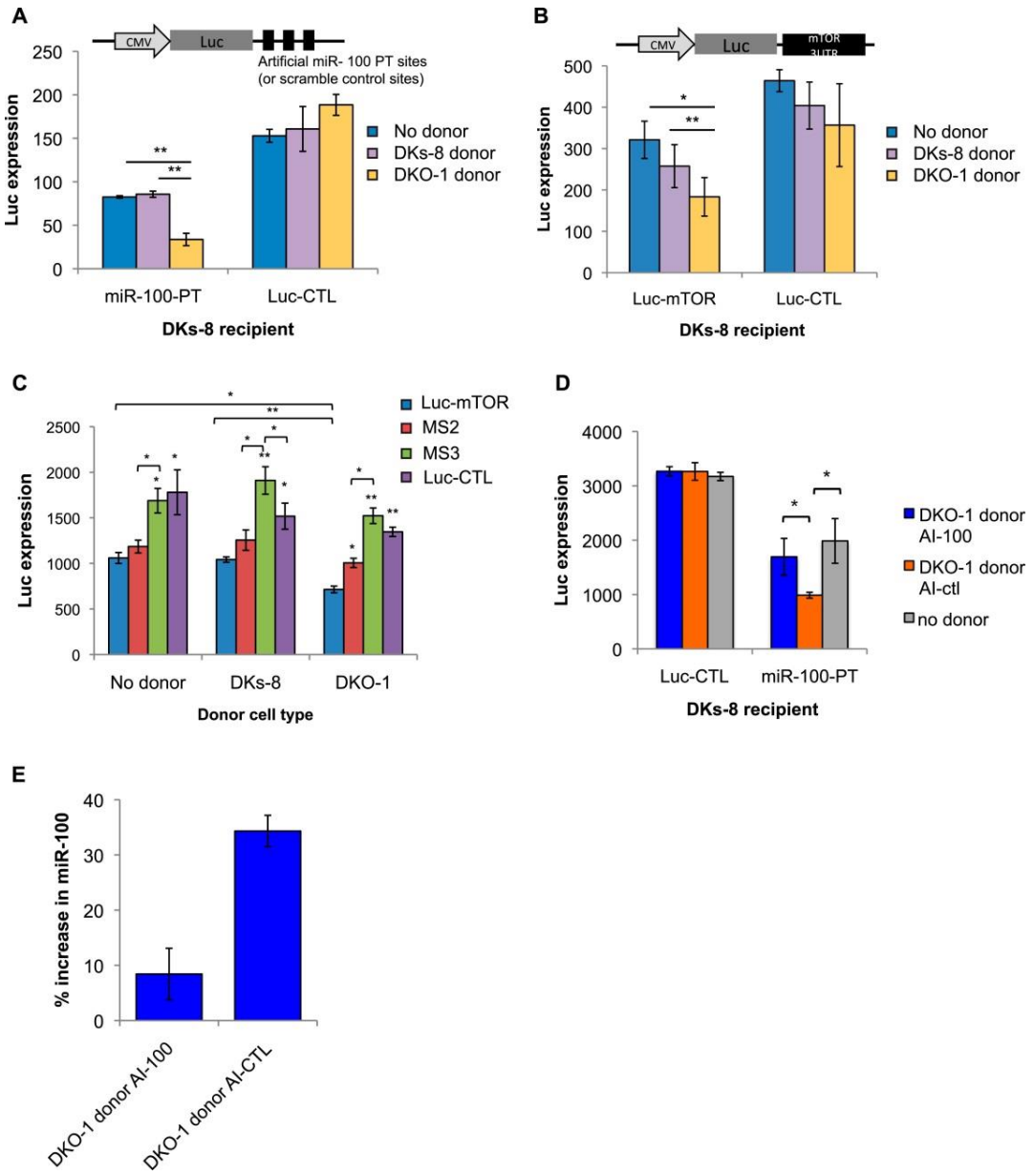

Figure 9. Transfer of extracellular miRNAs by mutant DKO-1 cells promotes target repression in wild-type DKs-8 cells. Transwell co-culture of DKs-8 recipient cells with or without DKs-8 or DKO-1 donor cells. Luciferase (Luc) expression was measured in DKs-8 recipient cells transiently expressing (**A**) Luc fused to three perfectly complementary synthetic*miR-100* target sites (*miR-100*-PT) or (**B**) Luc fused to the 3′UTR of mTOR, which harbors 3 endogenous target sites for *miR-100*. (**C**) Luc expression increased upon mutation of two (MS2) sites with full expression upon mutation of all three sites (MS3). Luc-CTL contains three random scrambled target sites that do not match any known miRNA sequence. (**D**) Luc expression was restored in recipient cells expressing *miR-100*-PT upon pretreatment of donor DKO-1 cells with 100 nM *miR-100* antagomirs (AI-100) compared to pre-treatment of donor DKO-1 cells with 100 nm control antagomirs (AI-CTL) targeting *cel-miR-67*. (**E**) Taqman qRT-PCR for *miR-100*. Compared to DKs-8 recipient cells grown without donor cells, *mir-100* levels increased by approximately 34% in the presence of mutant DKO-1 donor cells pre-treated with AI-CTL compared to an 8% increase in AI-100 pre-treated donor cells. Y axis is % increase in *miR-100*= $(CP_{AI\text{-}CTL}$ or $CP_{AI\text{-}100} - CP_{no\ donor}/CP_{no\ donor})^{*}100$, where CP = absolute copy number. All Luc values were normalized to co-transfected vectors expressing β-galactosidase; n = 3 independent experiments in **A**–**C**and n = 4 in **D**, **E**. All Luc assays were performed in technical triplicate. Significance was determined by two-tailed, paired t-tests where * are p values ≤ 0.05 and ** ≤0.01.

To further probe the repressive activity of *miR-100*, we performed co-culture experiments in which the recipient Dks-8 cells express Luc fused to the 3'UTR of mTOR, an endogenous *miR-100* targe(Nagaraja et al. 2010; Grundmann et al. 2011; Ge et al. 2014). As observed with *miR-100*-PT repression, Luc-mTOR was significantly repressed in the presence of mutant *KRAS* DKO-1, but not in the presence of wild type *KRAS* DKs-8 donor cells (Figure 9B). This suggests that *miR-100* repressive activity is specific to the presence of mutant *KRAS* DKO-1 donor cells. To confirm these results, we mutated the *miR-100* recognition elements within the mTOR 3'UTR and assayed for *miR-100* activity (A.10). Mutation of individual sites did not show significantly different Luc repression (data not shown). However, upon mutation of two MREs (MS2), we observed a partial rescue of Luc expression (Figure 9C). This was further augmented upon mutation of all three sites (MS3), with a complete rescue of *miR-100*-mediated repressive activity (Figure 9C).

As a final test of miRNA transfer in the Transwell co-culture experiments, we created vectors expressing Luc fused to a 3' UTR containing perfect sites for *miR-222* because *miR-222* is not detectable in DKs-8 recipient cells, unlike *miR-100*. In this case, silencing of Luc should be due to transfer of *miR-222* and not due to unforeseen changes in endogenous miRNA activity. We observed a greater than 2-fold repression of the *miR-222* Luc reporter in recipient cells (A.11). These results support the hypothesis that miRNAs secreted by mutant *KRAS* cells can be transferred to recipient cells.

2.4 Discussion

In this study, we comprehensively examined the composition of small ncRNAs from exosomes and cells of isogenic CRC cell lines that differ only in *KRAS* status. By employing small RNA transcriptome analyses, we found that oncogenic *KRAS* selectively alters the miRNA profile in exosomes and that ceramide depletion selectively promotes miRNA accumulation in mutant *KRAS* CRC cells. Distinct miRNA profiles between cells and their exosomes may be functionally coupled to mitogenic signaling.

KRAS status-specific patterns of secreted miRNAs supports the idea of using exosomes as potential biomarkers in CRC. Our finding that *miR-10b* is preferentially enriched in wild type

KRAS-derived exosomes while *miR-100* is enriched in mutant *KRAS*-derived exosomes raises interesting questions regarding how they are selected for secretion. *miR-10b* and *miR-100* are both part of the *miR-10/100* family and differ by only one base in the seed region, allowing regulation of distinct sets of target mRNAs (Tehler, Høyland-Kroghsbo, and Lund 2011). Whether the accumulation or export of these miRNAs is a result or a consequence of oncogenic signaling remains unknown. Preventing the export or retention of certain miRNAs, such as *miR-100 and miR-10b,* may serve a therapeutic role in reversing the tumorigenic effects seen with aberrant miRNA expression.

KRAS-dependent differential miRNA expression more prominently affected miRNA expression patterns observed in exosomes than in the parent cells. This could reflect a mechanism by cells to selectively export miRNAs so as to maintain specific growth or gene expression states. This is consistent with a recent report that found that the cellular levels of *miR-218-5p* could be maintained, despite changes in the abundance of its target, likely through a "miRNA relocation effect" where unbound miRNAs that are in excess have the potential to be sorted to exosomes(Squadrito et al. 2014). Another mechanism may be through sequence-specific motifs that direct miRNA trafficking by interaction with specific chaperone proteins(Bolukbasi et al. 2012; Villarroya-Beltri et al. 2013a). Although we did not find any globally significant motif overrepresented in exosomal miRNAs, we cannot rule out that individual miRNAs might undergo sequence-specific export. *miR-320* family members all contain the GGAG motif that has been proposed to serve as an exosomal targeting signal(Villarroya-Beltri et al. 2013a). We found that members of the *miR-320* family are preferentially enriched in exosomes independent of *KRAS* status; however, the GGAG sequence was not found in other miRNAs that are targeted to exosomes. It has been reported that the biogenesis of *miR-320* family members occurs by a non-canonical pathway that requires neither Drosha(Chong et al. 2010) nor XPO5(Xie et al. 2013). Instead, the 5' ends contain a 7-methyl guanosine cap that facilitates nuclear-cytoplasmic transport through XPO1(Xie et al. 2013). XPO1 is present in DKO-1, DKs-8 and DLD-1 exosomes as detected by mass spectrometry(Demory Beckler et al. 2012). It will be interesting to investigate whether alternate processing pathways and associated biogenic machinery contribute to the heterogeneity of extracellular vesicle cargo and affect miRNA secretion.

It was recently demonstrated that miRNAs in B-cell exosomes display enriched levels of nontemplate-directed 3'-uridylated miRNAs, while 3'-adenylated miRNA species are preferentially cell-enriched(Koppers-Lalic et al. 2014). In certain contexts, the addition of nontemplated uridine residues to cognate miRNAs accelerates miRNA turnover(Baccarini et al. 2011; Wei et al. 2012). Thus, it is possible that the stability/half-life of a miRNA affects whether it is retained or secreted. While the exact functional significance of 3'-end modifications of miRNAs detected in both cells and exosomes remains to be determined, it could be that differential export of "tagged" miRNAs could allow cells to export specific miRNAs. However, the lack of any apparent motif upon global analysis of miRNAs enriched in exosomes, coupled to the finding that even untagged miRNAs are differentially exported, suggests multiple strategies for loading of miRNAs into extracellular vesicles, and that not all extracellular vesicles and exosomes contain identical cargo. This further implies that different cell types secrete a heterogeneous population of vesicles. Although the biological relevance of these findings remain to be determined, the specific sorting of miRNAs into exosomes may enable cancer cells to discard tumor suppressive miRNAs so as to increase their oncogenic potential, or perhaps modulate gene expression in neighboring and distant cells to promote tumorigenesis. In support of this hypothesis, *miR-100*, which we found to be enriched in mutant *KRAS* exosomes, was found to down-regulate LGR5 in colorectal cancer cells and thereby inhibit migration and invasion of such cells(Zhou et al. 2014). In this context, removal of *miR-100* from the cell would be a tumor-promoting event.

In other contexts, *miR-100* can have contradictory activities, both inducing EMT by down-regulating E-cadherin through targeting SMARCA5, and inhibiting tumorigenicity by targeting HOXA1(D. Chen et al. 2014). Thus, although *miR-100* can function as a tumor suppressor under normal conditions, augmenting its levels, for example by extracellular vesicle uptake, could potentially promote EMT. In this regard, the role of *miR-100* in tumorigenesis would be two-fold, where its secretion in exosomes could function to maintain low intracellular levels within mutant cells, while inducing EMT in wild-type recipient cells. Along these lines, *miR-100* is part of the *miR-125b/let-7a-2/miR-100* cluster that is transcribed and expressed coordinately (Emmrich et al. 2014).Interestingly, in malignant colonic tissues from individuals with CRC, *miR-100* levels were significantly decreased while *let-7a* levels were strongly upregulated(Tarasov et al. 2014). Based on our finding that there is differential accumulation of

individual miRNAs within this cluster between mutant *KRAS* cells and exosomes, it will be interesting to determine whether cancer cells down-regulate specific miRNAs by active secretion, while simultaneously maintaining the levels of other miRNAs transcribed within the same cluster.

miRNAs are secreted from malignant breast epithelial cells after packaging into vesicles larger than conventional exosomes that are enriched in CD44, whose expression is linked to breast cancer metastasis(Palma et al. 2012). Normal cells tend to release miRNAs in more homogenous types of exosomes, suggesting that malignant transformation may alter the formation of secreted vesicles that could alter miRNA export and lead to differences in exosome content and morphology(Palma et al. 2012; Melo et al. 2014). In support of this, it was recently shown that in exosomes from breast cancer cells, CD43 mediates the accumulation of Dicer(Melo et al. 2014). These exosomes also contain other RISC proteins and pre-miRNAs, indicating that miRNA processing can occur in exosomes. These components were absent in exosomes derived from normal cells. It remains to be determined whether components of the RISC loading complex assemble within endosomes before their secretion as exosomes, or by the fusion of exosomes containing heterogeneous cargo after they are secreted. The observation that cells can selectively release miRNAs and also release a heterogeneous population of vesicles raises the possibility that differential release of miRNAs is associated with different classes of exosomes and microvesicles.

Recently, quantitative analysis of secreted miRNAs suggested that the levels of extracellular miRNAs are limited and raise the question as to how such levels can alter gene expression in recipient cells(Chevillet et al. 2014). The results of our Transwell co-culture experiments are most consistent with extracellular transfer of specific miRNAs to alter expression of reporter constructs. Nevertheless, the level of exosomal transfer that is needed to alter recipient cell gene expression *in vivo* remains an open question. Our finding that mutant *KRAS* protein can be functionally transferred in exosomes indicates that the full effect of exosomes on recipient cells can be due to a combination of both RNA delivery and protein-based signaling(Higginbotham et al. 2011a). This could include activation of Toll-like receptors with possible downstream effects following NFKB or MAPK cascades(Fabbri et al. 2012; X. Chen et al. 2013). The complexity of *miR-100* function in the tumor microenvironment underscores this argument by its potential for inhibiting mTOR expression which is required for proliferation of

Apc-deficient tumors in mouse models(Faller et al. 2015). In tumors where some cells have incurred activating mutations in *KRAS*, while others have not, *miR-100* could accumulate in wild-type *KRAS* tumor cells through exosomal transfer, inhibiting mTOR and cell growth. Conversely *miR-100* could be secreted from mutant *KRAS* cells giving them a growth advantage. In this way exosomal transfer of miRNAs might act to select for cells carrying specific tumor driver mutations. Our studies have direct implications for CRC and, together with other studies, indicate that delivery of exosomes to recipient cells can induce cell migration, inflammation, immune responses, angiogenesis, invasion, pre-metastatic niche formation, and metastasis(Kahlert and Kalluri 2013; Boelens et al. 2014; Melo et al. 2014).

Table 4. miRNAs enriched in cell*

DKO-1			
hsa-miR-548u	hsa-miR-16-1-3p	hsa-miR-33a-3p	hsa-miR-33a-5p
hsa-miR-31-5p	hsa-miR-181b-3p	hsa-miR-450a-5p	hsa-miR-424-5p
hsa-miR-9-5p	hsa-miR-219-5p	hsa-miR-190a	hsa-miR-573
hsa-miR-30d-3p	hsa-miR-204-5p	hsa-miR-1226-3p	hsa-miR-499a-5p
hsa-miR-450b-5p	hsa-miR-499b-3p	hsa-miR-3662	hsa-miR-20a-3p
hsa-miR-27b-5p	hsa-miR-5701	hsa-miR-4677-3p	hsa-let-7i-5p
hsa-miR-331-3p	hsa-miR-31-3p	hsa-miR-651	hsa-miR-1306-5p
hsa-miR-147b	hsa-miR-3611	hsa-miR-1305	hsa-miR-148a-3p
hsa-miR-27b-3p	hsa-miR-1306-3p	hsa-miR-374b-3p	hsa-miR-1260b
hsa-miR-3940-3p	hsa-miR-200c-5p	hsa-miR-548ar-3p	
DKs-8			
hsa-miR-132-5p	hsa-miR-484	hsa-miR-374a-5p	hsa-miR-1180
hsa-miR-1307-3p	hsa-miR-200a-5p	hsa-miR-548o-3p	hsa-miR-149-5p
hsa-miR-3615	hsa-miR-100-5p	hsa-miR-197-3p	hsa-miR-378a-5p
hsa-let-7a-3p			
DLD-1			
hsa-miR-141-3p	hsa-miR-26b-5p	hsa-miR-24-3p	hsa-miR-3074-5p
hsa-miR-15a-5p	hsa-miR-27a-3p	hsa-miR-3613-5p	hsa-miR-30b-5p
hsa-miR-29a-3p	hsa-miR-301a-5p	hsa-let-7i-3p	hsa-miR-185-5p
hsa-let-7g-5p	hsa-miR-23b-3p	hsa-miR-22-3p	
DKO-1 & DKs-8			
hsa-miR-141-5p	hsa-miR-582-5p		
DKO-1 & DLD-1			
hsa-miR-556-3p	hsa-miR-374a-3p	hsa-miR-106b-5p	hsa-miR-17-3p
hsa-miR-24-1-5p	hsa-miR-340-3p		
DLD-1 & DKs-8			
hsa-miR-24-2-5p	hsa-miR-106a-5p	hsa-miR-30e-5p	hsa-miR-107
hsa-miR-429	hsa-miR-98-5p	hsa-miR-425-5p	hsa-miR-140-5p
hsa-miR-93-5p	hsa-miR-210	hsa-miR-126-3p	hsa-miR-194-5p
hsa-miR-29b-3p	hsa-miR-15b-5p	hsa-miR-362-5p	hsa-miR-27a-5p
hsa-miR-454-3p	hsa-miR-452-5p	hsa-miR-196b-5p	
DKO-1, DLD-1 & DKs-8			
hsa-miR-32-5p	hsa-miR-582-3p	hsa-miR-542-3p	hsa-miR-96-5p
hsa-miR-101-3p	hsa-miR-18a-5p	hsa-miR-3529-3p	hsa-miR-7-5p
hsa-miR-19a-3p	hsa-miR-142-3p	hsa-miR-20a-5p	hsa-miR-32-3p
hsa-miR-130b-5p	hsa-miR-1278	hsa-miR-7-1-3p	hsa-miR-590-3p
hsa-miR-4473	hsa-miR-17-5p	hsa-miR-103a-3p	hsa-miR-103b
hsa-miR-19b-3p	hsa-miR-340-5p	hsa-miR-200a-3p	hsa-miR-34a-5p
hsa-miR-372			

*miRNAs differentially enriched in cells when comparing mean reads in exosomes versus cell.

Table 5. miRNAs enriched in exosomes *

DKO-1			
hsa-miR-139-5p	hsa-miR-3178	hsa-miR-151b	hsa-miR-125b-1-3p
hsa-miR-193b-3p	hsa-miR-935	hsa-miR-130b-3p	hsa-miR-628-3p
hsa-miR-139-3p	hsa-let-7d-3p	hsa-miR-589-3p	hsa-miR-4532
hsa-miR-451a	hsa-miR-6087	hsa-miR-151a-5p	hsa-miR-940
hsa-miR-222-3p	hsa-miR-766-5p	hsa-miR-505-5p	hsa-miR-3187-3p
hsa-miR-125a-3p	hsa-miR-3679-5p	hsa-miR-4436b-3p	hsa-miR-4787-3p
hsa-miR-2277-3p	hsa-miR-361-5p	hsa-miR-1293	hsa-miR-3183
hsa-miR-3162-5p	hsa-miR-642a-3p	hsa-miR-642b-5p	hsa-miR-197-5p
hsa-miR-324-3p	hsa-miR-145-3p	hsa-miR-3182	hsa-miR-3127-3p
hsa-miR-3127-5p	hsa-miR-4728-3p	hsa-miR-3184-5p	hsa-miR-125b-5p
hsa-miR-186-5p	hsa-miR-1	hsa-miR-100-5p	hsa-miR-423-3p
hsa-miR-766-3p	hsa-miR-4753-5p	hsa-miR-145-5p	hsa-miR-4724-5p
hsa-miR-373-3p	hsa-miR-223-5p	hsa-miR-1307-5p	hsa-miR-1914-3p
hsa-miR-3121-3p	hsa-miR-3613-3p	hsa-miR-205-5p	hsa-miR-98-3p
hsa-miR-23a-3p	hsa-miR-3124-5p	hsa-miR-3656	hsa-miR-3918
hsa-miR-4449	hsa-miR-378c	hsa-miR-3138	hsa-miR-1910
hsa-miR-3174	hsa-miR-4466	hsa-miR-3679-3p	hsa-miR-3200-5p
hsa-miR-6511b-5p	hsa-miR-1247-5p	hsa-miR-22-3p	hsa-miR-877-5p
hsa-miR-4687-3p	hsa-miR-1292-5p	hsa-miR-181c-5p	hsa-miR-6131
hsa-miR-6513-5p	hsa-miR-3661	hsa-miR-132-3p	hsa-miR-214-3p
hsa-miR-574-3p	hsa-miR-3190-3p	hsa-miR-326	hsa-miR-3191-5p
hsa-miR-3198	hsa-miR-3928	hsa-miR-629-3p	hsa-miR-4489
hsa-miR-4700-5p	hsa-miR-5006-5p	hsa-miR-5088	hsa-miR-2110
hsa-miR-3911	hsa-miR-3146		
DKs-8			
hsa-miR-1224-5p	hsa-let-7b-5p	hsa-miR-155-5p	hsa-let-7c
hsa-let-7a-5p	hsa-miR-146b-5p	hsa-miR-4647	hsa-miR-4494
hsa-miR-711	hsa-miR-1263		
DLD-1			
hsa-miR-1226-5p	hsa-miR-4745-5p	hsa-miR-4435	hsa-miR-939-5p
hsa-miR-409-3p	hsa-miR-1304-3p		
DKO-1 & DKs-8			
hsa-miR-146a-5p	hsa-miR-4508	hsa-miR-224-5p	hsa-miR-4429
hsa-miR-222-5p	hsa-miR-629-5p	hsa-miR-4492	hsa-miR-3653
hsa-miR-320a	hsa-miR-1290	hsa-miR-1262	hsa-miR-5010-5p
hsa-miR-204-3p	hsa-miR-4461	hsa-miR-5187-5p	
DKO-1 & DLD-1			
hsa-miR-483-5p	hsa-miR-4658	hsa-miR-4758-5p	hsa-miR-492
hsa-miR-5001-5p	hsa-miR-371a-5p	hsa-miR-1323	hsa-miR-371b-3p
hsa-miR-501-3p	hsa-miR-4446-3p	hsa-miR-6511a-5p	hsa-miR-30a-3p
hsa-miR-4727-3p			

DLD-1 & DKs-8			
hsa-miR-28-3p	hsa-miR-3934-5p		
DKO-1, DLD-1 & DKs-8			
hsa-miR-658	hsa-miR-320d	hsa-miR-4792	hsa-miR-1246
hsa-miR-320e	hsa-miR-4516	hsa-miR-320b	hsa-miR-4488
hsa-miR-1291	hsa-miR-320c	hsa-miR-4634	hsa-miR-3605-5p
hsa-miR-4741	hsa-miR-3591-3p	hsa-miR-122-5p	hsa-miR-486-3p
hsa-miR-184	hsa-miR-223-3p	hsa-miR-3651	hsa-miR-486-5p
hsa-miR-3180	hsa-miR-3180-3p	hsa-miR-3168	hsa-miR-4497
hsa-miR-423-5p	hsa-miR-3184-3p	hsa-miR-150-5p	hsa-miR-664a-5p
hsa-miR-182-5p			

*miRNAs differentially enriched in exosomes when comparing mean reads in exosomes versus cell.

2.5 Methods

Exosome isolation

Exosomes were isolated from conditioned medium of DKO-1, Dks-8, and DLD-1 cells as previously described, with slight modification[15]. Briefly, cells were cultured in DMEM supplemented with 10% bovine growth serum until 80% confluent. The cells were then washed 3 times with PBS and cultured for 24 hr in serum-free medium. The medium was collected and replaced with ionomycin-containing medium for 1 hr, after which ionomycin-containing medium was collected and pooled with the previously collected serum-free medium. Pooled media was centrifuged for 10 min at 300 X *g* to remove cellular debris, and the resulting supernatant was then filtered through a 0.22-mm polyethersulfone filter (Nalgene, Rochester, NY, USA) to reduce microparticle contamination. The filtrate was concentrated ~300-fold with a 100,000 molecular-weight cutoff centrifugal concentrator (Millipore, Darmstadt, Germany). The concentrate was then subjected to high-speed centrifugation at 150,000 X *g* for 2 hr. The resulting exosome-enriched pellet was resuspended in PBS containing 25 mM HEPES (pH 7.2) and washed by centrifuging again at 150,000 X *g* for 3 hr. The wash steps were repeated a minimum of 3 times until no trace of phenol-red was detected. The resulting pellet was resuspended in PBS containing 25 mM HEPES (pH 7.2) and protein concentrations were determined with a MicroBCA kit (Pierce/Thermo, Rockford, IL, USA). The number of exosomes per µg of protein was determined by means of nanoparticle tracking analysis (NanoSight, Wiltshire, UK). Analysis was performed on three independent preparations of exosomes.

RNA purification

Total RNA from exosomes and cells was isolated using TRIzol (Life Technologies/Thermo). In the case of exosomal RNA isolation TRIzol was incubated with 100 ul or less of concentrated exosomes for an extended 15 min incubation prior to chloroform extraction. RNA pellets were resuspended in 60 µl of RNase-free water and were then re-purified using the miRNeasy kit (Qiagen Inc., Valencia, CA, USA). Final RNAs were eluted with two rounds of 30 ul water extraction.

miRNA library preparation and sequencing

Total RNA from each sample was used for small RNA library preparation using NEBNext Small RNA Library Prep Set from Illumina (New England BioLabs Inc., Ipswich, MA, USA). Briefly, 3` adapters were ligated to total input RNA followed by hybridization of multiplex SR RT primers and ligation of multiplex 5' SR adapters. Reverse transcription (RT) was performed using ProtoScript II RT for 1 hr at 50°C. Immediately after RT reactions, PCR amplification was performed for 15 cycles using LongAmp Taq 2X master mix. Illumina-indexed primers were added to uniquely barcode each sample. Post-PCR material was purified using QIAquick PCR purification kits (Qiagen Inc.). Post-PCR yield and concentration of the prepared libraries were assessed using Qubit 2.0 Fluorometer (Invitrogen, Carlsbad, California, CA, USA) and DNA 1000 chip on Agilent 2100 Bioanalyzer (Applied Biosystems, Carlsbad, CA, USA), respectively. Size selection of small RNA with a target size range of approximately 146-148 bp was performed using 3% dye free agarose gel cassettes on a Pippin Prep instrument (Sage Science Inc., Beverly, MA, USA). Post-size selection yield and concentration of libraries were assessed using Qubit 2.0 Fluorometer and DNA high sensitivity chip on an Agilent 2100 Bioanalyzer, respectively. Accurate quantification for sequencing applications was performed using qPCR-based KAPA Biosystems Library Quantification kits (Kapa Biosystems, Inc., Woburn, MA, USA). Each library was diluted to a final concentration of 1.25 nM and pooled in equimolar ratios prior to clustering. Cluster generation was carried out on a cBot v8.0 using Illumina's Truseq Single Read (SR) Cluster Kit v3.0. Single End (SE) sequencing was performed to generate at least 15 million reads per sample on an Illumina HiSeq2000 using a 50-cycleTruSeq SBSHSv3 reagent kit. Clustered flow cells were sequenced for 56 cycles, consisting of a 50-cycle read, followed by a 6-cycle index read. Image analysis and base calling was performed using the standard Illumina pipeline consisting of Real Time Analysis (RTA) version v1.17 and demultiplexed using bcl2fastq converter with default settings.

Mapping of RNA reads

Read sequence quality checks were performed by FastQC (Babraham Bioinformatics (http://www.bioinformatics.babraham.ac.uk/projects/fastqc/). Adapters from the 3' ends of reads were trimmed using Cutadpt with a maximum allowed error rate of 0.1. Reads shorter than 15 nucleotides in length were excluded from further analysis. Reads were mapped to the human

genome hg19 using Bowtie version 1.1.1. Mapped reads were annotated using ncPRO-seq based on miRbase, Rfam and RepeatMasker (http://www.repeatmasker.org/) and expression levels were quantified based on read counts. Mature miRNA annotation was extended 2 bp in both upstream and downstream regions to accommodate inaccurate processing of precursor miRNAs. Reads with multiple mapping locations were weighted by the number of mapping locations.

Principal Component analysis

DESeq Version 1.16.0 was used to perform Principal Component analyses.

Enrichment analysis

Differential expression was analyzed using DESeq Version 1.16.0. Negative binomial distribution was used to compare miRNA abundance between cells versus exosomes and wild type versus mutant *KRAS* status. The trimmed mean of M values (TMM) method was used for normalization. Differential expression was determined based on log2 fold change (log2 fold change) and False Discovery Rate (FDR) with |log2 Fold Change| >= 1 and FDR <= 0.001.

Trimming and tailing

Trimming and tailing analysis was based on miRBase annotation. Only high confidence miRNAs (544) and corresponding hairpin sequences were used. Bowtie version 1.1.1 with 0 mismatch was used for mapping. miRNA reads were first mapped to hairpin sequences with unmapped reads then mapped to the human genome hg19. Remaining reads were trimmed 1 bp form the 3' end and remapped to hairpin sequences. The remapping process was repeated 10 times. Finally, all mapped reads were collected for further analysis.

qRT/PCR

Taqman small RNA assays (Life Technologies) (individual assay numbers are listed below) were performed for indicated miRNAs on cellular and exosomal RNA samples. Briefly, 10 ng of total RNA was used per individual RT reactions; 0.67 µl of the resultant cDNA was used in 10 µl qPCR reactions. qPCR reactions were conducted in 96-well plates on a Bio-Rad CFX96 instrument. All C(t) values were ≤ 30. Triplicate C(t) values were averaged and normalized to U6 snRNA. Fold-changes were calculated using the ΔΔC(t) method, where: $\Delta=C(t)_{miRNA}-C(t)_{U6}$

$_{snRNA}$, and $\Delta\Delta C(t) = \Delta C(t)_{exo} - \Delta C(t)_{cell}$, and $FC = 2^{-\Delta\Delta C(t)}$. Analysis was performed on three independent cell and exosomal RNA samples. Taqman probe #: U6 snRNA: 001973; *hsa-let-7a-5p*: 000377; *hsa-miR-100-5p*: 000437; *hsa-miR-320b*: 002844; hsa-miR-320a: 002277.

Generation of miRNA standard curves

RNase-free, HPLC-purified 5'-phosphorylated miRNA oligoribonucleotides were synthesized (Integrated DNA Technologies) for human *miR-100-5p* (5'-phospho-AACCCGUAGAUCCGAACUUGUG-OH-3') and *cel-miR-39-3p* (5'-phospho-UCACCGGGUGUAAAUCAGCUUG-OH-3'). Stock solutions of 10μM synthetic oligonucleotide in RNase-free and DNase-free water were prepared according to the concentrations and sample purity quoted by the manufacturer (based on spectrophotometry analysis). Nine 2-fold dilution series beginning with 50pM synthetic oligonucleotide were used in 10ul RT reactions (Taqman small RNA assays) and qPCR was performed. Each dilution was performed in triplicate from three independent experiments. Linear regression was used to determine mean C(t) values plotted against log(miRNA copies/ul).

miRNA *in situ* hybridizations and ceramide dependence

Cells were plated in 6-well plates containing coverslips at a density of ~2.5×10^5 cells and cultured in DMEM supplemented with 10% bovine growth serum for 24 hr. The cells were then washed 3 times with PBS and cultured for 24 hr in serum-free medium containing either 5 uM GW4869 (Cayman Chemicals # 13127, Ann Arbor, MI, USA) or DMSO. Medium was removed and cells were washed 3 times with PBS and fixed with 4% PFA for ~15 min at room temperature. After, cells were washed 3 times in DEPC-treated PBS and permeabilized in 70% ethanol for ~4 hr at 4°C, and rehydrated in DEPC-treated PBS for 5 min. Pre-hybridization was performed in hybridization buffer (25% formamide, 0.05 M EDTA, 4X SSC, 10% dextran sulfate, 1X Denhardts solution 1mg/ml *E.coli* tRNA) in a humidified chamber at 60°C for 60 min. Hybridization buffer was removed and replaced with 10 nM of probe (probe numbers are listed below) diluted in hybridization buffer and incubated at either 55°C (*miR-100* and *miR-10b*) or 57°C for scrambled and U6 probes for 2 hr. Coverslips were then washed in series with pre-heated SSC at 37°C as follows: 4X SSC briefly, 2X SSC for 30 min., 1x SSC for 30 min, and 0.1x SSC for 20 min. miRNA detection was conducted using Tyramide Signal Amplification

(TSA) (Perkin Elmer, # NEL741001KT, Waltham, MA, USA). Briefly, coverslips were blocked in blocking buffer (0.1 M TRIS-HCl, pH 7.5, 0.15 M NaCl, 0.5% Blocking Reagent [Roche, #11096176001, Basel, Switzerland]) at 4°C overnight. Blocking buffer was replaced with anti-DIG-POD (Roche, # 11207733910) diluted 1:100 in blocking buffer and incubated for 60 min. Coverslips were washed 3 times, 5 min per wash, in wash buffer (0.1 M TRIS-HCl, pH 7.5, 0.15 M NaCl, 0.5% Saponin) followed by incubation with 1X Fluorescein diluted in 1X amplification reagent for 5 min. Fluorescent coverslips were then washed 2 times, 5 min per wash, in wash buffer. To preserve fluorescent signals, coverslips were fixed with 2% PFA containing 2% BSA in 1X PBS for 15 min. After fixation, coverslips were washed 2 times, 5 min per wash, in wash buffer, followed by a final wash in 1X PBS for 5 min. Coverslips were then mounted in Prolong Gold (Life Technologies) and visualized on a Zeiss LSM510 at 63X objective. 3'-DIG labeled probes for *in situ* hybridizations- U6 snRNA: 99002-05; Scramble: 99004-05; *miR-10b-5p*: 38486-05; *miR-100-5p*: 18009-05 (Exiqon, Woburn, MA, USA).

Co-culture and luciferase reporter assays

Recipient cells were plated in 6-well plates at a density of ~$2.5x10^5$ cells and cultured in DMEM supplemented with 10% bovine growth serum for 24 hr. Media was replaced and cells were co-transfected (Promega, E2311, Madison, WI, USA) with 1.5 ug of Luc-reporter plasmid and 1.5 ug β-gal plasmid DNA/well. Donor cells were plated in 0.4 um polyester membrane Transwell filters (Corning, 3450, Corning, NY, USA) at ~$2.5x10^5$ cells/well for 24 hrs. Media from donor Transwells and recipient 6-well plates were removed and replaced with DMEM without FBS. Co-culture of donor and recipient cells were conducted for either 24 or 48 hrs before recipient cells were harvested. Lysates were prepared in 1X Reporter lysis buffer (Promega, E2510) and luciferase assays were performed according to the manufacturer's protocol (Promega, E2510). β-Gal expression was simultaneously determined from the lysates according to the manufacturer's protocol (Promega, E2000). Differences in transfection efficiency were accounted for by normalizing Luc expression to β-Gal expression (Luc/β-Gal). All assays were performed on 3 biological replicates, each with 3 technical replicates.

Antagomir treatment

Donor cells were plated in 0.4 μm polyester membrane Transwell filters (Corning, 3450,

Corning, NY, USA) at ~1.4x10^4 cells/well for 24 hrs. Medum was replaced and donor cells were transfected with either *miR-100* hairpin antagomirs (# IH-300517-05, GE Life Sciences) or negative control hairpin antagomirs corresponding to *cel-miR-67* (# IN-001005-01, GE Life Sciences) to produce a final concentration of 100 nM of antagomir for 24 hrs. Medium from donor Transwells and recipient 6-well plates was removed and replaced with DMEM without FBS. Co-culture of donor and recipient cells was conducted for 24 hrs before recipient cells were harvested for RNA isolation.

Plasmid construction

For the pLuc-mTOR construct, the 3'UTR of *mTOR* was PCR amplified (primer sequences in Supplemental Table 5) from genomic DNA isolated from DKs-8 cells. The amplicon was cloned into pMiR-Report (Life Technologies) via SpeI/HinDIII restriction sites. Mutation of *miR-100* binding sites in mTOR 3UTR (MS) was performed on pLuc-mTOR using forward or reverse primers targeting either all three MRE's, or MRE 2 & 3 with QuikChange Lightning Multi-Site Directed Mutagenesis (Agilent, Santa Clara, CA, USA) according to manufacturer's protocol. To create the reporter construct containing three *miR-100* perfect sites (miR-100-PT), oligonucleotides were annealed to produce a synthetic fragment containing the perfect sites with CTAGT and AGCTT overhangs. The fragment was cloned into pMiR-report via SpeI/HinDIII restriction sites. All plasmids were sequence verified (GeneWiz, South Plainfield, NJ, USA).

Author contributions

DJC and JLF designed and performed most of the experimental work with help from JNH and MDB. NP and SL performed the sequencing analyses. YD, QL, and BZ performed computational, bioinformatics, and statistical analyses. JGP, RJC, AMW and KV conceived and directed the project. DJC, JLF, RJC, AMW, YD, BZ, and JGP wrote the manuscript.

Acknowledgements

This work was supported by grants from the National Institutes of Health, U19CA179514, RO1 CA163563 and a GI Special Program of Research Excellence (SPORE) P50 95103 to RJC, and a pilot in P30 DK058404 to JLF. Vanderbilt Digestive Disease Research Center (P30 DK058404) and associated Cores.

Chapter 3

Circular RNAs are down-regulated in *KRAS* mutant colon cancer cells and can be transferred to exosomes[2]

3.1. Abstract

Recent studies have shown that circular RNAs (circRNAs) are abundant, widely expressed in mammals, and can display cell-type specific expression. However, how production of circRNAs is regulated and their precise biological function remains largely unknown. To study how circRNAs might be regulated during colorectal cancer progression, we used three isogenic colon cancer cell lines that differ only in *KRAS* mutation status. Cellular RNAs from the parental DLD-1 cells that contain both wild-type and G13D mutant *KRAS* alleles and isogenically-matched derivative cell lines, DKO-1 (mutant *KRAS* allele only) and DKs-8 (wild-type *KRAS* allele only) were analyzed using RNA-Seq. We developed a bioinformatics pipeline to identify and evaluate circRNA candidates from RNA-Seq data. Hundreds of high-quality circRNA candidates were identified in each cell line. Remarkably, circRNAs were significantly down-regulated at a global level in DLD-1 and DKO-1 cells compared to DKs-8 cells, indicating a widespread effect of mutant *KRAS* on circRNA abundance. This finding was confirmed in two independent colon cancer cell lines HCT116 (*KRAS* mutant) and HKe3 (*KRAS* WT). In all three cell lines, circRNAs were also found in secreted extracellular-vesicles, and circRNAs were more abundant in exosomes than cells. Our results suggest that circRNAs may serve as promising cancer biomarkers.

---

2. Yongchao Dou, Diana J. Cha, Jeffrey L. Franklin, James N. Higginbotham, Dennis K Jeppesen, Alissa M. Weaver, Nripesh Prasad, Shawn Levy, Robert J. Coffey, James G. Patton & Bing Zhang. "Circular RNAs are down-regulated in *KRAS* mutant colon cancer cells and can be transferred to exosomes." *Sci. Rep.* **6**, 37982; doi: 10.1038/srep37982 (2016).

3.2. Introduction

Circular RNAs (circRNAs) were first reported more than 30 years ago(Cocquerelle et al. 1993; Saad et al. 1992; Nigro et al. 1991), but had long been perceived as occasional RNA splicing errors until recent genome-wide analyses powered by next generation sequencing (NGS) technologies have shown these are bona fide RNA species. Studies during the past several years have identified a large number of exonic and intronic circRNAs across the eukaryotic lineage, including human, mouse, zebrafish, worms, fungi, and plants(Memczak et al. 2013; P. L. Wang et al. 2014). Based on the assumption that the abundance of circRNAs is much lower than that of linear RNAs, early studies typically use RNase R, a magnesium-dependent 3′ to 5′ exoribonuclease, to deplete linear RNAs before sequencing(Cheng and Deutscher 2005). However, recent work showed that the abundance of circRNAs is similar to or higher than that of linear transcripts for about one in eight human genes(Jeck et al. 2013), which can be partially explained by higher cellular stability and longer half-life of circRNAs compared to linear mRNAs(Jeck and Sharpless 2014). The observed high abundance of circRNAs suggests that RNase R treatment is likely to be unnecessary in NGS-based analysis of circRNAs, consistent with the identification of 7112 circRNA candidates from non-poly(A)-selected libraries generated by the ENCODE project(Guo et al. 2014; Consortium 2004). It is now clear that circRNAs are evolutionarily conserved, exhibit cell-specific expression patterns, and are regulated independent of their linear transcripts(Jeck et al. 2013; Salzman et al. 2013). For example, circRNAs are enriched in brain and accumulate to the highest levels in the aging central nervous system(Westholm et al. 2014; Rybak-Wolf et al. 2015). Recent studies also showed that circRNAs can be transferred to human exosomes(Y. Li et al. 2015), where they are enriched and stable. These findings suggest that circRNAs are prevalent, abundant, and potentially functional.

Knowledge about the general sequence features, biogenesis, and putative functions of circRNAs, especially exonic circRNAs, has gradually accumulated(Jeck and Sharpless 2014). Because both circRNAs and linear RNAs are spliced from pre-mRNAs, the competition between circularization and linear splicing may play a role in the regulation of gene expression(Ashwal-Fluss et al. 2014). Moreover, introns between exons may be retained when exons are circularized(Z. Li et al. 2015). Circularization of exonic circRNAs typically involves the canonical GU-AG splice site pairs(Black 2003) and can contain one or multiple exons. On

average, single-exon circRNAs form with exons that are three times longer than non-circularized exons(Jeck and Sharpless 2014). Exon circularization is promoted by pairing of reverse complementary sequences within introns bracketing circRNAs; reverse complimentary sequences are primarily Alu repeats(X.-O. Zhang et al. 2014; D. Liang and Wilusz 2014; A. Ivanov et al. 2015). Two possible mechanisms for the formation of exonic circRNAs have been proposed, and both involve the canonical spliceosome(Jeck and Sharpless 2014). Two circRNAs in mammals have been shown to function as miRNA sponges(Memczak et al. 2013), but significant enrichment of miRNA binding sites was not found for the majority of circRNA candidates(Guo et al. 2014; Consortium 2004).

Although other non-coding RNAs have been shown to play critical roles in cancer, the association between circRNAs and cancer is largely unknown(Hansen, Kjems, and Damgaard 2013; Bachmayr-Heyda et al. 2015). In this study, we performed deep RNA-Seq analysis of rRNA-depleted total RNA libraries to characterize circRNA expression in three isogenically-matched human colon cancer cell lines that differ only in the mutation status of the *KRAS* oncogene. The parental DLD-1 cells contain both wild-type and G13D mutant*KRAS* alleles, whereas the isogenically-matched derivative cell lines DKO-1 and DKs-8 contain only a mutant *KRAS* and a wild-type *KRAS* allele, respectively.

KRAS mutations occur in approximately 34–45% of colon cancers(Vogelstein et al. 1988) and have been associated with a wide range of tumor-promoting effects(Velho and Haigis 2011). We developed an integrated bioinformatics pipeline to identify, confirm and annotate circRNAs based on RNA-Seq data. Using the pipeline, we studied both cellular and exosomal circRNAs in the three cell lines, with confirmation of altered circRNAs in a second set of isogenically matched cell lines. To our knowledge, this is the first report describing the impact of a well-established oncogene on the abundance of circRNAs.

3.3. Results

Bioinformatics pipeline

Exonic circRNAs largely result from back-spliced exons, in which splice junctions are formed by an upstream 5′ splice acceptor and a downstream 3′ splice donor. Back-splice reads mapping to such junctions are the most important indicator for circRNAs that can be gleaned

from RNA-Seq data(Memczak et al. 2013; Jeck and Sharpless 2014; Westcott et al. 2014; X.-O. Zhang et al. 2014; Hansen et al. 2013). Similar to the existing pipeline used by Memczak *et al*.(Memczak et al. 2013), our pipeline (Fig. 10A) uses the presence of back-splice reads to identify exonic circRNA candidates. However, multiple mapping positions are allowed when mapping anchors in our pipeline. Find-circ only reports a random mapping position and may therefore miss some circRNAs (false negatives). Moreover, because one read may be considered as a back-splicing candidate at one position or a linear gapped mapping at another position, find-circ may also introduce false positives. Thus, allowing multiple mapping positions in our pipeline may help reduce both false positives and false negatives. Briefly, one paired-end read was used as two single-end reads for mapping to the genome. Mappable reads were discarded because back-splice reads cannot be mapped to the genome directly. The 5′ and 3′ termini of unmapped reads were then extracted as anchors, which were aligned to the genome independently with multiple mapping allowed. Because multiple mapping is allowed, all possible pairs of anchor alignments were evaluated. If any of these pairs correspond to a normal linear gapped mapping, the read was discarded. For the remaining reads, all the possible extensions that could be extended to reconstruct the original read with a maximum of two mismatches were further considered. Then we will search the GU/AC splice sites for each extension. If any extensions with the GU/AC splice sites, the read was considered as with GU/AC splice sites. Extended alignments flanked by GU/AG splice sites were used to define a back-splice read.

Contamination from other biological sources may affect both the identification and quantification of circRNAs. To check possible contaminations from bacteria and viruses, we built a database with all bacterial and viral sequences and blasted all back-splicing mates against the database. For cellular RNAs, 99.6% to 99.8% of the mates had no hits to the database and none of them had a hit with two or less mismatches. For exosomal RNAs, 91.8% to 99.4% of the mates had no hits to the database and only a few had a hit with two or less mismatches. Next, all back-splicing mates were mapped to the bovine genome(Elsik et al. 2016) both linearly and using the back-splicing detection algorithm. The linear mapping percentages were close to 0 for all samples, and no more than 2.2% of the back-splicing mates could be back-splicing-mapped to the bovine genome. These results show that the vast majority of the identified circular RNAs are not from bacterial and viral contamination and the potential contamination from the bovine sources is very limited. We discarded all back-splicing reads that can be mapped to bacterial,

viral, or bovine genomes from downstream analysis to avoid any influence from possible contamination.

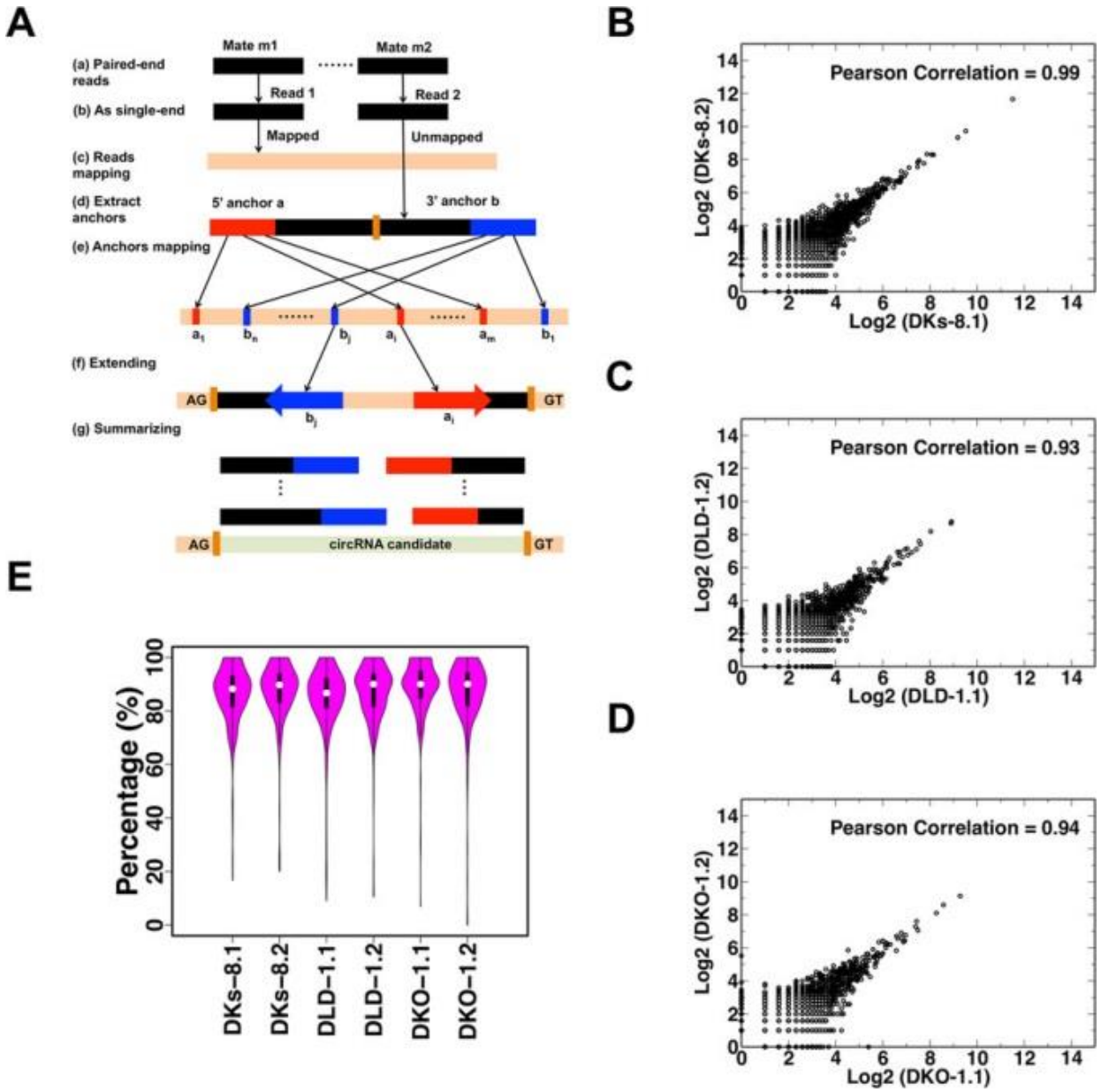

Figure 10: Bioinformatics pipeline and analysis of cell circRNAs (**A**) Computational pipeline. (**B**–**D**) Pearson Correlation analysis between cell replicates for DKs-8, DLD-1, and DKO-1 colorectal cell lines, respectively. (**E**) Distribution of percentages of back-splice mates with corresponding mates that can be mapped (PCMM) for each sample.

Identification of circRNA candidates in colorectal cancer cells

We prepared cellular RNA libraries from the three isogenic-*KRAS* CRC cell lines, each with two biological replicates. RNase R treatment was not applied during library construction.

Sequence fragments supported by two or more remaining back-splice reads were considered as circRNA candidates, and those supported by ten or more back-splice reads were considered as high quality candidates. Finally, circRNA candidates with sequence fragment lengths between 100 and 1000,000 bp were reported by the pipeline.

Sequencing was performed at high depth, with ~100 million reads per sample. Applying the above-described pipeline to cellular RNAs from the three cell lines identified thousands of circRNA candidates and hundreds of high quality circRNA candidates in each biological replicate (Table 6). Among the 1620 high quality candidates detected in our study, 1395 (86.1%) were found in the circBase database(Glažar, Papavasileiou, and Rajewsky 2014).

Table 6: Identification of circRNA candidates in the three cell lines.

Read type	**Samples**					
	DKs-8.1	**DKs-8.2**	**DLD-1.1**	**DLD-1.2**	**DKO-1.1**	**DKO-1.2**
Paired-end reads	88746986	111215656	100025762	97930613	107392430	91024681
Back-splice reads	65319	80701	47941	44717	40657	37403
circRNA candidates	11061	13565	8771	8182	7348	6827
High quality candidates	932	1211	651	571	488	428
Host genes	676	866	509	455	392	342
Genes with >1 high quality candidates	158	192	87	72	57	53

.

To assess the reproducibility of the data, we generated scatter plots comparing the back-splice read counts of individual circRNAs from replicates of the three cell lines (Fig. 10B–D). As shown, the vast majority of all candidates were supported by consistent identification of back-splice reads in all replicates. Person's correlations between replicates were 0.99, 0.93, and 0.94 for DKs-8, DLD-1, and DKO-1, respectively. These scatter plots show circRNA candidates with higher read counts are closer to the diagonal, suggesting that reproducibility tended to be higher for circRNA candidates with high back-splice read counts. Therefore, our downstream

analyses focused only on high quality candidates with at least ten back-splice reads.

To further evaluate the reliability of the identified circRNA candidates, we leveraged the paired end information. If one mate of a paired end read mapped to a back-splice junction (Mate a), the corresponding mate could be mapped to the candidate circRNA sequence either within the circle (Mate b') or crossing the back-splice junction (Mate b). For each high quality candidate, we calculated the Percentage of back-splice mates with Corresponding Mates that can be mapped to the candidate circRNA sequence (PCMM), *i.e.* the percentage of properly paired back-splice mates. As shown in Fig. 8E, the median percentages ranged from 88.2% to 90.0% across the six samples, suggesting high reliability of these circRNA candidates. We also tested RNase R resistance of circRNAs in the DKO-1 and DKs-8 cell lines with the top four most abundant circRNAs. As shown in Figure 11, these circRNAs were enriched by RNase R (R+) treatment compared to mock treated controls (R−). Thus circRNAs are resisted to RNase R treatment. Taken together, these results suggest that a large number of circRNAs can be reliably and reproducibly identified and quantified in the three cell lines.

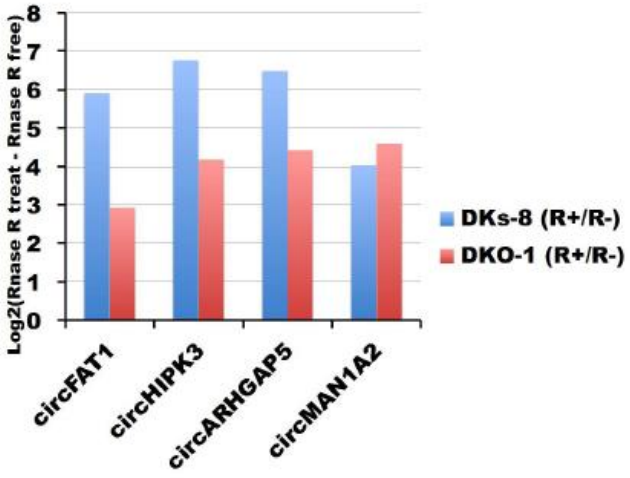

Figure 11. Enrichment after RNase R treatment. qRT-PCR was performed on RNA isolated from either DKs-8 cells (blue) or DKO-1 cells (red) treated with or without RNase R. RNase R (R+) treatment enriches for circRNA species compared to mock treated RNA samples. This enrichent is greater in DKs-8 samples compared to DKO-1 (orange) samples.

Down-regulation of circRNAs in *KRAS* mutant cells

To test whether the expression levels of circRNAs are regulated by *KRAS*, we compared the levels of circular RNA candidates between the mutant and wild-type *KRAS* cell lines. circRNAs were globally down-regulated in the mutant *KRAS* DKO-1 (Fig. 10A) and DLD-1 (Fig. 10B) cell lines compared to the wild-type *KRAS* DKs-8 cell line. Specifically, 443 and 305

circRNAs were significantly down-regulated in DKO-1 and DLD-1 cells, respectively (False Discovery Rate [FDR] < 0.01 and Fold Change [FC] >2). In contrast, only 5 and 13 circRNAs were significantly up-regulated in DKO-1 and DLD-1 cells, respectively. Among the top ten most abundant circRNAs in distinct genes, seven were significantly down-regulated in DKO-1 cells and five of them were also significantly down-regulated in DLD-1 cells (Table 7). These results suggest that circRNAs are down-regulated in *KRAS* mutant cells at a global level.

Table 7. Top10 most abundant circRNAs in distinct genes in DKs-8

		DLD-1/DKs-8		DKO-1/DKs-8	
		Log2FC	FDR	Log2FC	FDR
chr4:187627717-187630999	FAT1	−2.71	0	−2.41	2.01E-267
chr11:33307959-33309057	HIPK3	−0.81	1.26E-22	−1.07	1.40E-35
chr14:32559708-32563592	ARHGAP5	−1.12	2.37E-34	−1.10	2.67E-32
chr1:117944808-117963271	MAN1A2	−1.27	1.52E-25	−1.59	9.14E-36
chr5:95091100-95099324	RHOBTB3	−1.00	1.97E-16	−1.54	4.30E-32
chr2:55209651-55214834	RTN4	−1.81	2.69E-33	−2.04	1.93E-39
chr17:20107646-20109225	SPECC1	−0.45	5.15E-04	−0.94	4.83E-12
chr4:144464662-144465125	SMARCA5	−0.81	2.43E-09	−1.07	1.32E-14
chr4:25789846-25804084	SEL1L3	−0.07	9.05E-01	−0.17	3.72E-01
chr20:30954187-30956926	ASXL1	−0.50	9.78E-04	−0.66	1.68E-05

We next sought to determine whether circRNA down-regulation was due to down-regulation of corresponding host genes. Figure 12 shows a direct comparison of the differential expression results for circRNAs and their host genes between each of the two mutant cell lines and the wild-type cell line. While the log-fold changes of the host genes exhibited a symmetrical distribution around 0, the log-fold changes of circRNAs were negatively shifted toward decreased abundance in mutant *KRAS* cell lines. The correlations between log-fold changes of circRNAs and host genes were 0.19 and 0.16, respectively, for the two comparisons. Using the most abundant circRNA candidate circRNA chr4:187627717-187630999 as an example, we found that this circRNA was down regulated by 6.6- and 5.3-fold in DLD-1 and DKO-1 cells, respectively compared to DKs-8 cells. In contrast, the host gene FAT1 was only down-regulated by 1.7- and 1.8-fold, respectively. These data suggest that circRNAs can be regulated independently of their corresponding host genes.

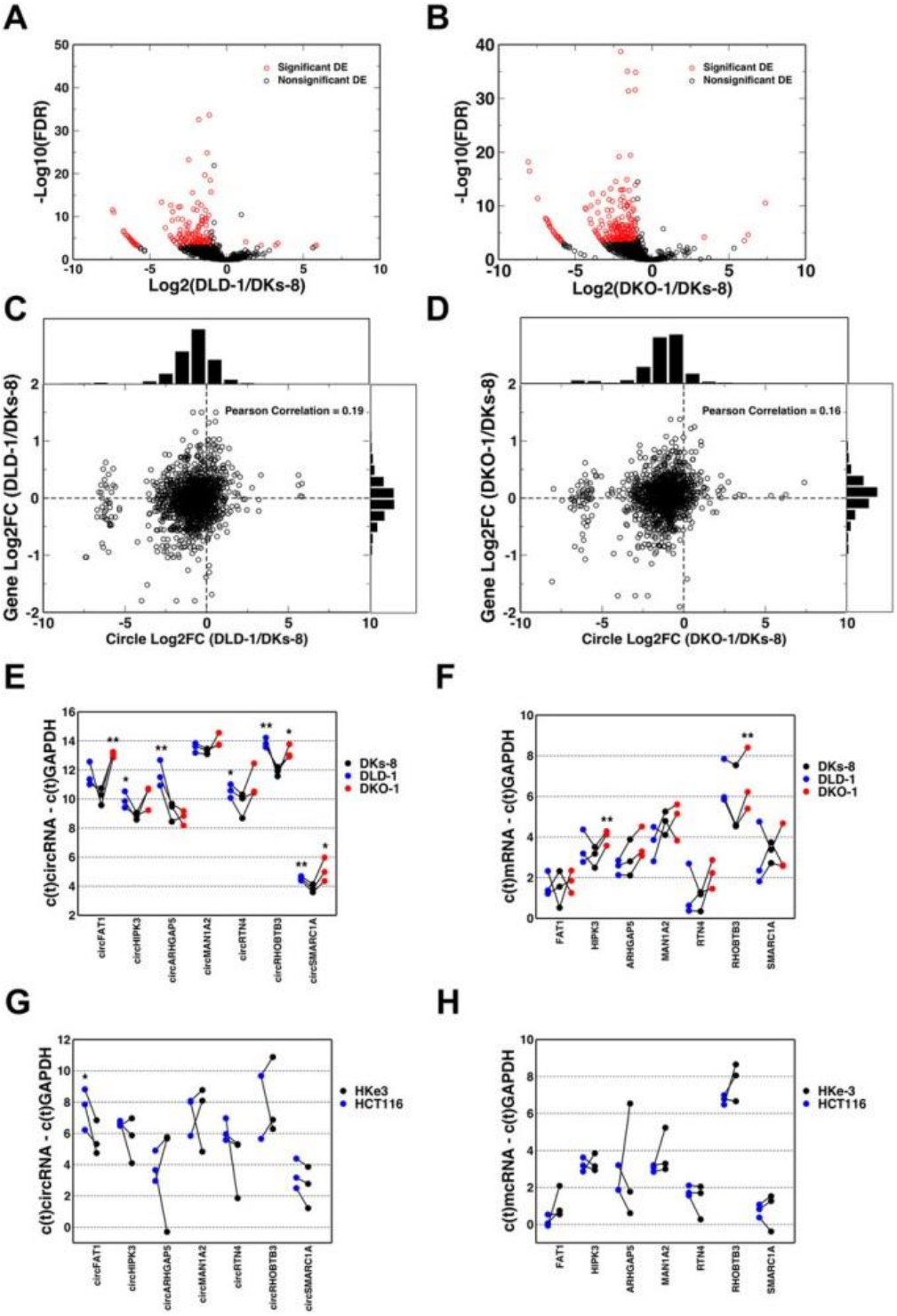

Figure 12. Differential expression analysis for cellular circRNAs. (**A**,**B**) circRNA differential expression analysis between mutant and wild-type *KRAS* cells. (**C**,**D**) Differential expression results for circRNAs and their host genes. Histograms of each gene and corresponding circRNAs log2FCs are shown above the X and Y-axes, respectively. (**E**) qRT-PCR results for seven selected circRNAs between mutant and wild-type cells. (**F**) qRT-PCR results for host genes of selected circRNAs. (**G**) qRT-PCR results for seven selected circRNAs between HCT116 and HKe3 cells. (**H**) qRT-PCR results for host genes between HCT116 and HKe3 cells. (Two-tailed, paired t-test was used for the analysis. *denote p values ≤ 0.1 and **≤ 0.05).

To validate our findings, we performed qRT-PCR analysis for seven out of the ten most abundant circRNA candidates. As shown in Fig. 12E, all were confirmed by qRT-PCR and six out of the seven circRNA candidates were significantly down-regulated in at least one mutant cell line compared with the wild-type cell line (two-tailed, paired t-tests was used for the analysis, where *are p values ≤ 0.1 and **≤ 0.05). As a comparison, Fig. 12F shows different trends for the host genes of these circRNAs. These results further confirm our finding that circRNAs are down-regulated in mutant *KRAS* cells and that the regulation of circRNAs can occur independent of their host genes.

To further strengthen our conclusion, we performed additional experiments using another pair of isogenically-matched human colon cancer cell lines, HCT116 and HKe3. Derived from a completely different cancer, HCT116 harbors mutant G13D *KRAS* while its clonal derivative HKe3 contains wild-type *KRAS*(Senji Shirasawa et al. 1993). Consistent with our previous results, all seven circRNAs assayed were down regulated in the HCT116 cells compared to the HKe3 cell line as shown in Fig. 12G. Among them, circFAT1 was significantly down-regulated in the mutant*KRAS* cell line (HCT116). Furthermore, the host genes for these candidates were not significantly differentially expressed between HCT116 and HKe3 cell lines (Fig. 12H). These results support our finding that circRNAs are down-regulated in mutant *KRAS* cells and that the regulation of circRNAs can occur independently of their host genes.

circRNAs in exosomes

Several recent reports have identified extracellular circRNAs(Y. Li et al. 2015). To test whether circRNAs could be detected in the exosomes of colon cancer cell lines, we performed RNA-Seq analysis for exosomal RNAs from the three cell lines, each with three biological replicates. High quality circRNA candidates were identified in all three cell lines. However, the number of high quality candidates varied among the replicates. Because the variation between DKs-8 exosomal replicates was relatively low, we focused our downstream analyses on data from DKs-8 derived exosomes. High quality exosomal circRNA candidates identified in this cell line were well supported by paired end information. Specifically, the median percentages of properly paired back-splice mates were 90.0%, 91.3%, and 91.7% for the three replicates, respectively (Fig. 13A). Table 8 shows the ten most abundant exosomal circRNA candidates in distinct genes in DKs-8 cells. Interestingly, seven of these circRNAs were also the top ten most

abundant circRNAs candidates in DKs-8 cells (Table 7).

Table 8. Top10 most abundant circRNAs in exosomes

Candidates	Gene	DKs-8.1		DKs-8.2		DKs-8.3	
		BSR[1]	PCMM[2]	BSR[1]	PCMM	BSR[1]	PCMM2
chr5:95091100-95099324	RHOBTB3	81	95.1%	141	92.2%	89	95.5%
chr11:33307959-33309057	HIPK3	75	81.3%	97	88.7%	51	90.2%
chr4:187627717-187630999	FAT1	69	88.4%	78	94.9%	60	90.0%
chr4:144464662-144465125	SMARCA5	44	97.7%	95	95.8%	61	88.5%
chr1:117944808-117963271	MAN1A2	36	83.3%	65	95.4%	37	94.6%
chr20:30954187-30956926	ASXL1	28	85.7%	60	85.0%	33	90.9%
chr12:120592774-120593523	MIR4498	40	92.5%	44	97.7%	28	89.3%
chr2:55209651-55214834	RTN4	28	85.7%	43	88.4%	35	100.0%
chr9:138773479-138774924	CAMSAP1	21	95.2%	36	91.7%	34	82.4%
chrM:2003-2226	MT-RNR2	67	92.5%	18	90.9%	3	100.0%

Abbreviations: BSR[1]= Back-spliced reads; PCMM[2]= Percentage of back-splice mates with Corresponding Mates

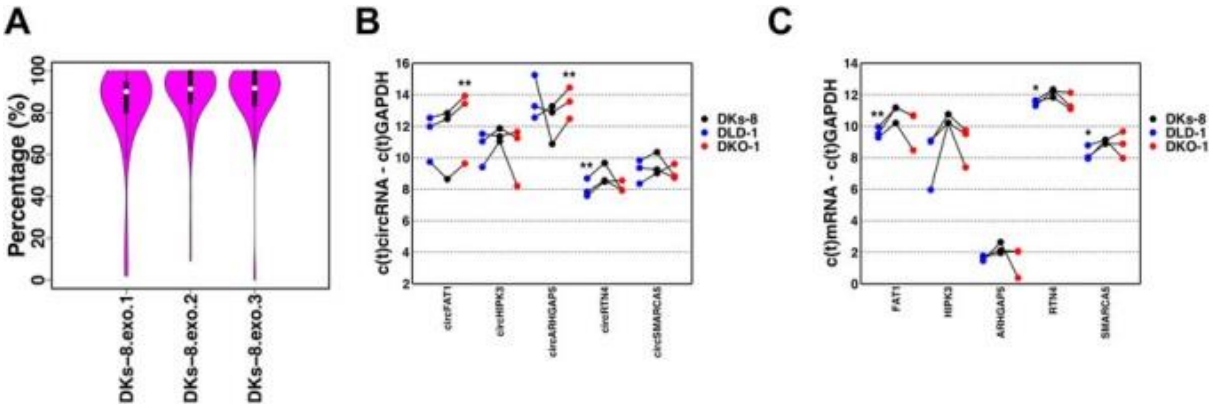

Figure 13: Bioinformatics analysis of circRNAs in exosomes. (**A**) Distribution of PCMM values for three DKs-8 exosomes replicates. (**B**) RT-PCR results for five selected circRNAs between mutant and wild-type cell lines in exosomes. (**C**) RT-PCR results for host genes of confirmed circRNAs in exosome. (Two-tailed, paired t-test was used for the analysis. *Denote p values ≤ 0.1 and **≤0.05).

To validate the RNA-Seq results, qRT-PCR analysis was also performed on these consistently present and abundant circRNA candidates in exosomes. As shown in Fig. 13B, five of these circRNAs were confirmed as present in exosomes and three of them were differentially

expressed in at least one set of mutant cell line derived exosomes compared with the wild-type cell line exosomes (two-tailed, paired t-tests was used for the analysis, where *are p values ≤ 0.1 and **≤ 0.05). Among them, circFAT1 was significantly down regulated in DKO-1 as compared to DKs-8 exosomes (Fig. 13B); this circRNA followed the same trend in cells (Fig. 12E). Meanwhile, circRTN4 was significantly up regulated in DLD-1 exosomes (Fig. 13B), while it was significantly down regulated in DLD-1 cells (Fig. 12E). The mRNA expression levels of these circRNA host genes were also tested by qRT-PCR and the results shown in Fig. 13C. The mRNA expression levels of both FAT1 and RTN4 were up regulated in exosomes from mutant *KRAS* cells. Therefore the shift in the relative circRNA levels was not the same as that for their linear mRNA host genes when comparing mutant and wild-type *KRAS*-derived exosomes. These results suggested that there is a complex exosomal trafficking mechanism for circular RNAs. This is interesting given the increased abundance of RNA-binding proteins present in wild-type *KRAS* as compared to mutant *KRAS* cell-derived exosomes(Demory Beckler et al. 2012). Results from the proteomic analysis of these exosomes may explain both the relative differences in circRNA and linear RNA content in DKs-8 as compared to DKO-1 and DLD-1 exosomes, as well as the relatively consistent levels of such RNAs in DKs-8 exosomes, given that such RNAs might be trafficked by these specifically exosomally-localized DKs-8 enriched RNA-binding proteins.

Relative abundance of circular and linear transcripts

Because RNAse R treatment was not applied during the RNA library construction in this study, the resulting RNA-Seq data allowed us to directly compare the abundance of circRNAs and their linear host RNAs. Similar to previous studies(Salzman et al. 2013; Rybak-Wolf et al. 2015), we used the ratio between Expression level of exons With Circular RNAs and Expression level of exons with No Circular RNAs (EWC/ENC) to quantify the relative abundance of these two types of transcripts.

For cellular RNAs, the median EWC/ENC ratios ranged from 1.57 to 1.84 across the three cell lines (Fig. 14A). Similar analysis was performed on exosomal RNAs, where the median EWC/ENC ratios were much higher and ranged from 2.56 to 4.26 (Fig. 14B). Figure 14C and D show the read coverage depth plots for the most abundant circRNA circFAT1 (chr4:187627717-187630999) in DKs-8 cells and exosomes, respectively. The exon

corresponding to circFAT1 (red) had a much higher read depth compared with other exons (blue). The EWC/ENC ratios were 3.5 and 3.0 for the two cell replicates, respectively, and 7.1, 7.6, and 7.7 for the three exosome replicates, respectively. These results are consistent with recent reports that circRNAs are more abundant than their host linear RNAs(Salzman et al. 2013; Rybak-Wolf et al. 2015) and provide additional evidence that circRNAs are likely to be more stable than their linear transcripts(Jeck and Sharpless 2014). In addition, our results suggest that cirRNAs are enriched in exosomes, which is consistent with a recent publication(Dou et al. 2016).

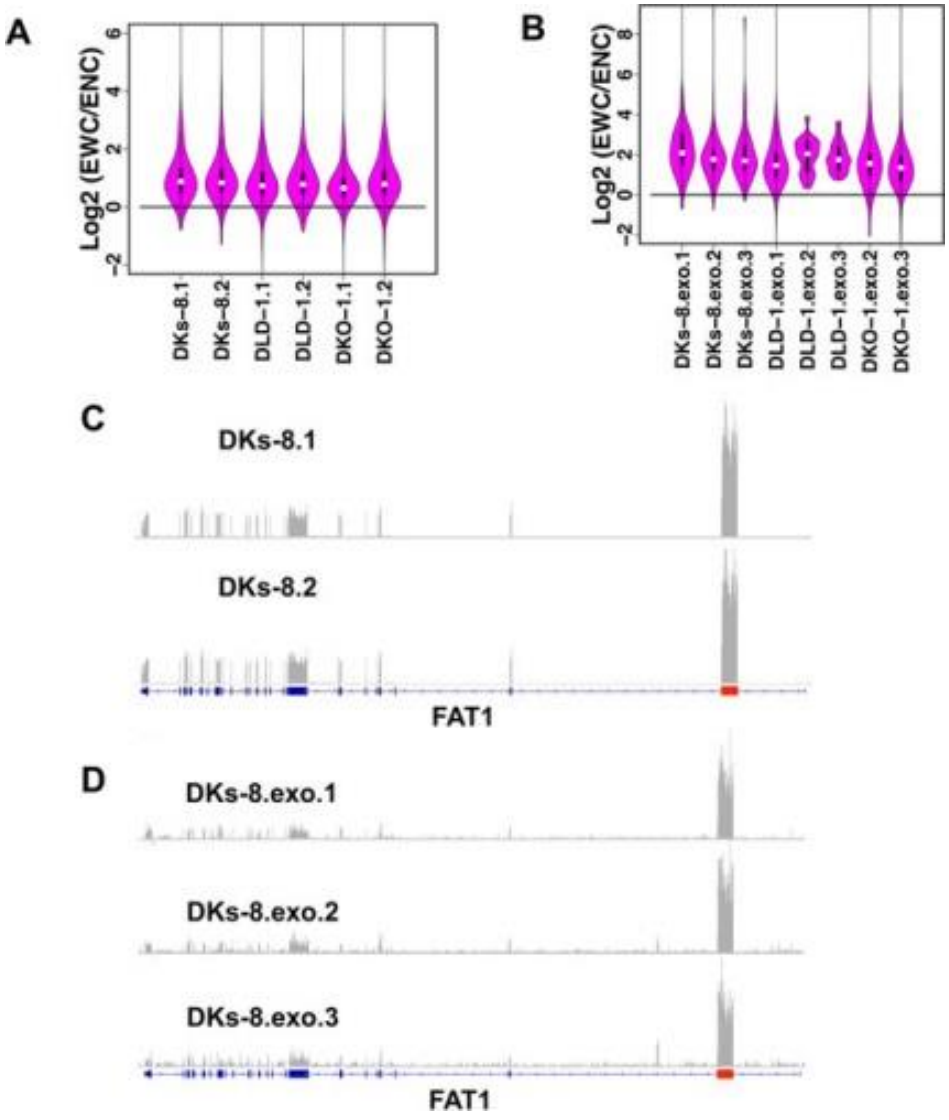

Figure 14: Relative expression levels of circRNAs compared to linear transcripts. (**A**,**B**) Distribution of EWC/ENC values for cellular and exosomal RNAs, respectively. DKO-1.exo.1 was excluded because only 2 high quality candidates were identified in this replicate. (**C**,**D**) Expression levels of exons with and without circRNA with the FAT1 gene in DKs-8 cells and exosomes, respectively.

3.4. Discussion

In this work, we determined the circRNA expression profiles in both cells and exosomes from three CRC cell lines that differ only in *KRAS* mutation status. Hundreds of high quality circRNA candidates were identified in cellular RNAs and we discovered that they could be transferred to exosomes. circRNAs tended to be more abundant in exosomes. Importantly, we showed that circRNA abundance was down-regulated at a global level in mutant *KRAS* cell lines, suggesting a potential involvement of circRNAs in oncogenesis.

There are complex regulatory mechanisms for both circRNA and host gene expression. Although circRNAs were down-regulated in both DLD-1 and HCT166 based cell lines, it is difficult to conclude that the circRNAs are directly regulated by *KRAS*. One possibility is that down-regulation of circRNAs in *KRAS* mutant cells is caused by their increased exporting to exosomes. However, as shown in Fig. 14B, the EWC/ENC median values were 2.77, 4.15, 3.38, 2.96 and 2.56 for *KRAS* mutant exosomes and were 4.26, 3.43 and 3.25 for *KRAS* WT exosomes (Fig. 12B). The median values in *KRAS* mutant exosomes were comparable to that in *KRAS* WT exosomes. Moreover, Fig. 13B shows that two of three significantly regulated circRNAs between *KRAS* mutant and WT exosomes were down-regulated in *KRAS* mutant (circFAT1 and circARHGAP5). These data suggest that circRNAs are not enriched in exosomes of the *KRAS* mutant cells. We also examined the expression levels of the RNA-editing enzymes *ADAR* and the RNA-binding protein QKI, which were reported as circRNA regulators(A. Ivanov et al. 2015; Conn et al. 2015). The *ADAR* was decreased in the *KRAS* mutant cells, which may lead to an increase of circRNAs. QKI was down-regulated in *KRAS* mutant cells, which may lead to down-regulation of circRNAs. More broadly, we studied the expression levels of all RNA-binding proteins from RBPDB(Cook et al. 2011), following the approach taken by Conn *et al*.(Conn et al. 2015). Six were found to be differentially expressed (FDR < 0.01 and absolute log2FC > 1) in *KRAS* mutant cell lines compared with wild-type cell lines (*ELAVL2, RBMS3, BICC1, MSI1, RBM44, and LARP6*). Three of these were up regulated and the others were down regulated. The most up-regulated gene, *ELAVL2*, can function as an alternative pre-mRNA splicing regulator in mammalian neurons(Ince-Dunn et al. 2012; J. M. Izquierdo 2008). The most down-regulated gene, *MSI1*, is also an important post-transcriptional regulator(Katz et al. 2014; Ratti et al. 2008). These genes may serve as candidate circRNA regulators. However, our

previous work shows that the correlation of mRNA and protein expression level is low for RNA-binding proteins(B. Zhang et al. 2014). Further investigation will be needed to precisely define how circRNAs are regulated.

3.5. Methods

Cell Culture

Cells were cultured in DMEM supplemented with 10% bovine growth serum until 80% confluent. To collect exosomes, cells were then washed 3 times with PBS and cultured for 24 hr in serum-free medium. The medium was collected and replaced with ionomycin-containing media for 1 hr, after which ionomycin-containing media was collected and pooled with the previously collected serum-free medium.

Exosome isolation

Exosomes were isolated from conditioned medium of DKO-1, Dks-8, and DLD-1 cells, with slight modification(Demory Beckler et al. 2012). Pooled media as describted above was centrifuged for 10 min at 300 × g to remove cellular debris, and the resulting supernatant was then filtered through a 0.22-um polyethersulfone filter (Nalgene, Rochester, NY) to reduce microparticle contamination. The filtrate was concentrated ~300-fold with a 100,000 molecular-weight cutoff centrifugal concentrator (Millipore). The concentrate was then subjected to high-speed centrifugation at 150,000 × g for 2 hr. The resulting exosome-enriched pellet was resuspended in PBS containing 25 mM HEPES (pH 7.2) and washed by centrifuging again at 150,000 × g for 3 hr. The wash steps were repeated a minimum of 3 times until no trace of phenol-red was detected. The resulting pellet was resuspended in PBS containing 25 mM HEPES (pH 7.2) and protein concentrations were determined with a MicroBCA kit (Pierce). The number of exosomes per ug of protein was determined by nanoparticle tracking analysis (NanoSight, Wiltshire, UK).. Analysis was performed on three independent preparations of exosomes.

RNA purification

Total RNA from exosomes and cells was isolated using TRIzol (Life Technologies). In the case of exosomal RNA isolation TRIzol was incubated with 100 ul or less of concentrated exosomes

for an extended 15 min incubation prior to chloroform extraction. RNA pellets were resuspended in 60 µl of RNase-free water and were then re-purified using the miRNeasy kit (QIAGEN). Final RNAs were eluted with two rounds of 30 ul water extraction.

mRNA library preparation and sequencing

Total RNA containing both long RNA as well as miRNA fractions was extracted from exosomes or cell lines using Trizol followed by miRNeasy Kit purification. Final elution was in 60 µl RNase free sterile distilled water. The concentration and integrity of the extracted total RNA was estimated by Qubit® 2.0 Fluorometer (Invitrogen, Carlsbad, California), and Agilent 2100 Bioanalyzer (Applied Biosystems, Carlsbad, CA), respectively. RNA samples with a RIN value of at least 7.0 or higher were used for further processing.

Approximately 500 ng of total RNA was required for proceeding to downstream RNA-seq applications. Briefly, a Ribo-zero Magnetic Gold rRNA removal kit (Epicenter, IIlumina Inc.) was used to remove ribosomal RNA from the total RNA. Next, first strand synthesis was performed using NEBNext RNA first strand synthesis module (New England BioLabs Inc., Ipswich, MA, USA). Immediately, directional second strand synthesis was performed using NEBNExt Ultra Directional second strand synthesis kit. Following this, cDNAs were used for standard library preparation protocol using NEBNext® DNA Library Prep Master Mix Set for Illumina® with slight modifications. Briefly, end-repair was performed followed by polyA addition and custom adapter ligation. Post-ligated materials were individually barcoded with unique in-house genomics service lab (GSL) primers. Library quality was assessed by Qubit 2.0 Fluorometer, and the library concentration was estimated by utilizing a DNA 1000 chip on an Agilent 2100 Bioanalyzer. Accurate quantification for sequencing applications was determined using the qPCR-based KAPA Biosystems Library Quantification kit (Kapa Biosystems, Inc., Woburn, MA). Each library was diluted to a final concentration of 12.5 nM and pooled equimolar prior to clustering. Paired-End (PE) sequencing was performed on all samples. Raw reads were de-multiplexed using a bcl2fastq conversion software v1.8.3 (Illumina, Inc.) with default settings.

circRNA identification

Reads with length 100 bp were mapped to the UCSC hg19 human genome (with mitochondrial

sequences) by Bowtie 2 with up to 2 mismatches (version 2.2.3). Paired 3′ and 5′ end anchors with length 20 bp were extracted for each unmapped read. Anchor pairs were mapped to the above genome with no mismatches and up to 40 mapping positions using Bowtie 2. Refseq gene annotations from UCSC were used to annotate circRNA candidates. Custom PERL scripts were used to implement the pipeline.

Contamination analysis

We built a database with all bacterial and viral sequences from the NCBI nt database(ftp://ftp.ncbi.nlm.nih.gov/genomes/refseq/bacteria/assembly_summary.txt and ftp://ftp.ncbi.nih.gov/genomes/Viruses/). All back-splicing mates were blasted (ncbi-blast-2.3.0+) against the database with default parameters. Next, back-splicing mates were linearly mapped to the bovine genome by Tophat2 (version 2.0.12) with up to 2 mismatches. Moreover, these mates were mapped to the bovine genome using the back-splicing detection algorithm described above.

Differential expression analysis

To count reads mapped normally to genes, paired end reads were mapped to the hg19 human genome using Tophat2 with up to 2 mismatches. Htseq-count (version 0.6.0) with default parameters was used to count reads mapped to genes with the refSeq annotation. It is worth noting that host gene expression was quantified using reads from both linear and circRNAs because existing tools cannot separate linear and circRNA counts based on RNA-Seq data from total RNAs. Accordingly, our results may have underestimated the difference between linear and circRNAs levels. The correlation between the regulation of linear and circRNAs would be even lower if we were able to separate the read counts. The EdgeR R package (version 3.6.8) was used for differential expression analysis. This package uses the Trimmed Mean of M-values (TMM) normalization method to remove systematic technical effects that occur in the data to minimize the impact of technical bias on differential expression analysis results. Moreover, the empirical Bayes method used in the package enables gene-specific variation estimates even when the number of replicate samples is very small. This method has been demonstrated in experiments with only two replicates, and thus is particularly appropriate for our study. For differential expression analysis of circRNAs, back-splicing read counts of circRNAs were added to the

bottom of gene count list as new genes for the normalization purpose. The cutoffs for log2 fold change (log2FC) and FDR were $|log2FC| > 1$ and $FDR < 0.01$.

Evaluate circRNA candidates by paired end information

To evaluate circRNA candidates by paired end sequencing information, corresponding mates of paired end reads were initially extracted for back-splice mapped mates. Then, fragments from the 5′ ends of linear transcripts of circRNAs with length 100 nt were copied to the 3′ end of these linear transcripts. These mates were then mapped to the modified linear sequences using Tophat2 with up to 2 mismatches. PCMM values were calculated as the number of reads both mates are mappable/the number of reads with back-splice mapped mate.

Compare expression levels between circRNAs and linear transcripts

To compare the relative expression levels between exons with and without circRNA candidates, DEPTH tool from Samtools package (version 0.1.19–44428 cd) was used to report read depths for genes with circRNA candidates. The mean value of read depths from an exon was used as the read depth of the exon. EWC/ENC value was calculated as the mean depth of exons with circRNAs/without circRNAs.

RT-PCR

To validate circRNA species, 0.5 ug of total RNA was reverse transcribed in a 30 µl reaction using AccuScript Hi-Fi RT kit with random hexamers according to manufactures protocol (#200820, Agilent Technologies). The resultant cDNA was diluted 4-fold in RNase- and DNase-free water and approximately 14 ng was used as template for each qPCR reaction. qPCR was performed in technical triplicates for each amplicon using SsoAdvanced Universal SYBR®Green Supermix (Bio-Rad). qPCR reactions were conducted on a Bio-Rad CFX384 instrument and relative expression levels were obtained using cycle threshold (Ct) values obtained by instrument software. All Ct values ≥31 were considered as background and discarded from further analysis. Triplicate C(t) values were averaged and normalized to U6 snRNA. Fold-changes were calculated using the ΔΔC(t) method, where: Δ = C(t)circRNA - C(t)U6 snRNA, and $\Delta\Delta C(t) = \Delta C(t)$DKO or DLD − $\Delta C(t)$DKs, and FC = 2^ΔΔC(t). Analysis was performed on three independent cell and exosomal samples. Forward (F) and reverse (R) primers used in qPCR

analysis were designed against head-to-tail junctions of putative circRNA products as follows: FAT1- (F) ACGCCAGAGCCATCTCTAAT, (R) GCAATGGGGAGACATTTGGC; HIPK3- (F) ATGGCCTCACAAGTCTTGGT, (R) TGGCCGACCCAAAGTCTATT; ARHGAP5- (F) TGATCTTGAAGATGTTTCTGCACAG, (R) CATCTAACTCCTGGTCAGAAGTG; MAN1A2- (F) TTCGAGCTGATCATGAGAAGG, (R) GCAAGTAGGCCTCCAATAAA; RHOBTB3- (F) TAAAGGCTGAAGCGTCACATTAT, (R) CTCGATTACATTTGAAACATCCCCA; RTN4- (F) CAACTAAGAAGAGGCGCCTG, (R) AGACTGGAGTGGTGTTTGGT; SMARCA5- (F) GGCTTGTGGATCAGAATCTGAACA, (R) TCTCTATAGTCTTCTCCTTCGAAGT. All primer sequences are 5′ to 3. The primer sequences were blasted against the NCBI human genomic + transcript database to ensure specific amplification of the intended targets. Moreover, the melt curves showed that each primer set only had one specific peak, suggesting that the amplicon was specific and no other secondary targets were being amplified.

Acknowledgements

This work was supported by a grant from the NIH, U19 CA179514.

Contributions

Y.D. and B.Z. designed the study. Y.D. performed all computational, bioinformatics, and statistical analyses. D.J.C., J.L.F., J.N.H., D.K.J., A.M.W., R.J.C. and J.G.P. developed the experimental protocol and prepared the samples. N.P. and S.L. performed the RNA-Seq experiments. D.J.C. performed all RT-PCR analysis. Y.D., J.G.P., J.L.F. and B.Z. wrote the manuscript with comments and final approval from all authors

Chapter 4

Diverse long-RNAs are differentially expressed in exosomes secreted by mutant *KRAS* colorectal cancer cells

4.1. Abstract

There is growing evidence for the regulatory roles of extracellular RNAs in mediating cell-to-cell communication. Although much is known about extracellular microRNAs (miRNAs), the identity and functional roles of non-miRNA biotypes are largely unknown. We have previously shown that mutant *KRAS* colorectal cancer (CRC) cells release exosomes containing distinct proteomes, miRNAs, and circular RNAs. To test whether mutant *KRAS* might regulate the composition of other RNA species, particularly long RNAs (mRNAs and lncRNAs), we comprehensively profiled RNAs of cells and matched exosomes from isogenic CRC cell lines differing only in *KRAS* status. We show that distinct RNAs, such as pseudogene and antisense transcripts, are enriched in exosomes compared to cellular profiles. Additionally, specific transcripts are differentially expressed dependent on mutant *KRAS.* For example, we observe strong enrichment of *Rab13,* as well as other novel ncRNAs in mutant *KRAS* exosomes. In co-culture experiments, we have implemented a novel RNA-tracking system to monitor the delivery of extracellular RNAs to recipient cells. Uptake of a guide-RNA fusion from donor cells activates reporter expression in recipient cells. Here, we present comprehensive data to identify the broad and diverse classes of extracellular RNAs secreted in exosomes and we demonstrate that export of specific RNAs can be regulated by *KRAS* status. Collectively, this will advance our understanding of exRNA biology in CRC and facilitate the development of potential exRNA biomarkers.

4.2. Introduction

It is now known that the majority of genome is transcribed into RNA but only ~2-3% of the genome encodes proteins. The remaining non-coding RNAs (ncRNAs) play important regulatory roles in mediating gene expression in eukaryotes and prokaryotes, and in nearly every biological context (Reinhart et al. 2000, 7). Recently, numerous studies have demonstrated the presence of distinct types of extracellular RNA (exRNAs) in diverse biological fluids (Valadi et al. 2007; Andrey Turchinovich et al. 2011). With respect to exRNAs, studies have focused primarily on microRNAs (miRNAs) which are well annotated with known regulatory functions (Kozomara and Griffiths-Jones 2011; Alvarez-Garcia and Miska 2005). However, the diversity of exRNAs is extensive and miRNAs are often not the most abundant class of RNA found in EVs (Balkom et al. 2015). The biological functions of these non-miRNA species are largely unknown.

Circulating RNAs are protected within ribonucleoprotein complexes (RNPs) (Arroyo et al. 2011), complexed with lipids (Vickers et al. 2011; Tabet et al. 2014), or incorporated into extracellular vesicles (EVs) (Valadi et al. 2007). EVs are an umbrella term referring to membrane-delimited nanovesicles released by all cells (Maas, Breakefield, and Weaver 2016), including exosomes, microvesicles, and other secreted vesicles (for review, see (Graça Raposo and Stoorvogel 2013)). Each class of vesicle is unique in its origin, and thus, differs in its composition of lipid, protein and RNA cargo (Colombo, Raposo, and Théry 2014; Patton et al. 2015). Here, we will focus on exosomes, small vesicles (40-100nm) that arise through the endosomal pathway (Graça Raposo and Stoorvogel 2013).

It has been suggested that protein cargo transfer by EVs between cells is associated with tumor aggressiveness and metastasis(Skog et al. 2008; Higginbotham et al. 2011b; Hoshino et al. 2013). However, numerous reports have also demonstrated that specific RNA species are sorted into exosomes and EVs and can function in cell-to-cell communication (Squadrito et al. 2014; Villarroya-Beltri et al. 2013b; Bellingham, Coleman, and Hill 2012). Dysregulation of various RNAs, such as miRNAs and lncRNAs, have been associated with disease, including cancer. Secretion of any of these various RNAs could contribute to modulation of the tumor microenvironment and metastasis through extracellular signaling. Therefore, identifying the full complement of circulating RNAs in normal and disease states could serve as useful biomarkers

in the diagnosis and prognosis of different types of malignancies, as well as for potentially monitoring the response to treatments (Creemers, Tijsen, and Pinto 2012; Berrondo et al. 2016). Elucidation of the potential mechanisms for selective sorting of cargo into exosomes is critical to understanding extracellular signaling by RNA.

KRAS mutations occur in approximately 34-45% of colon cancers(Wong and Cunningham 2008). In our ongoing efforts to understand the biological and pathological role of exRNAs regulated by oncogenic signaling, we utilized three isogenic colorectal cancer cell lines that differ only in the mutational status of the *KRAS* gene. The parental DLD-1 cell line contains both wild-type and G13D mutant *KRAS* alleles, while the isogenically-matched derivative cell lines contain either one mutant *KRAS* allele (DKO-1) or one WT KRAS allele (DKs-8)(Senji Shirasawa et al. 1993). We have previously shown that exosomes from mutant *KRAS* CRC cells can be transferred to wild type cells to induce cell growth and migration(Higginbotham et al. 2011b; Demory Beckler et al. 2012). Additionally, we found that the miRNA profiles of exosomes from all three cell lines are distinct from the parental cell, and segregate depending on the mutation status of KRAS (Cha et al. 2015). More recently, we identified a global downregulation of circular RNAs (circRNAs) in mutant *KRAS* cells with an inverse upregulation in exosomes (Dou et al. 2016).

In this study, we extended our RNA-seq analysis on DLD-1 CRC cells and isogenic derivatives, as well as their secreted exosomes. We conducted comprehensive analysis of long RNAs to determine whether long coding and noncoding transcripts are selectively sorted to exosomes.

4.3. Results

Distinct RNA classes are differentially distributed in exosomes

Because exosomes derived from mutant *KRAS* cell lines have distinct proteomes (Demory Beckler et al. 2012), and miRNA profiles (Cha et al. 2015) compared to both exosomes from WT cells and from parental cellular profiles, we hypothesized that *KRAS* signaling could alter sorting of long RNA species in exosomes. We performed directional RNA-seq on ribosomal RNA-depleted total RNA libraries from isogenically matched CRC cell lines that differ only in KRAS status (Table 3) and their cognate exosomes. Exosomes were isolated through a series of differential centrifugations, as previously described (Higginbotham et al. 2011b), and consisted of EVs approximately 40-130 nm in diameter (Demory Beckler et al. 2012). Sequence alignment to the human genome revealed that the mapping percentages were much higher in cellular datasets compared to exosomes. For all cellular profiles, 76-78% of paired reads were mapped to the genome, while in exosomes, mapping percentages were much lower (DKs-8=35-56%, DKO-1=49-54%, DLD-1=37-49%)(Table 9). The decreased abundance of mappable reads is not due to amplification and sequencing of contaminating RNAs but rather due to the fact that numerous mismatches were detected in exosomal RNA compared to parental RNA populations. It appears that many RNAs detected in exosomes are enriched in base modifications that could alter base reads during reverse transcription and PCR amplification.

Table 9. Percent of reads mapping to the human genome

Data	Total	Paired reads		Left mate		Right mate	
		Mapped	Unique mapped	Mapped	Unique mapped	Mapped	Unique mapped
DKO-1.cell.1	111585679	77.6%	68.1%	83.1%	72.4%	85.2%	74.2%
DKO-1.cell.2	120022437	77.3%	68.5%	82.8%	72.9%	84.8%	74.6%
DKO-1.cell.3	120636161	77.3%	67.8%	82.6%	71.9%	84.8%	73.8%
DLD-1.cell.1	122984756	77.7%	68.8%	83.1%	73.0%	85.1%	74.9%
DLD-1.cell.2	131668189	76.6%	67.5%	82.6%	72.2%	84.2%	73.6%
DLD-1.cell.3	118751417	77.6%	69.1%	83.3%	73.7%	85.0%	75.3%
DKs-8.cell.1	120608612	77.2%	67.2%	82.7%	71.6%	84.8%	73.2%
DKs-8.cell.2	126181872	77.8%	69.1%	83.3%	73.5%	85.3%	75.3%
DKs-8.cell.3	131998156	78.4%	70.2%	84.3%	74.9%	85.8%	76.2%
DKO-1.exo.1	114041294	53.9%	47.0%	64.2%	55.6%	62.3%	53.9%
DKO-1.exo.2	109044100	54.9%	47.1%	64.6%	55.0%	63.7%	54.1%
DKO-1.exo.3	125124227	48.8%	45.1%	57.4%	53.0%	56.6%	52.1%
DLD-1.exo.1	120736524	37.2%	30.4%	45.2%	36.6%	45.9%	36.7%
DLD-1.exo.2	119110502	47.2%	40.8%	57.9%	49.3%	56.3%	47.9%
DLD-1.exo.3	120405815	48.5%	40.3%	57.6%	47.1%	57.2%	46.3%
DKs-8.exo.1	120350227	35.1%	26.5%	41.3%	29.7%	41.7%	30.0%
DKs-8.exo.2	113418948	54.0%	46.7%	63.8%	54.6%	62.8%	53.6%
DKs-8.exo.3	115990041	56.1%	49.9%	67.4%	59.6%	64.8%	57.3%

After mapping to known gene regions and performing pairwise analyses between samples, cell replicates showed very high correlation (r=0. 91-0.94), while exosomal replicates were less correlated (r=0.76-0.95) (Figure 15). This is likely due to the inherent heterogeneity of purified EV preparations compounded by batch variance in sequencing runs. However, RNA profiles from exosomes compared to their parental cells showed the least correlation (DKO-1 r=0.68-0.72, DKs-8 r=0.68-0.78, DLD-1 r=0.66-0.73) (Figure 15). In cellular datasets, a high percentage of reads corresponded to annotated gene regions (~57-62%), but only a small percentage was observed in exosomal profiles (5-16%) (Figure 16a). In addition to base modifications than might alter sequence reads, some transcripts likely represent novel RNA species that map to unannotated loci.

To determine the different biotypes of RNA in cell and exosomes, we mapped reads against genotypes (Hg19, UCSC). Although the majority of reads mapped to known protein coding sequences in both cellular and exosomal datasets, we identified reads from various classes of RNA, with differential enrichment between cell and exosomes (Figure 16b). For example, we observed enrichment for transcripts derived from pseudogenes and antisense RNAs in exosomes, which was almost undetectable in cell samples (≤0.3%)(Figure 16b). Because these pseudogenes contain miRNA binding sites in their 3'UTRs, they have the potential to regulate their corresponding coding gene expression by competing for miRNA binding (Poliseno et al. 2010). The tumor suppressor gene *PTEN* and the oncogene *KRAS* both have pseudogenes, *PTENP1* and *KRAS1P*, respectively (Poliseno et al. 2010). *PTENP1* has been shown to regulate PTEN levels and exert a growth-suppressive role. Furthermore, down regulation of *PTEN* expression was associated with focal copy number losses at the *PTENP1* locus in sporadic colon cancer patient samples (Poliseno et al. 2010). A similar relationship was observed between oncogene *KRAS* and its pseudogene *KRAS1P*, where transcript levels are positively correlated in different tumors(Poliseno et al. 2010), suggesting a proto-oncogenic role for *KRAS1P*. In cell datasets, a higher percentage of transcripts corresponding to protein coding and lincRNAs were observed. These data suggest that distinct biotypes of RNAs are selectively sorted to exosomes or retained within the cell, independent of KRAS status.

Figure 15. Pairwise similarity between all samples. Spearman correlation analysis was performed on all cellular and exosomal samples. DKO-1, DLD-1 and DKs-8 cell samples showed high correlation (r=0.91-0.92; 0.91; 0.92-0.93, respectively). Exosome samples were more varied (r=0.91-0.94 DKO-1, 0.82-0.93 DLD-1, 0.76-0.95 DKs-8).

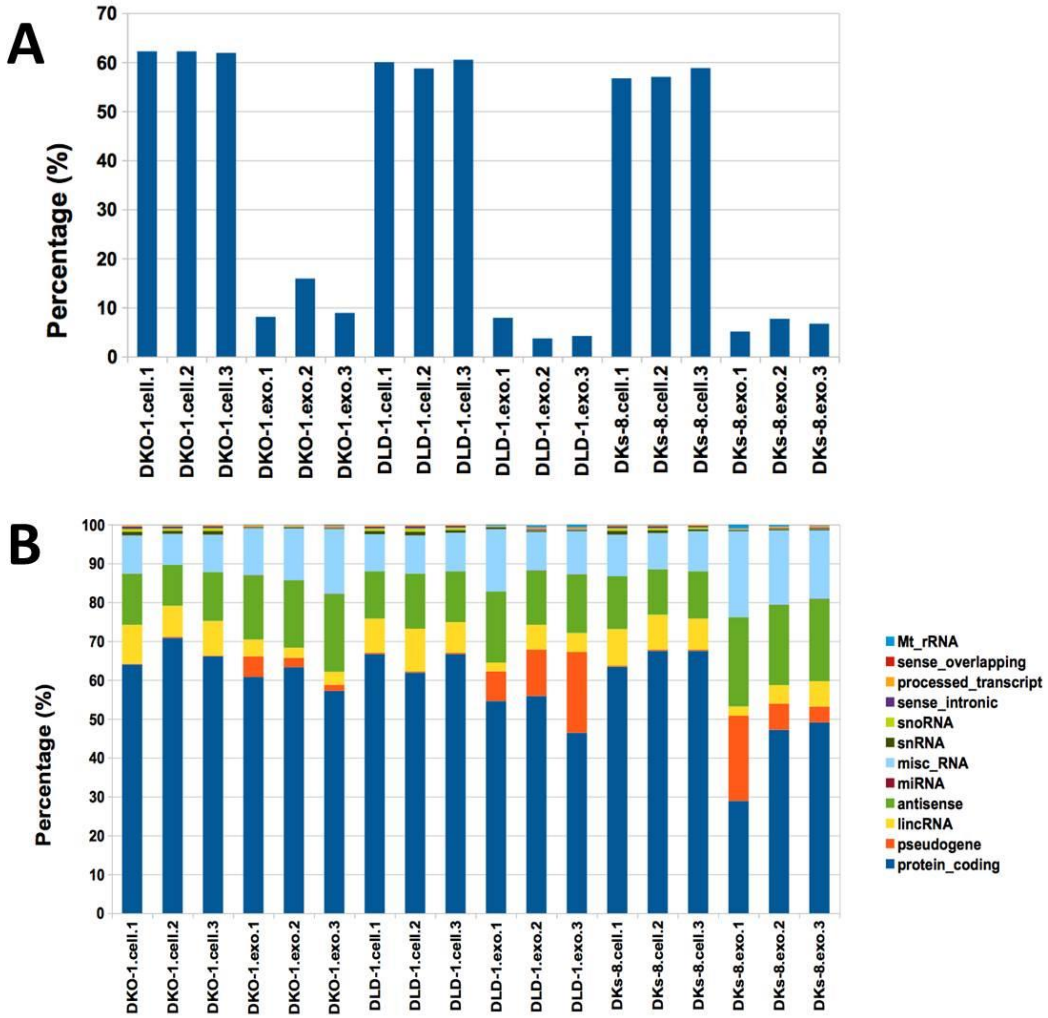

Figure 16. Long sequencing analysis of cellular and exosomal RNAs from CRC cell lines. Shown are total percentage of mapped reads to (A) gene regions, and (B) different gene types. The majority of reads map to protein coding sequences (dark blue) in both cellular and exosomal datasets. In cells, many more reads map to lincRNAs (yellow), whereas in evosomes, transcripts mapping to pseudogenes (orange) and antisense (dark green)) are increased.

To determine whether the overall long RNA profiles are distinct between cells and exosomes and between wild-type and mutant KRAS status, we performed Principal Component Analysis (PCA). PCA analysis revealed that the repertoire of long RNAs is clearly distinct when comparing parental cell RNA profiles and their secreted exosomal RNAs (Figure 17a). When comparing cellular profiles across the three lines, the RNA expression patterns clustered together, suggesting that KRAS-driven differential RNA expression is more pronounced when comparing exosomes to cells as opposed to comparing between the three cell lines. It is worth noting that the exosomal profiles varied from batch to batch, suggesting that secreted RNAs may be much more sensitive to various factors and are dynamically regulated.

Differential gene expression analyses were performed comparing cellular RNAs to their cognate exosomes, cellular RNAs between the three cell lines differing in KRAS status (mutant cell/WT cell), and exosomal RNA profiles differing in KRAS status (mutant exo/WT exo). When comparing exosomes to their parent cells, we found 16,000 RNAs enriched in DKO-1 exosomes, while only 2,400 and 1,600 RNAs were enriched in DLD-1 and DKs-8 exosomes, respectively (Figure 17b). This suggests that the diversity of transcripts when comparing mutant DKO-1 exosomes to its cognate cell line is much more different than when comparing the exosomes and cells from either WT (DKs-8) or heterozygote (DLD-1) cells, similar to what we observed in our previous miRNA profiles (Cha et al. 2015).

Differential enrichment of RNA transcripts in exosomes

We observed several transcripts to be overrepresented in exosomes compared to their parental cells. Several transcripts were much more abundant in mutant DKO-1 exosomes compared to WT DKs-8 exosomes, several of which have known roles in oncogenesis. *Rab13* was >21-fold up-regulated in DKO-1 exosomes, whereas in DKs-8 exosomes, enrichment for *Rab13* was <4-fold. We observed reads spanning the entire coding sequence for Rab13 in both cellular and exosomal datasets. Because a caveat of long RNA sequencing is that it cannot precisely distinguish between full-length or fragmented sequences, we performed RT-PCR to determine transcript lengths. PCR analysis on Poly(A)-selected RNAs confirmed the presence of full-length Rab13 in both exosomes and cells. Interestingly, RAB13 protein was also enriched in mutant exosomes in our previous proteomic analysis (Demory Beckler et al. 2012). In our libraries

In addition to protein coding sequences, we found enrichment of several lincRNAs in mutant *KRAS* exosomes. RP11-946L20.4, more recently annotated as LINC01609 in ENSEMBL, is a novel lincRNA ~456 nt in length with no characterized functions.

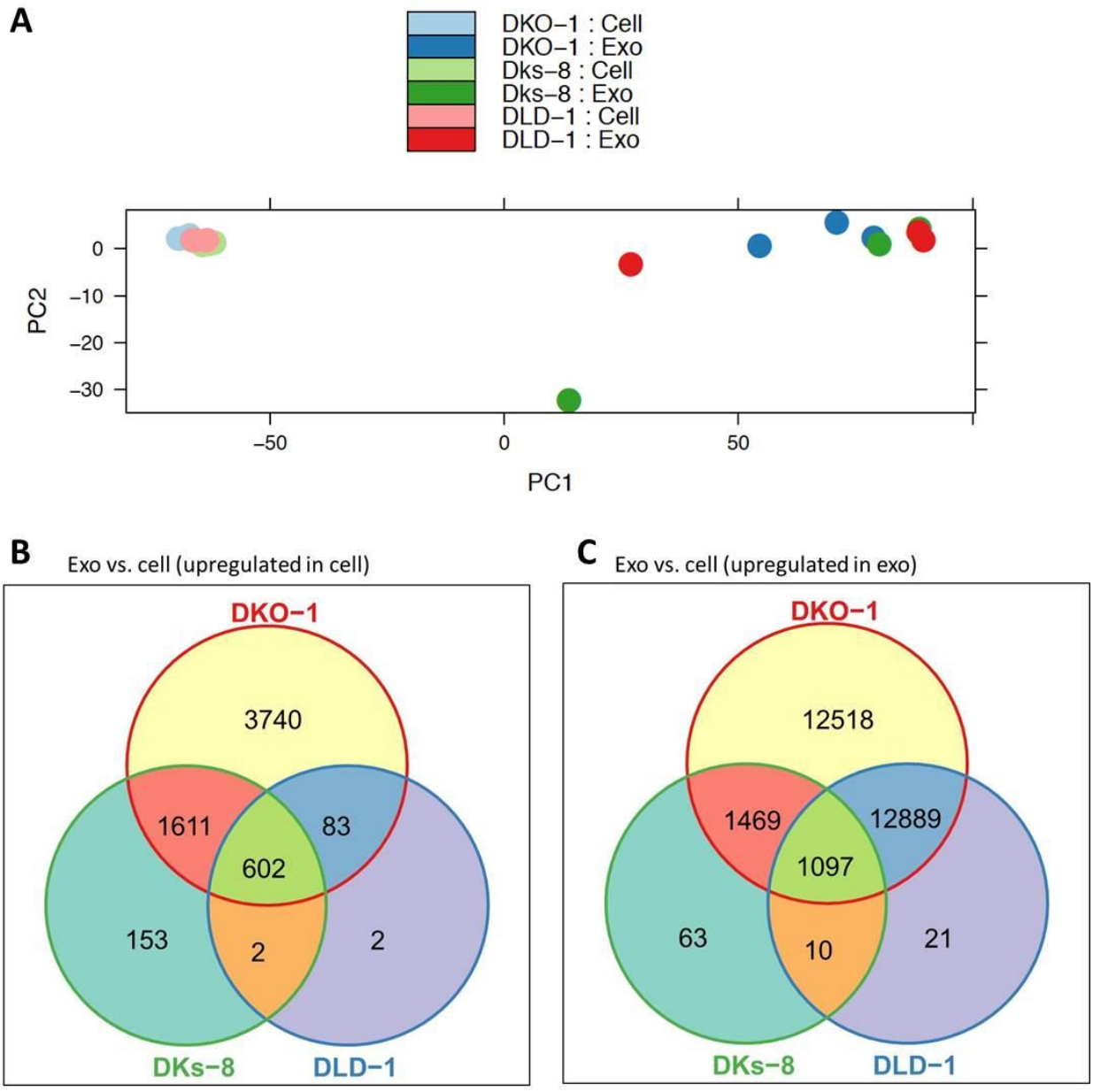

Figure 17. Long RNAs are differentially enriched in cells and exosomes. A) Comparative Principal Component Analysis (PCA) reveals that cellular long RNA profiles are clustered together and are similar, independent of KRAS status (light colors). Exosome profiles are distinct from the parent cell, and are more variable between replicates. Venn diagram shows that several RNA transcripts are differentially represented in B) cells and D) exosomes.

Table 10. Top 50 Differentially Expressed RNA Transcripts In Exosomes

Gene	Gene symbol	Detail of gene name	DKO1 E/C[1]	DLD1 E/C[1]	DKs8 E/C[1]
ENSG00000205176.2	REXO1L1	REX1, RNA exonuclease 1 homolog (S. cerevisiae)-like 1	159.17	73.06	123.48
ENSG00000253103.1	RP11-946L20.4	NULL	86.91	39.18	39.13
ENSG00000213121.2	AL590867.1	NULL	56.22	26.47	26.43
ENSG00000213121.2	AL590867.1	NULL	56.22	26.47	26.43
ENSG00000173198.4	CYSLTR1	cysteinyl leukotriene receptor 1	52.48	26.83	25.68
ENSG00000248360.3	LINC00504	NULL	47.55	24.50	26.06
ENSG00000173212.4	MAB21L3	mab-21-like 3 (C. elegans)	44.28	23.10	22.99
ENSG00000249614.1	RP11-703G6.1	NULL	41.68	18.95	19.99
ENSG00000259380.1	RP11-346D14.1	NULL	39.50	19.81	19.28
ENSG00000225914.1	XXbac-BPG154L12.4	NULL	36.74	18.25	16.90
ENSG00000069431.6	ABCC9	ATP-binding cassette, sub-family C (CFTR/MRP), member 9	30.12	14.88	15.31
ENSG00000165805.5	C12orf50	chromosome 12 open reading frame 50	28.95	14.74	13.56
ENSG00000143545.4	RAB13	RAB13, member RAS oncogene family	21.82	5.76	3.52
ENSG00000236008.1	AC011747.4	NULL	21.28	12.18	14.46
ENSG00000249348.1	UGDH-AS1	UGDH antisense RNA 1	20.70	10.24	10.96
ENSG00000249731.1	RP11-259O2.3	NULL	18.48	9.25	10.56
ENSG00000150477.10	KIAA1328	KIAA1328	17.22	9.84	10.25
ENSG00000237515.6	SHISA9	shisa homolog 9 (Xenopus laevis)	16.00	8.02	7.02
ENSG00000269821.1	KCNQ1OT1	KCNQ1 opposite strand/antisense transcript 1 (non-protein coding)	12.84	6.13	6.13
ENSG00000233251.3	AC007743.1	NULL	12.80	6.88	5.59
ENSG00000133138.15	TBC1D8B	TBC1 domain family, member 8B (with GRAM domain)	12.55	6.59	6.59
ENSG00000181458.6	TMEM45A	transmembrane protein 45A	12.39	6.00	5.53
ENSG00000115993.7	TRAK2	trafficking protein, kinesin binding 2	10.11	2.43	1.14
ENSG00000151338.14	MIPOL1	mirror-image polydactyly 1	9.63	5.33	2.02
ENSG00000173848.14	NET1	neuroepithelial cell transforming 1	9.30	1.93	1.41
ENSG00000129250.7	KIF1C	kinesin family member 1C	9.17	2.41	1.72
ENSG00000136938.8	ANP32B	acidic (leucine-rich) nuclear phosphoprotein 32 family, member B	7.26	1.36	1.59
ENSG00000153179.7	RASSF3	Ras association (RalGDS/AF-6) domain family member 3	7.04	1.37	1.02
ENSG00000143951.11	WDPCP	WD repeat containing planar cell polarity effector	4.99	2.54	3.12
ENSG00000198786.2	MT-ND5	NULL	4.82	0.40	0.45
ENSG00000079482.11	OPHN1	oligophrenin 1	4.09	2.43	2.02
ENSG00000139974.11	SLC38A6	solute carrier family 38, member 6	3.61	2.03	1.30
ENSG00000069869.11	NEDD4	neural precursor cell expressed, developmentally down-regulated 4, E3 ubiquitin protein ligase	3.13	2.01	3.31
ENSG00000140450.7	ARRDC4	arrestin domain containing 4	3.04	0.96	0.49
ENSG00000166377.15	ATP9B	ATPase, class II, type 9B	2.57	1.59	1.76
ENSG00000104164.6	BLOC1S6	biogenesis of lysosomal organelles complex-1, subunit 6, pallidin	2.43	1.53	1.93
ENSG00000137831.10	UACA	uveal autoantigen with coiled-coil domains and ankyrin repeats	2.34	0.97	0.64
ENSG00000198585.7	NUDT16	nudix (nucleoside diphosphate linked moiety X)-type motif 16	2.05	0.67	0.29
ENSG00000143850.8	PLEKHA6	pleckstrin homology domain containing, family A member 6	1.89	0.51	0.35

ENSG00000198899.2	MT-ATP6	NULL	1.87	0.24	0.26
ENSG00000130517.9	PGPEP1	pyroglutamyl-peptidase I	1.76	0.36	0.21
ENSG00000020577.9	SAMD4A	sterile alpha motif domain containing 4A	1.66	0.59	0.62
ENSG00000147224.6	PRPS1	phosphoribosyl pyrophosphate synthetase 1	1.65	0.44	0.22
ENSG00000185963.9	BICD2	bicaudal D homolog 2 (Drosophila)	1.60	2.05	0.86
ENSG00000170759.10	KIF5B	kinesin family member 5B	1.49	0.23	0.30
ENSG00000122484.8	RPAP2	RNA polymerase II associated protein 2	1.31	0.68	0.83
ENSG00000236824.1	BCYRN1	brain cytoplasmic RNA 1	1.28	0.90	2.89
ENSG00000112096.12	SOD2	superoxide dismutase 2, mitochondrial	1.27	0.80	0.93
ENSG00000245532.4	NEAT1	nuclear paraspeckle assembly transcript 1 (non-protein coding)	0.24	0.03	0.10
ENSG00000251562.3	MALAT1	metastasis associated lung adenocarcinoma transcript 1 (non-protein coding)	0.08	0.02	0.09

Abbreviations: E/C^1=reads in exosomes / reads in cell; represents fold-change in exosomes compared to cells

Extracellular transfer of RNA

Unlike miRNAs which have clear functional roles in recipient cells, functional transfer of non-coding RNAs is much more difficult to assay. To test transfer of lncRNAs, we utilized a modified version of the CRISPR-Display system (Shechner et al. 2015). This system uses a short guide RNA (sgRNA) with an engineered loop that allows insertion of any RNA sequence of interest, either coding or non-coding. The sgRNA is used to target a dead Cas9 (dCas9) protein that is fused to VP64, a transcriptional activator to reporter constructs encoding luciferase (Shechner et al. 2015). To determine whether secreted long RNAs function in recipient cells, we designed a sgRNA containing miR-100 since we know that miR-100 is enriched in exosomes. This construct served as a positive control and showed 2-fold increase in luciferase expression compared to the unmodified sgRNA (Figure 18). Baseline activation of luciferase was measured in recipient DKs-8 cells co-cultured with donor cells expressing the empty control sgRNA (sgRNA-CTL). To test a lncRNA, we inserted the colorectal neoplasia differentially expressed (CRNDE) lncRNA within the sgRNA loop region (sgRNA-CRNDE). CRNDE transcripts were up-regulated in exosomes from our RNA-seq analysis (data not shown). This construct was therefore expressed in donor cells and co-cultured with DKs-8 recipient cells expressing dCas9-VP64 and the luciferase reporter (Figure 19). In co-culture experiments where donor cells express the sgRNA-CRNDE construct, we observed a modest increase in luciferase activation (Figure 18).

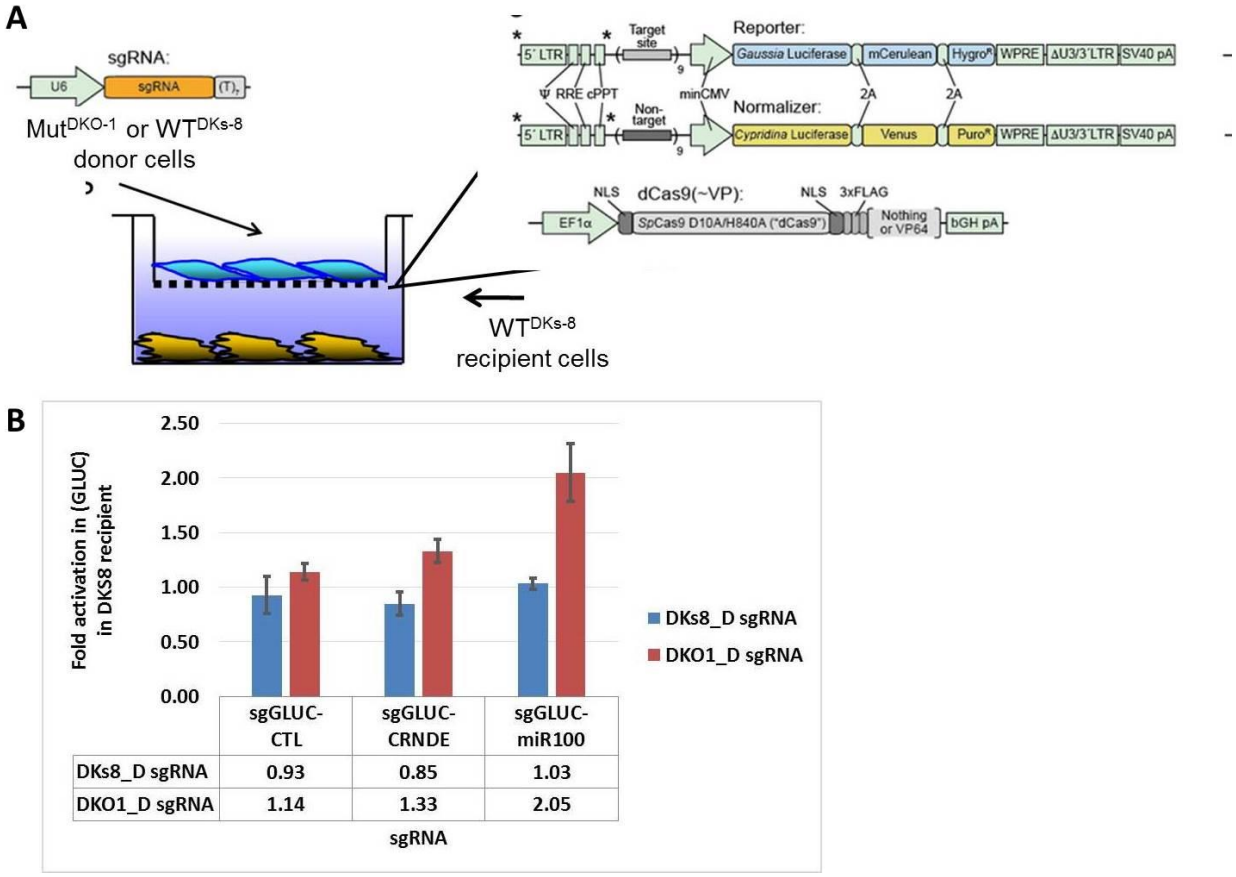

	sgGLUC-CTL	sgGLUC-CRNDE	sgGLUC-miR100
DKs8_D sgRNA	0.93	0.85	1.03
DKO1_D sgRNA	1.14	1.33	2.05

Figure 18. CRISPR-display to track RNA transfer. A) Mutant DKO-1 or wild-type DKs-8 donor cells transiently expressing a short guide RNA (sgRNA) with an engineered loop (sgGLUC-CTL) containing CRNDE (sgGLUC-CRNDE), a non-coding RNA, or miR-100 (sgGLUC-miR100), a miRNA known to traffic to mutant exosomes. Recipient cells transiently expressing dCas9 fused to VP64, a CLUC normalizer, and a GLUC reporter that is activated only in the presence of the sgRNA. B) 24-hr co-culture reveals sgRNA-mediated GLUC activation in recipient DKs-8 cells in the presence of mutant DKO-1 donor cells expressing sgGLUC-miR100 and sgGLUC-CRNDE, but not sgGLUC-CTL.

4.4. Discussion

From our analyses, we find that the RNA profiles are dramatically different in exosomes compared to the parent cells. We also find that certain transcripts are significantly enriched in mutant exosomes compared to WT-exosomes, suggesting that some RNAs are differentially regulated by *KRAS*-status. For example, *Rab13* is up-regulated in mutant DKO-1 exosomes. Interestingly, *Rab13* mRNA has been specifically detected in protrusions of metastatic breast cancer cells (Jakobsen et al. 2013). Unlike miRNA loading, which is presumably thought to occur at late endosomes (Gibbings et al. 2009), one possibility is that mRNA sorting occurs at the site of exosome release, thus favoring transcripts that localize to the periphery of the cell. Interestingly, analysis of fragmented and full-length mRNAs secreted by glioblastoma cells revealed that many of the full-length transcripts have functions in the extracellular matrix (Batagov and Kurochkin 2013). This supports the idea that mRNA loading and unloading into EVs occurs at sites that are functionally relevant.

Despite numerous reports demonstrating the presence of mRNA in biofluids, it remains controversial whether these mRNAs are full-length or fragmented transcripts(Noerholm et al. 2012). A caveat of long RNA sequencing is that it cannot distinguish between full-length or fragmented transcripts. Although an mRNA is assumed to be full-length when individual sequencing reads are mapped along the entire coding sequence, validation by RT-PCR is required to confirm the length of the transcript. In our libraries, we observed reads spanning the entire coding sequence for some mRNAs, such as Rab13, in both cellular and exosomal datasets, suggesting that these sequences are full-length. According to Ensembl, *Rab13* has five known splice variants, three of which do not code for protein. Whether certain isoforms are specifically sorted to exosomes and whether these non-coding variants that arise from coding sequences have regulatory roles remains to be determined.

Currently, it unknown what the approximate size limitation is for inclusion into EVs. Given that the majority of EV-associated RNAs fall within a size distribution of 25-700 nt from a variety of biofluids (Pegtel et al. 2010; Noerholm et al. 2012), it is likely that most of the RNA transcripts present in EVs consist of short transcripts. These could represent full-length mRNAs that are <700 nt, or alternately, truncation of longer mRNAs. In addition to size limitations, it is unknown whether secreted long RNAs are characterized by a specific fragmentation or cleavage

pattern. In certain contexts, EV-associated mRNAs are largely enriched for 3'-UTR fragments (Batagov and Kurochkin 2013). Although we did not observe enrichment of these sequences in our libraries, this may have important implications in regulating gene expression in target cells since the 3'-UTRs of mRNAs are rich in regulatory sequences. Although the precise mechanisms for how 3'UTRs are selected for secretion are unknown, one possibility is that mRNAs undergo post-transcriptional cleavage to produce 3'UTR fragments, as reported by Mercer et al. (Mercer et al. 2011). Another possibility is that exosome-associated mRNAs undergo degradation after secretion via extracellular RNases. This seems unlikely, however, as we and others observe sequencing reads spanning both full-length transcripts as well as smaller/fragmented transcripts, suggesting that these fragments are generated within the cell before sorting into exosomes.

Sorting of RNAs can occur by several processes. In certain contexts, RNAs can be trafficked to exosomes by *cis*-regulatory signals, such as sequence-specific motifs (elaborate). Furthermore, certain RNAs may localize to distinct cellular compartments based on biological functions. Our data reveal several potential long RNA CRC biomarkers and potential novel genes that, collectively, will advance our understanding of EV biology in CRC and accelerate the development of EV-based diagnostics and therapeutics."

4.5. Methods

Exosome isolation

Exosomes were isolated from conditioned medium of DKO-1, Dks-8, and DLD-1 cells, with slight modification44. Pooled media as describted above was centrifuged for 10 min at 300 × g to remove cellular debris, and the resulting supernatant was then filtered through a 0.22-um polyethersulfone filter (Nalgene, Rochester, NY) to reduce microparticle contamination. The filtrate was concentrated ~300-fold with a 100,000 molecular-weight cutoff centrifugal concentrator (Millipore). The concentrate was then subjected to high-speed centrifugation at 150,000 × g for 2 hr. The resulting exosome-enriched pellet was resuspended in PBS containing 25 mM HEPES (pH 7.2) and washed by centrifuging again at 150,000 × g for 3 hr. The wash steps were repeated a minimum of 3 times until no trace of phenol-red was detected. The resulting pellet was resuspended in PBS containing 25 mM HEPES (pH 7.2) and protein concentrations were determined with a MicroBCA kit (Pierce). The number of exosomes per ug of protein was determined by nanoparticle tracking analysis (NanoSight, Wiltshire, UK). Analysis was performed on three independent preparations of exosomes.

RNA purification

Total RNA from exosomes and cells was isolated using TRIzol (Life Technologies). In the case of exosomal RNA isolation TRIzol was incubated with 100 ul or less of concentrated exosomes for an extended 15 min incubation prior to chloroform extraction. RNA pellets were resuspended in 60 µl of RNase-free water and were then re-purified using the miRNeasy kit (QIAGEN). Final RNAs were eluted with two rounds of 30 ul water extraction.

mRNA library preparation and sequencing

Total RNA containing both long RNA as well as miRNA fractions was extracted from exosomes or cell lines using Trizol followed by miRNeasy Kit purification. Final elution was in 60 µl RNase free sterile distilled water. The concentration and integrity of the extracted total RNA was estimated by Qubit® 2.0 Fluorometer (Invitrogen, Carlsbad, California), and Agilent 2100 Bioanalyzer (Applied Biosystems, Carlsbad, CA), respectively. RNA samples with a RIN value of at least 7.0 or higher were used for further processing.

Approximately 500 ng of total RNA was required for proceeding to downstream RNA-seq applications. Briefly, a Ribo-zero Magnetic Gold rRNA removal kit (Epicenter, IIlumina Inc.) was used to remove ribosomal RNA from the total RNA. Next, first strand synthesis was performed using NEBNext RNA first strand synthesis module (New England BioLabs Inc., Ipswich, MA, USA). Immediately, directional second strand synthesis was performed using NEBNExt Ultra Directional second strand synthesis kit. Following this, cDNAs were used for standard library preparation protocol using NEBNext® DNA Library Prep Master Mix Set for Illumina® with slight modifications. Briefly, end-repair was performed followed by polyA addition and custom adapter ligation. Post-ligated materials were individually barcoded with unique in-house genomics service lab (GSL) primers. Library quality was assessed by Qubit 2.0 Fluorometer, and the library concentration was estimated by utilizing a DNA 1000 chip on an Agilent 2100 Bioanalyzer. Accurate quantification for sequencing applications was determined using the qPCR-based KAPA Biosystems Library Quantification kit (Kapa Biosystems, Inc., Woburn, MA). Each library was diluted to a final concentration of 12.5 nM and pooled equimolar prior to clustering. Paired-End (PE) sequencing was performed on all samples. Raw reads were de-multiplexed using a bcl2fastq conversion software v1.8.3 (Illumina, Inc.) with default settings.

Read Mapping

Reads sequencing quality check were performed using fastQC (v0.11.2). Results are shown in the folder: /dors/bioinfo/exrna/human/dld/rnaseq_batch3_gencode/02RawQC. Reads were mapped to the human genome hg19 (UCSC) using tophat2 (v2.0.13) with bowtie2 (version 2.2.3). Parameters for the mapping are -p 12 -g 10 -r 50 --mate-std-dev 50 --library-type fr-firststrand -G gencode.v19.annotation.gtf. The above gene annotation is form Gencode project version 19. Htseq-count (version 0.6.1p1) was used for counting with parameters: -f bam -s reverse -r name -a 10 and with the same annotation to mapping. DESeq (version 1.16.0), based on negative binomial distribution, was used to differential analysis and PCA analysis.. The trimmed mean of M values (TMM) method was used as normalization method in the analysis. The cutoffs for log2 fold change (log2FC) and PDR are |log2FC| >= 1 and FDR <= 0.001.

Chapter 5

Discussion

There is growing evidence for the regulatory roles of EV-associated exRNAs in transferring genetically encoded messages to mediate cell-to-cell communication. They have been implicated in normal developmental processes, such as fetal-maternal exchange during pregnancy (Adam et al. 2017) and antigen presentation in immunity (Graca Raposo et al. 1996), as well as in the progression of several diseases, including neurodegeneration (Lehmann et al. 2012), cardiovascular dysfunction (Bang et al. 2014), and cancer (D'Souza-Schorey and Clancy 2012). EVs are present in various body fluids, and can potentially reflect the status of the source cell, making them attractive candidates as clinical biomarkers to monitor disease (Cortez et al. 2011). Additionally, since EVs can transfer RNA and protein cargo, they are being explored as delivery vehicles for therapeutic purposes (Andaloussi et al. 2013). The field of EV and exRNA research is relatively new, and although much progress has been made in characterizing the various classes and composition of EVs, the precise mechanisms of their biogenesis and function in biological systems are still largely elusive. This section will address the significance and future directions of this work, as well as discuss the current challenges in the field.

5.1. Significance

Colon cancer is the third most commonly diagnosed cancer, and is the second leading cause of cancer-related deaths in the US (www.cancer.org). Activating mutations in *KRAS* occur in approximately 34-45% of colon cancers (Wong and Cunningham 2008), and can predict resistance to anti-EGFR monoclonal antibodies used to treat patients with metastatic CRC. Given the potential of cancer-derived secreted RNAs in driving formation of the pre-metastatic niche, identifying the mechanisms for cargo sorting into EVs is critical to understand extracellular signaling by RNA. In these studies, we comprehensively examined the composition of RNAs from exosomes and cells of isogenic CRC cell lines that differ only in *KRAS* status. We show that certain RNAs are selectively enriched (described below) in mutant *KRAS*-derived exosomes compared to the parent cell and to wild type exosomes. *KRAS* status-specific patterns of secreted

RNAs support the idea of using exRNAs as potential biomarkers in CRC, and suggest a new mode of action for oncogenic *KRAS*. These studies have not only expanded our understanding of *KRAS* mutations in CRC, but also provided insights to novel elements of exRNA regulated by oncogenic signaling that are important for cancer biology and are of general relevance to multiple fields.

In our small RNA sequencing analyses, we identified transcripts from various classes of RNA, with enrichment of specific biotypes in cellular and exosomal profiles. Given that microRNAs (miRNAs) are perhaps the best characterized class of small noncoding RNAs that have been detected in extracellular fluids (Valadi et al. 2007), and they have the potential to regulate hundreds of transcripts within a genome(Bartel 2004), our initial studies focused on defining extracellular miRNAs. We found that specific miRNAs are preferentially secreted by mutant *KRAS* cells (*miR-100)*, whereas other miRNAs, such as *miR-320* family members, are secreted in exosomes, independent of *KRAS* status. Neutral sphingomyelinase inhibition caused accumulation of both miRNAs only in mutant *KRAS* cells, suggesting that lipid composition and/or RNA export may be differentially regulated by oncogenic signaling. Finally, secretion of *miR-100* from mutant *KRAS* donor cells mediated target repression in wild type recipient cells. This supports the hypothesis that extracellular miRNAs can function beyond the cell of origin.

In our long RNA sequence analyses, we found that circular RNAs (circRNAs) are globally downregulated in mutant *KRAS* cells, but in contrast, tended to be more abundant in exosomes, suggesting a potential involvement of circRNAs in oncogenesis. SMARCA5 was among the top ten circRNA candidates enriched in exosomes. Interestingly, linear SMARCA5 is targeted by miR-100 which subsequently promotes epithelial to mesenchymal transition (D. Chen et al. 2014). It remains to be determined whether *miR-100* can also regulate levels of circular SMARCA5. Although the precise function(s) of circRNAs remains largely unknown, it has been proposed that they can act as miRNA sponges (Hansen, Kjems, and Damgaard 2013).Whether circRNA in exosomes might function as competing exogenous RNA in recipient cells will require further investigation.

In addition to circRNAs, we identified enrichment of pseudogenes and antisense transcripts in exosomes compared to cellular profiles. The most upregulated transcript in exosomes was RNA exonuclease 1 homologue (S. cerevisiae)-like 1 gene (REXO1L1), a pseudogene cluster that lies within a 12 kb tandem repeat in 8q21.2, one of the largest variable

number tandem repeat arrays in the human genome (Warburton et al. 2008). REXO1L1 is a member of the 3'-5' exonuclease DEDD superfamily that has been associated with inflammatory diseases (Hollox and Hoh 2014) and RNA virus infections (Barber et al. 2017). Although additional experiments are needed to elucidate the functional consequences of these transcripts, pseudogenes can be processed into siRNAs and function through the RNAi pathway, or can act as miRNA decoys, and thus, have the potential to regulate their cognate coding gene (Poliseno et al. 2010; Pink et al. 2011).

Overall, we present comprehensive data to identify the broad and diverse classes of exRNAs secreted in exosomes and we show that exports of specific RNAs are differentially regulated by oncogenic *KRAS.* Understanding the correlation of exRNAs with disease progression and therapy response will facilitate the use of liquid biopsies as a clinical tool for cancer diagnosis, precluding the need for direct tumor sampling. Furthermore, since exRNAs can potentially regulate a variety of cellular processes in the tumor microenvironment and the tumor proper, we can use this information to develop novel drug delivery vehicles and alternate therapies for CRC.

5.2. Discussion and future directions

Composition of RNA secreted in EVs

Differential RNA expression is more prominently affected in secreted RNAs than in the parent cells. This could reflect the dynamic regulation of RNAs that are often times kept at steady states, and thus, masked witihin the cell. This also suggests that cells may implement mechanisms to selectively export certain RNAs to maintain specific growth or gene expression states. In the context of miRNAs, this is consistent with a recent report that found that the cellular levels of certain miRNAs could be maintained, despite changes in the abundance of its target, likely through a "miRNA relocation effect" where unbound miRNAs that are in excess have the potential to be sorted to exosomes(Squadrito et al. 2014) . As circRNAs are reported to bind miRNAs to function as a miRNA sponge (Hansen et al. 2013), it was demonstrated that exogenous expression of *miR-7* in MCF-7 cells caused significant decrease in exosomal levels of CDR1as exosomes (Y. Li et al. 2015), a circRNA known to act as a *miR-7* sponge (Hansen et al. 2013). This suggests that sorting of circRNAs to EVs are regulated, at least in part, by changes in

expression level of its associated miRNA in the parent cell.

In contrast to cellular profiles which displayed an enrichment of miRNA sequences (~70%), miRNA sequences make up just a small percentage in exosomes (<18%) compared to other class of ncRNA (repeat sequences, tRNAs, rRNAs). It was recently shown that lymphoma cell-derived exosomes are predominantly enriched with human yRNA fragments (Koppers-Lalic et al. 2014). Although the biological relevance of yRNAs in exosomes is unclear, yRNAs are known to be specifically packed in enveloped and non-eveloped viral particles (Garcia et al. 2009). The selective enrichment of these RNAs from the host cell into viral particles and exosomes implies that common molecular mechanisms may be regulating their packaging. Given that the RNA profiles in exosomes do not simply reflect the cell or origin, it remains to be determined exactly how these small ncRNAs are trafficked to exosomes.

Despite initial reports identifiying mRNAs in EVs (Valadi et al. 2007), it remains controversial whether these mRNAs are full-length or fragmented transcripts(Noerholm et al. 2012). Intact mammalian mRNAs vary in length from 400 nucleotides (nt) up to >100,000 nt, with the average transcript being ~2,100 nt in size (Lander et al. 2001). However, the majority of EV-associated RNAs profiled from various normal and cancer cell lines indicate secreted RNAs with a size distribution between 25-700 nt (Pegtel et al. 2010; Noerholm et al. 2012). This suggests that most of the RNA transcripts present in these EVs consist of short transcripts. In the case of mRNAs, the simplest explanation would be that EVs contain full-length mRNAs that are <700 nt, or alternately, are enriched for truncated/fragmented mRNAs. Truncation of mRNAs appears to be tightly regulated as recent studies have shown that RNA transcripts can undergo widespread post-transcriptional cleavage to produce a range of small coding and noncoding RNAs (Mercer et al. 2010). At present, it is unknown whether secreted RNAs are characterized by a specific fragmentation or cleavage pattern.

In certain contexts, EV-associated mRNAs are largely enriched for 3'-UTR fragments (Batagov and Kurochkin 2013). This may have important implications in regulating gene expression in target cells since the 3'-UTRs of mRNAs are rich in regulatory sequences. As a single 3'-UTR contains many miRNA binding sites, transfer of 3'UTR-derived mRNA fragments have the potential to directly compete with endogenous miRNAs for the silencing machinery, leading to deregulation of mRNAs (Wilczynska and Bushell 2015). Although the precise mechanisms for how 3'UTRs are selected for secretion are unknown, one possibility is

that mRNAs undergo post-transcriptional cleavage to produce 3'UTR fragments, as reported by Mercer et al. (Mercer et al. 2011). Another possibility is that exosome-associated mRNAs undergo degradation after secretion via extracellular RNases. This seems unlikely, however, as we and others observe sequencing reads spanning both full-length transcripts as well as smaller/fragmented transcripts, suggesting that these fragments are generated within the cell before sorting into exosomes.

RNA sorting into EVs

The mechanisms that dictate RNA sorting into EVs is not fully understood, particularly for long RNAs. For miRNAs, however, one possibility is through association with AGO proteins, a component of the RISC machinery previously found to associate with late endosomes (Gibbings et al. 2009). Work done in collaboration with the Weaver lab has shown that Ago2 sorting into exosomes is regulated by MEK-ERK signaling downstream of activated KRAS (McKenzie et al. 2016). In this context, secretion of Ago2 in exosomes was observed in wild type *KRAS* cells (Appendix A.12), but aberrant KRAS signaling prevented Ago2 association with MVBs and inclusion into exosomes via phosphorylation on serine-387 (S387) (McKenzie et al. 2016). Ago2 depletion in wild type *KRAS* cells did not affect cellular miRNA levels, but levels of exosomal miRNAs were significantly reduced (e.g. *let-7a* and *miR-100)*(Appendix A.12)(McKenzie et al. 2016). This is consistent with others that report decreased export of EV-associated miRNAs upon Ago2 knock out(Guduric-Fuchs et al. 2012).

Despite low levels of exosomal Ago2 secreted by mutant *KRAS* CRC cells, comparable levels of miRNA and other small RNA were observed in mutant *KRAS* exosomes (Cha et al. 2015), suggesting Ago2-independent mechanisms are also likely to control sorting of miRNAs. Protein alignment of human AGOs indicates serine-387, a phosphorylation site that has been shown to affect slicer activity and its localization to P-bodies (Horman et al. 2013; Zeng et al. 2008), is conserved in Ago-1, -2 and -4, but is absent in Ago3 (Appendix A.13). Interestingly, Ago3 is more abundant in mutant *KRAS* exosomes (Appendix A.13). It is tempting to speculate that Ago3 might be resistant to oncogenic signaling and can thus preferentially associate with endosomes. Although circulating Ago2 has been abundantly detected in non-vesicular protein complexes (Arroyo et al. 2011; Andrey Turchinovich et al. 2011) as well as EVs (Melo et al. 2014; McKenzie et al. 2016, 2), it remains to be determined whether Ago1, 3 or 4 have roles in

exRNA communication.

In addition to the Ago proteins, other RBPs may regulate exRNA sorting to EVs. For example, *miR-223-3p* was shown to be dependent on Y-Box protein 1 (YBX1) in HEK293T cells (Shurtleff et al. 2016). Interestingly, circulating *miR-223* is one of the most abundant miRNAs associated with HDL in patients with familial hypercholesterolemia(Vickers et al. 2011). In addition to miRNAs, YBX1 has also been shown to associate with other small RNAs, including tRNA fragments and snoRNAs (Goodarzi et al. 2015; Liu et al. 2015, 1), raising the possibility that YBX1 contributes to the secretion of various RNA classes. Another mechanism may be through sequence-specific motifs that direct RNA trafficking by interaction with specific RNA binding proteins. This has been described in T-cells where miRNAs containing the 'GGAG' motif are preferentially sorted to exosomes (Squadrito et al. 2014). Although we and others did not find enrichment of sequences containing the 'GAGG'exo-motif in EVs (Cha et al. 2015; Shurtleff et al. 2016) , it is likely that sequence-specific export depends on the donor cell, or only affects a subpopulation of RNAs.

Another sorting mechanism may be through post-transcriptional modifications of the RNA. It was demonstrated that miRNAs in exosomes were preferentially 3'-uridylated, while 3'-adenylated miRNA species were mostly cell-enriched (Koppers-Lalic et al. 2014). We also observed enrichment of miRNAs containing non-templated A in cellular samples; however, we did not detect significanty more 3'-uridylated miRNAs in exosomes (Appendix A.6). Interestingly, non-templated terminal nucleotide additions (NTAs) predispose miRNA association with RISC (Burroughs et al. 2010), affecting their target effectiveness. Furthermore, adenylation and uridylation affect the stability and activity of some miRNAs, and in certain context, U-addition is destabilizing (Burroughs et al. 2010). Consistent with this, exRNAs reportedly have shorter half-lives (~1.8x shorter) than cellular RNAs (Batagov, Kuznetsov, and Kurochkin 2011). Apart from human and viral miRNAs, adenylation and uridylation can also occur at the 3' ends of yRNA fragments. These uridylated yRNA fragments are also reportedly enriched in exosomes(Koppers-Lalic et al. 2014). Exactly how uridylated RNAs are trafficked to exosomes is unknown. In mammalian cells, ZCCHC11 (TUT4) and ZCCHC6 (TUT7) mediate terminal U-additions to miRNAs (Thornton et al. 2014). One possibility is that these TUTs are exported to EVs, although quantitative proteomic analysis argues against the presence of such enzymes in exosomes (Exocarta: http://www.exocarta.org/). Another possibility is that 3'

uridylated miRNAs have a higher turnover in cells compared to exosomes. The functional significance of 3'-end modifications in secreted RNAs remains to be determined.

Specific lipids appear to be another important component regulating the sorting of RNA into EVs. It has been shown that miRNAs secreted in exosomes are dependent on hydrolysis of sphingomyelin into ceramide by neutral sphingomyelinase 2 (N. Kosaka et al. 2010). Ceramide is also abundant in lipid rafts (Hannun and Obeid 2002), and certain RNAs demonstrate enhanced affinity to these phospholipid bilayers (Khvorova et al. 1999). It was demonstrated that RNAs with a specific secondary structure bind to rafted (liquid-ordered) domains in sphingomyelin-cholesterol-phosphatidylcholine vesicles that resemble liquid-ordered lipid phase of exosomal membranes (Janas, Janas, and Yarus 2006). Furthermore, posttranscriptional changes involving hydrophobic modifications, such as methlation of *miR-125b* by NSun2, can also increase the lipophilicity of RNAs (Hussain et al. 2013). It remains to be determined whether the sorting of longer RNA species into EVs are also regulated by lipids.

The physiological role of exRNA

The functional role of secreted RNAs has been controversial since the first reports of exRNA. Although numerous studies have shown that miRNAs can be transferred to neighboring cells in experimental settings, evidence demonstrating transfer of miRNAs in biologically significant quantities *in vivo* is lacking.

Although the number of studies suggesting functional roles for exRNAs in disease as well as in normal development is growing, it is not well understood mechanistically how they target and function in distant cells *in vivo*. EV-mediated miRNA transfer between cells has been proposed to be a mechanism for intercellular signaling, and EV-associated miRNAs in biofluids have been implicated as potential minimally invasive biomarkers for multiple human diseases. However, standard preparations of EVs reportedly do not contain many RNA molecules, at least this is true of miRNAs (Chevillet et al. 2014). This may require a reevaluation of current models suggesting cell-to-cell communication by exRNA. The stoichiometric analysis will be valuable for the study of the various classes of RNAs associated with EVs and RNPs, and determining the physiologically relevant concentration of exRNAs. In general, long RNAs make up a minority of the RNAs secreted in EVs; however, some lncRNAs are suspected to have functional activity at low copy numbers (Wilusz, Sunwoo, and Spector 2009).

To conclude, there is promising potential for EV-derived exRNAs as disease biomarkers and their applications in cancer immunotherapy. However, the mechanisms involved in EV secretion and cargo loading, as well as their interaction with target cells is only beginning to emerge. It is important to recognize that apart from mRNAs and miRNAs, other RNA classes may act as signaling molecules.Essential questions that remain are (2) the major sources of various RNAs in bodily fluids, (3) detection and measurement of RNAs in circulation, (4) selectivity of export and import, (5) sensitivity and specificity of export to target cells, and (6) cell-, tissue-, organ-, and organism-wide impacts of exRNA mediated cell-to-cell communication.

APPENDIX

A

Supplemental figures

A.1.

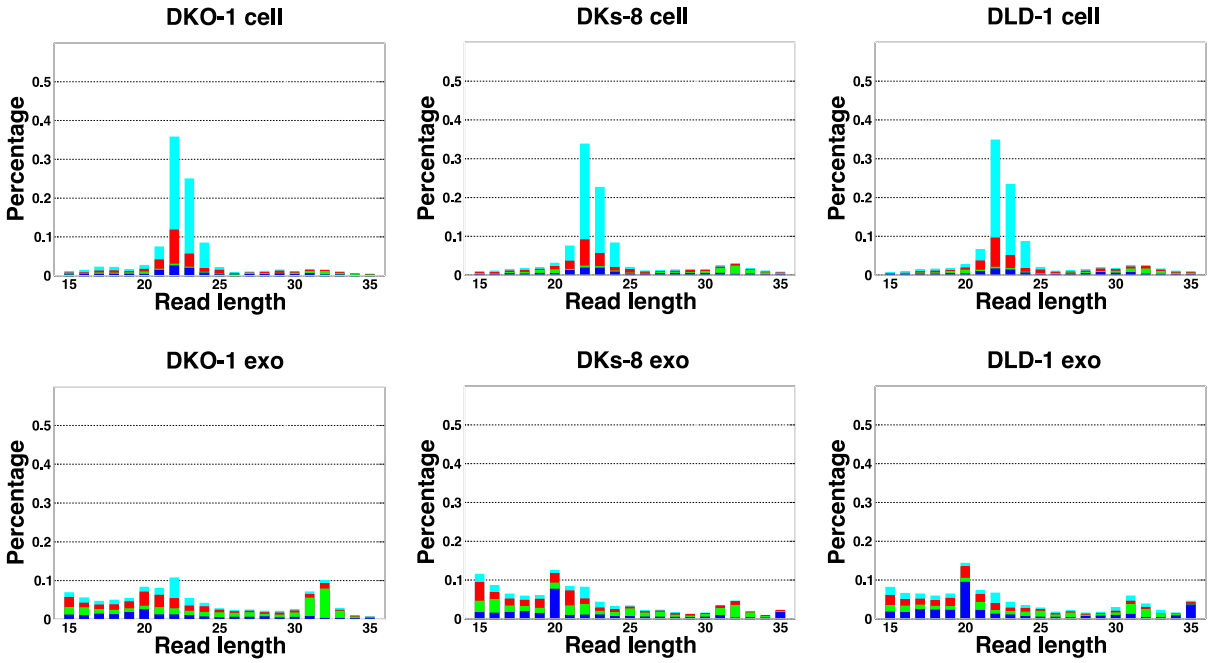

A.1. Length distribution of small RNA reads to genome. The small RNA read length distribution from serum starved cells and from purified exosomes was determined, as well as the 5' nucleotide from each read. The pattern from total cellular small RNA is consistent with primarily miRNA reads, the distribution from exosomes is much broader, encompassing a number of small reads derived from many sources (see Figure 1C,D). Colors represent nucleotide identify for the 5' base, T (cyan), A (red), G (green), and C (blue).

A.2.

A.2. Spearman correlations between miRNA expression profiles in cells and exosomes. Pairwise similarity between the RNA sequencing data sets derived from cells and exosomes. Spearman correlations are shown between the cell samples (R=0.93-0.96), between exosomes and cognate cells (R=0.64-0.83) and between exosome samples (R=0.74-0.86). Results were generated using the DESeq "pooled" method.

A.3.

A.3. Spearman correlations between miRNA expression profiles in cells and exosomes. Similar to Supplemental Figure 2A. Differential analysis using the DESeq "per condition" method.

A.4.

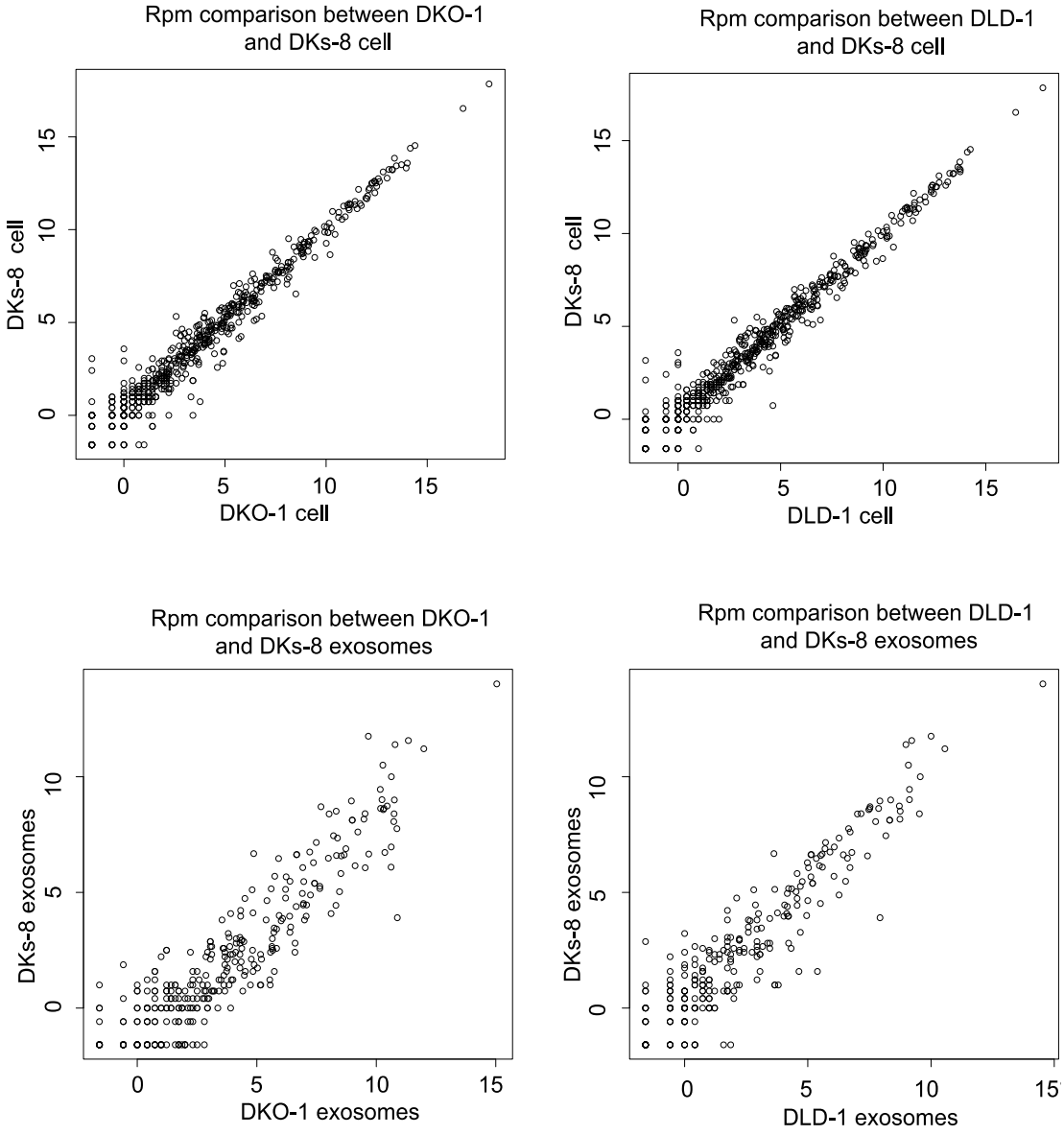

A.4. Spearman correlations between miRNA expression profiles in cells (top) and exosomes (bottoms) in reads per million (RPM).

A.5.

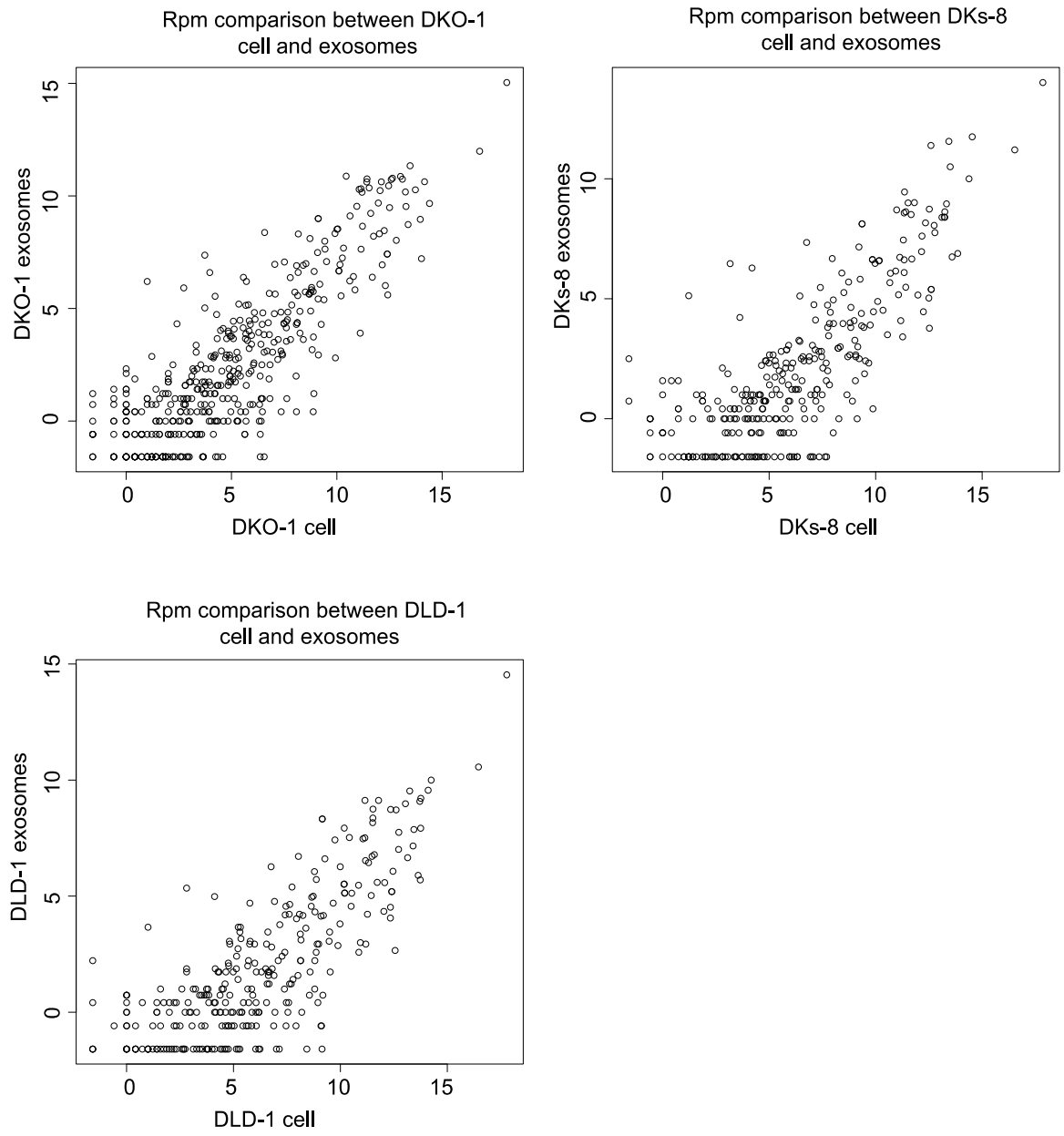

A.5. Spearman correlations comparing miRNA expression profiles in exosomes to parent cell in RPM.

A.6.

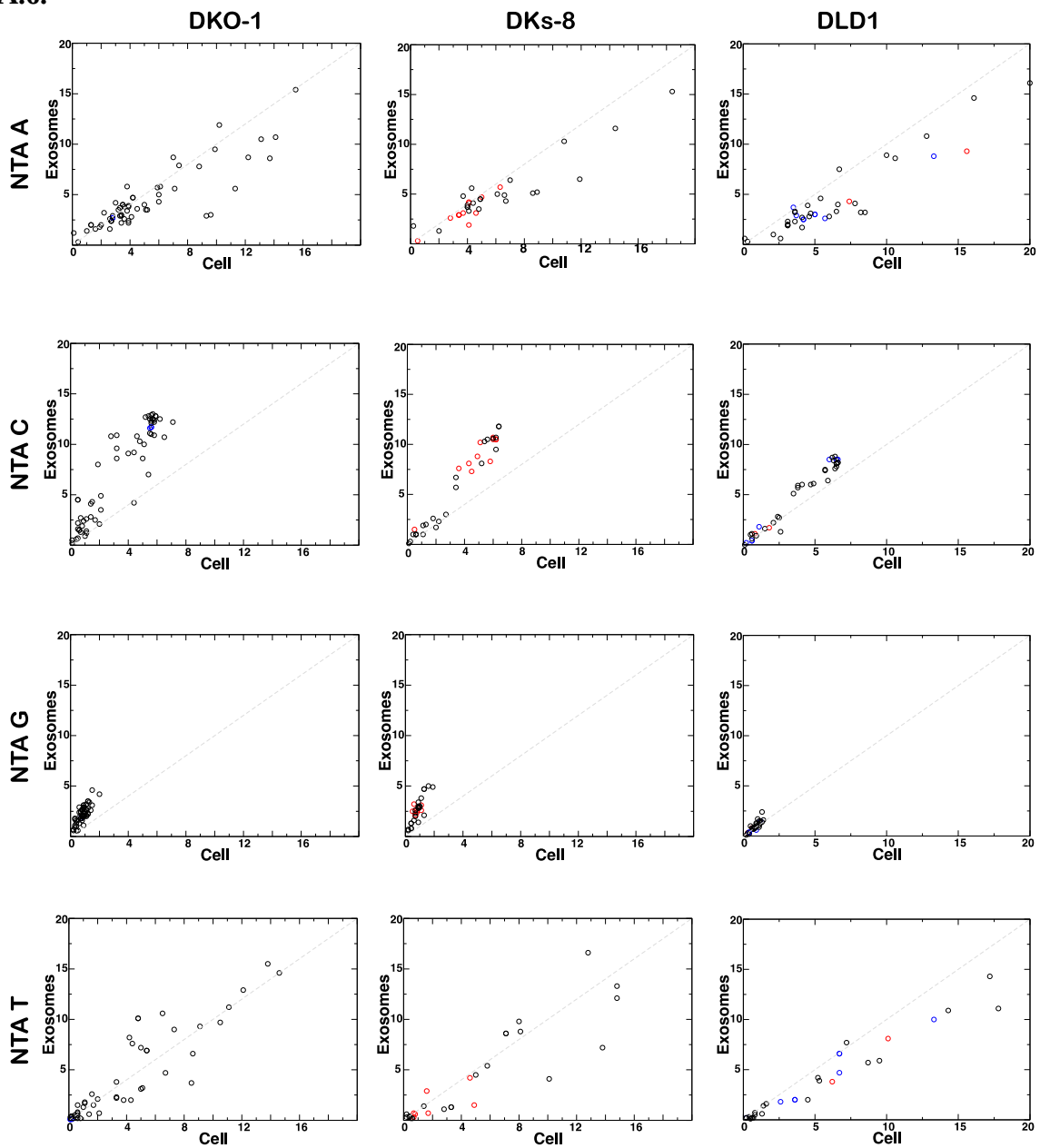

A.6. Non-Templated Addition (NTA) of Nucleotides to 3' Ends of miRNAs. 3' NTA of A-tailed miRNAs are enriched in cells independent of *KRAS* status whereas NTA of C-residues are more abundant in wild type *KRAS* DKs-8 exosomes. miRNAs with read counts ≥ 500 reads in both cells and exosomes were used in the analysis. Reads mapping to hairpin sequences were considered as templated miRNAs (untrimmed). Reads ≥18 nucleotides that did not map to hairpin or genome sequences were trimmed one nucleotide at the 3'-termini and mapped again to hairpin sequences. This was repeated three times to account for NTA's extending up to three nucleotides from the 3'-terminus. miRNAs significantly enriched in exosomes or cells are represented by red and blue circles, respectively.

A.7.

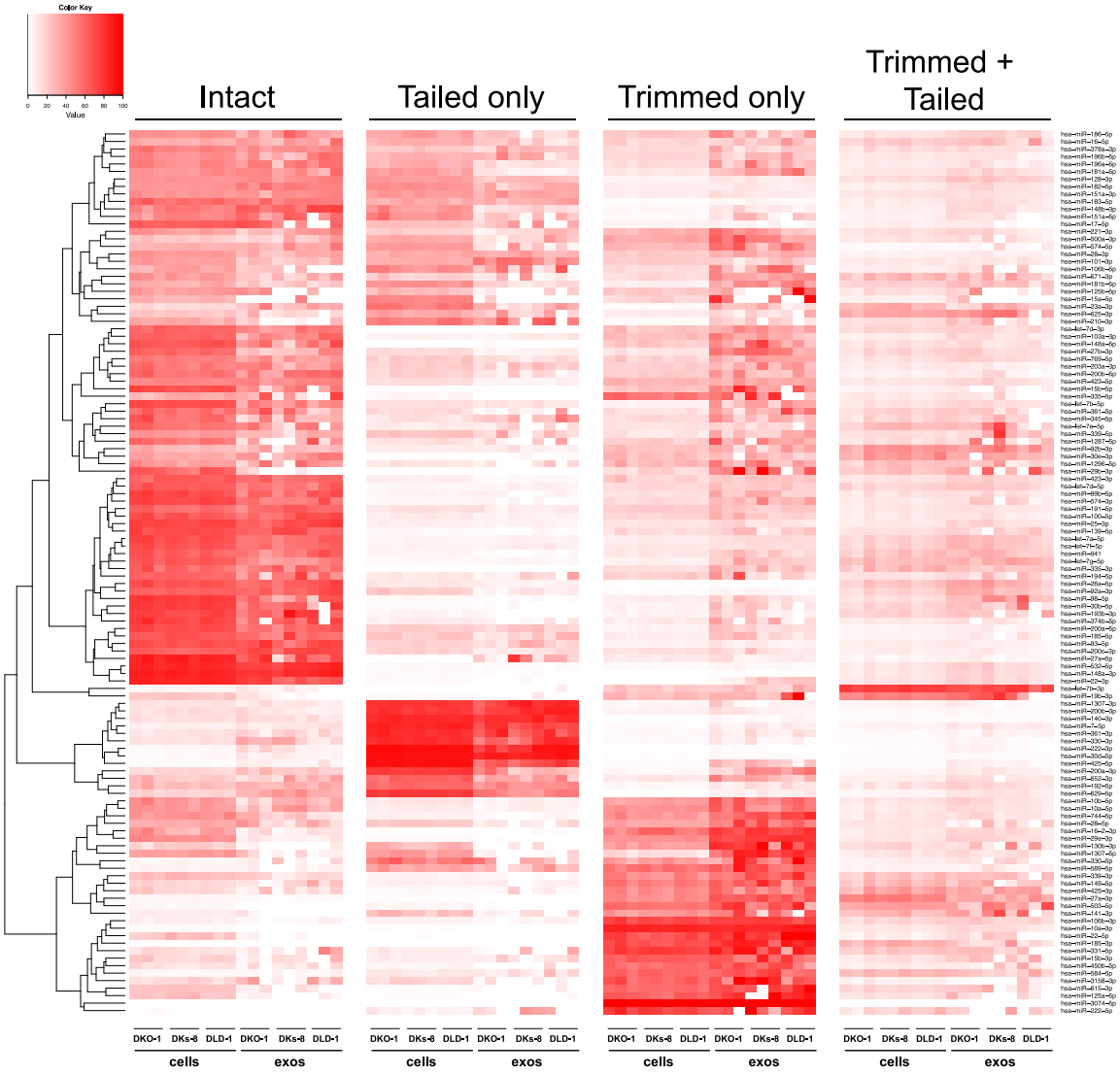

A.7. Comparison of miRNA 3' trimming and tailing between cells and exosomes. Heat maps show the extent of either 3' nucleotide additions (tailing) or 3' resection (trimming) compared to full length miRNA sequences (intact).

A.8.

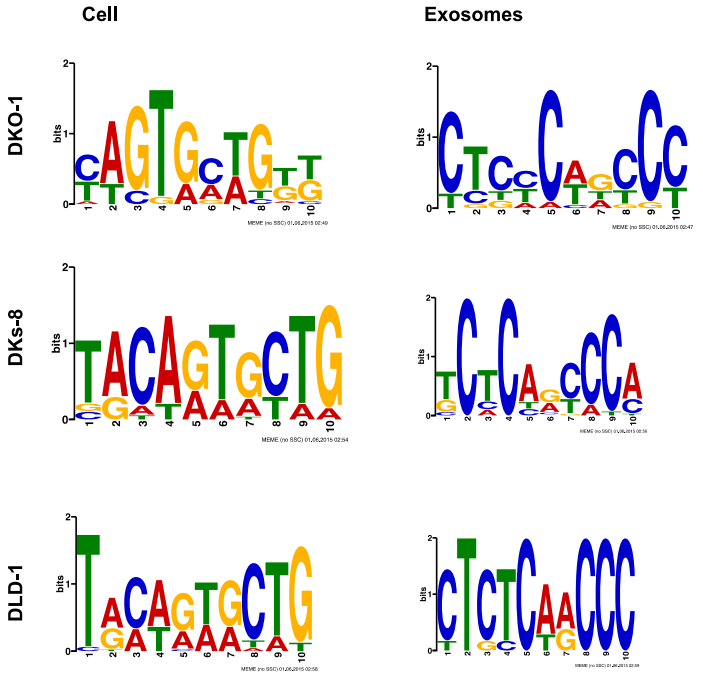

	Top 1	
	sites	e-value
Upregulated in DKO-1 exo	51	1.5e-009
Upregulated in DKO-1 cell	28	1.5e-007
Upregulated in DKs-8 exo	22	1.7e-010
Upregulated in DKs-8 cell	19	7.6e-007
Upregulated in DLD-1 exo	8	2.3e-003
Upregulated in DLD-1 cell	23	3.3e-012

A.8. MEME analysis of miRNA sequence in exosomes. MEME analysis was performed to attempt to identify sequence motifs that might target miRNAs for export into exosomes. The top most abundant motifs found in miRNAs in Tables 1 and 2 are shown for both cells and exosomes from either DKO-1, DKs-8 or DLD-1 cell lines.

A.9.

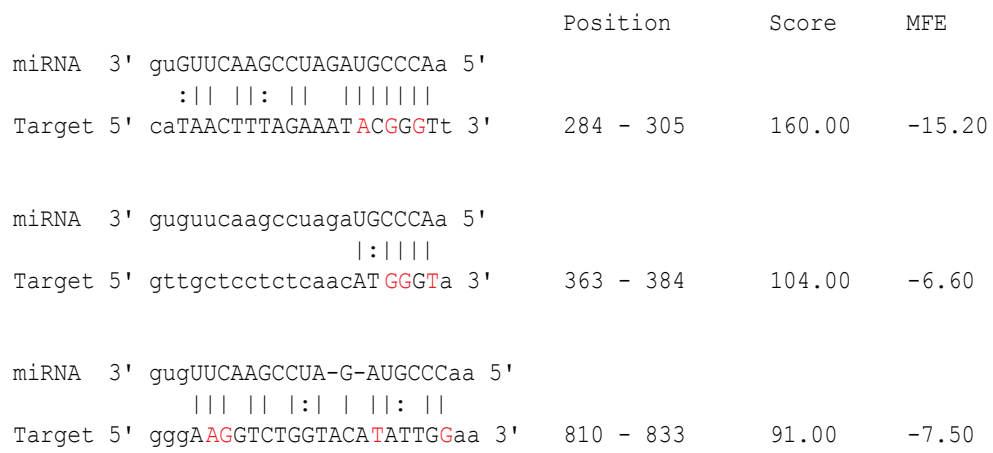

A.9. *miR-100* binding sites in the mTOR 3'UTR. *miR-100* binding sites within the mTOR 3'UTR. Mutated nucleotides indicated in red (oligonucleotide sequences in Supplemental Table 5).

A.10.

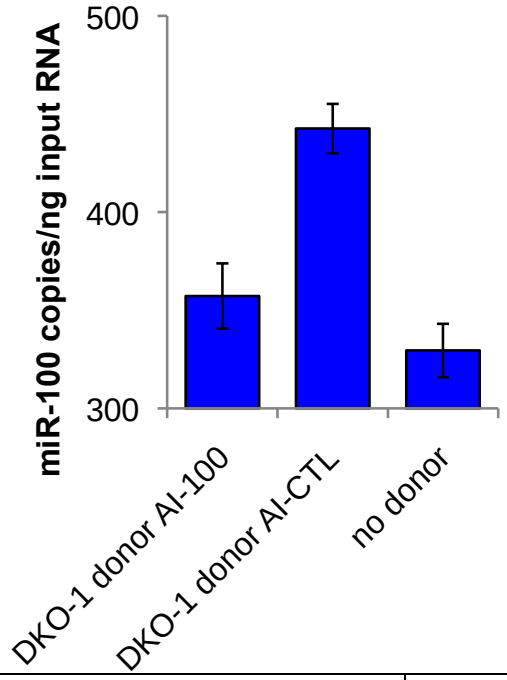

	miR-100 (copies/ng input RNA)	std dev
DKO-1 donor AI-100	357.230	16.654
DKO-1 donor AI-CTL	442.581	12.590
no donor	329.480	13.615

A.10. Presence of mutant DKO-1 donor cells augments *miR-100* levels in DKs-8 recipient cells. Taqman qRT-PCR for *miR-100*. *miR-100* levels increased by approximately 114 copies in recipient cells cultured with DKO-1 donor cells pre-treated with control antagomir (AI-CTL) compared to recipient cells cultured without donor cells. Pre-treatment of mutant DKO-1 donor cells with *miR-100* antagomir inhibitor (AI-100) attenuated this effect. Absolute levels of *miR-100* determined by standard curve generation of synthetically derived *miR-100* (see Methods).

A.11.

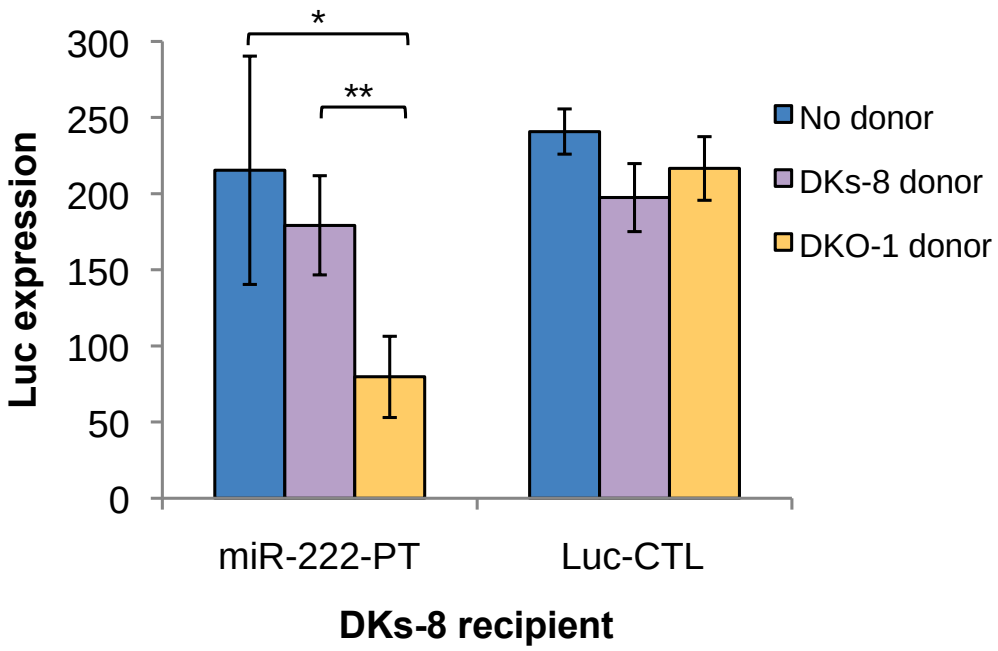

A.11. Transfer of extracellular miRNAs by mutant DKO-1 cells promotes target repression in wild type DKs-8 cells. Transwell co-culture of DKs-8 recipient cells with or without DKs-8 or DKO-1 donor cells. Luciferase (Luc) expression was measured in DKs-8 recipient cells expressing Luc fused to three perfectly complementary synthetic *miR-222* target sites (miR-222-PT)

A.12.

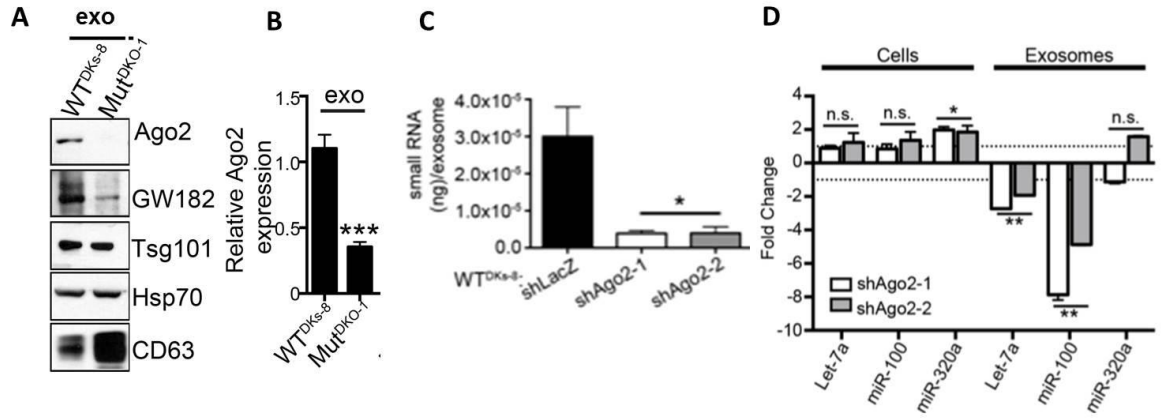

A.12. Mutant *KRAS* affects Ago2 secretion in exosomes. A) Representative western blots and B) quantification from three independent experiments of equal numbers of exosomes secreted from WT (DKs-8) and mutant (DKO-1) cells. Bands normalized to Hsp70. Ago2 depletion by shRNAs C)significantly decreases the amount of small RNA in exosomes. D) qRT-PCR of select miRNAs from exosomal and cellular RNA isolated from control and Ago2-knock down cells. Graph shows fold change compared to shLacZ. Dotted lines indicate no fold change. *p<0.05; **p<0.01; ***p<0.001; n.s., not significant.

This figure is part of a published manuscript:

McKenzie, Andrew J., Daisuke Hoshino, Nan Hyung Hong, Diana J. Cha, Jeffrey L. Franklin, Robert J. Coffey, James G. Patton, and Alissa M. Weaver. 2016. "KRAS-MEK Signaling Controls Ago2 Sorting into Exosomes." *Cell Reports* 15 (5): 978–87. doi:10.1016/j.celrep.2016.03.085.

A.13.

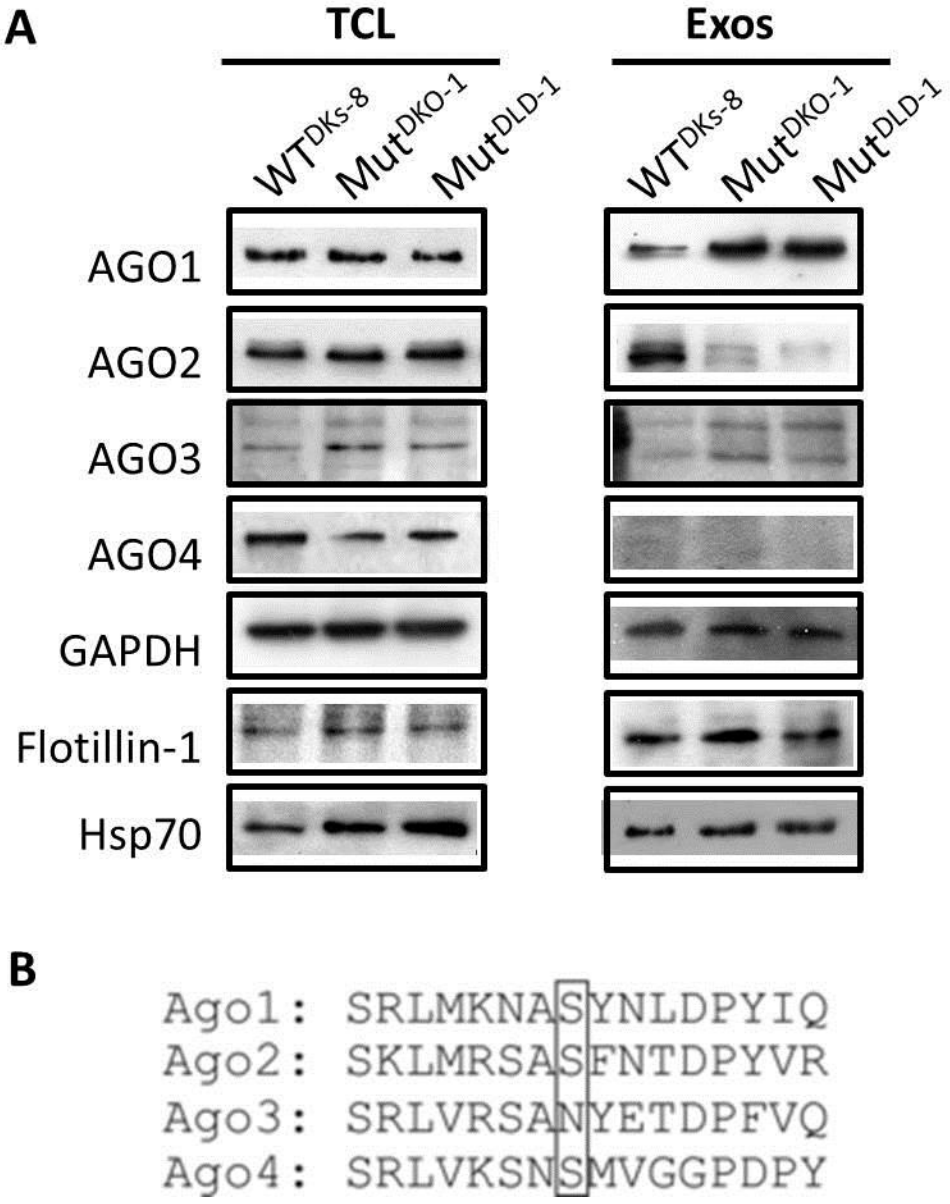

A.13. Differential AGO expression in CRC exosomes compared to cells. A) Representative expression levels of AGO1-4 are comparable in total cell lystates (left panel) by western blot analysis. AGO2 is enriched in wild-type *KRAS* (DKs-8) exosomes, while AGO1 and AGO3 levels are increased in mutant DKO-1 and DLD-1 exosomes (right panel). AGO4 was not detected in exosomal lysates. **B)** Protein sequence alignment of human AGOs at amino acids 380-395. AGO3 lacks the serine-387 phosphorylation site.

REFERENCES

Adam, Stefanie, Omar Elfeky, Vyjayanthi Kinhal, Suchismita Dutta, Andrew Lai, Nanthini Jayabalan, Zarin Nuzhat, Carlos Palma, Gregory E. Rice, and Carlos Salomon. 2017. "Review: Fetal-Maternal Communication via Extracellular Vesicles – Implications for Complications of Pregnancies." *Placenta*. Accessed April 5. doi:10.1016/j.placenta.2016.12.001.

Alvarez-Garcia, Ines, and Eric A. Miska. 2005. "MicroRNA Functions in Animal Development and Human Disease." *Development* 132 (21): 4653–62. doi:10.1242/dev.02073.

Andaloussi, Samir EL, Imre Mäger, Xandra O. Breakefield, and Matthew JA Wood. 2013. "Extracellular Vesicles: Biology and Emerging Therapeutic Opportunities." *Nature Reviews Drug Discovery* 12 (5): 347–357.

Arroyo, Jason D., John R. Chevillet, Evan M. Kroh, Ingrid K. Ruf, Colin C. Pritchard, Donald F. Gibson, Patrick S. Mitchell, et al. 2011. "Argonaute2 Complexes Carry a Population of Circulating microRNAs Independent of Vesicles in Human Plasma." *Proceedings of the National Academy of Sciences* 108 (12): 5003–8. doi:10.1073/pnas.1019055108.

Ashwal-Fluss, Reut, Markus Meyer, Nagarjuna Reddy Pamudurti, Andranik Ivanov, Osnat Bartok, Mor Hanan, Naveh Evantal, Sebastian Memczak, Nikolaus Rajewsky, and Sebastian Kadener. 2014. "circRNA Biogenesis Competes with Pre-mRNA Splicing." *Molecular Cell* 56 (1): 55–66. doi:10.1016/j.molcel.2014.08.019.

Baccarini, Alessia, Hemangini Chauhan, Thomas J. Gardner, Anitha D. Jayaprakash, Ravi Sachidanandam, and Brian D. Brown. 2011. "Kinetic Analysis Reveals the Fate of a MicroRNA Following Target Regulation in Mammalian Cells." *Current Biology* 21 (5): 369–76. doi:10.1016/j.cub.2011.01.067.

Bachmayr-Heyda, Anna, Agnes T. Reiner, Katharina Auer, Nyamdelger Sukhbaatar, Stefanie Aust, Thomas Bachleitner-Hofmann, Ildiko Mesteri, Thomas W. Grunt, Robert Zeillinger, and Dietmar Pils. 2015. "Correlation of Circular RNA Abundance with Proliferation - Exemplified with Colorectal and Ovarian Cancer, Idiopathic Lung Fibrosis, and Normal Human Tissues." *Scientific Reports* 5 (January). doi:10.1038/srep08057.

Balkom, Bas W. M. van, Almut S. Eisele, D. Michiel Pegtel, Sander Bervoets, and Marianne C. Verhaar. 2015. "Quantitative and Qualitative Analysis of Small RNAs in Human Endothelial Cells and Exosomes Provides Insights into Localized RNA Processing, Degradation and Sorting." *Journal of Extracellular Vesicles* 4 (0). http://www.journalofextracellularvesicles.net/index.php/jev/article/view/26760.

Bang, Claudia, Sandor Batkai, Seema Dangwal, Shashi Kumar Gupta, Ariana Foinquinos, Angelika Holzmann, Annette Just, et al. 2014. "Cardiac Fibroblast–derived microRNA Passenger Strand-Enriched Exosomes Mediate Cardiomyocyte Hypertrophy." *Journal of Clinical Investigation* 124 (5): 2136–46. doi:10.1172/JCI70577.

Barber, John C. K., Andrew J. Sharp, Edward J. Hollox, and Christine Tyson. 2017. "Copy Number Variation of the REXO1L1 Gene Cluster; Euchromatic Deletion Variant or Susceptibility Factor?" *European Journal of Human Genetics* 25 (1): 8–9. doi:10.1038/ejhg.2016.104.

Bartel, David P. 2004. "MicroRNAs: Genomics, Biogenesis, Mechanism, and Function." *Cell* 116 (2): 281–97. doi:10.1016/S0092-8674(04)00045-5.

Batagov, Arsen O., and Igor V. Kurochkin. 2013. "Exosomes Secreted by Human Cells Transport Largely mRNA Fragments That Are Enriched in the 3′-Untranslated Regions." *Biology Direct* 8 (1): 12. doi:10.1186/1745-6150-8-12.

Batagov, Arsen O., Vladimir A. Kuznetsov, and Igor V. Kurochkin. 2011. "Identification of Nucleotide Patterns Enriched in Secreted RNAs as Putative Cis-Acting Elements Targeting Them to Exosome Nano-Vesicles." *BMC Genomics* 12 (3): S18. doi:10.1186/1471-2164-12-S3-S18.

Beatty, Meabh, Jasenka Guduric-Fuchs, Eoin Brown, Stephen Bridgett, Usha Chakravarthy, Ruth Esther Hogg, and David Arthur Simpson. 2014. "Small RNAs from Plants, Bacteria and Fungi within

the Order Hypocreales Are Ubiquitous in Human Plasma." *BMC Genomics* 15 (1). doi:10.1186/1471-2164-15-933.

Bellingham, Shayne A., Bradley M. Coleman, and Andrew F. Hill. 2012. "Small RNA Deep Sequencing Reveals a Distinct miRNA Signature Released in Exosomes from Prion-Infected Neuronal Cells." *Nucleic Acids Research* 40 (21): 10937–49. doi:10.1093/nar/gks832.

Bergsmedh, Anna, Anna Szeles, Marie Henriksson, Anders Bratt, M. Judah Folkman, Anna-Lena Spetz, and Lars Holmgren. 2001. "Horizontal Transfer of Oncogenes by Uptake of Apoptotic Bodies." *Proceedings of the National Academy of Sciences* 98 (11): 6407–11. doi:10.1073/pnas.101129998.

Bernstein, Emily, Amy A. Caudy, Scott M. Hammond, and Gregory J. Hannon. 2001. "Role for a Bidentate Ribonuclease in the Initiation Step of RNA Interference." *Nature* 409 (6818): 363–66. doi:10.1038/35053110.

Berrondo, Claudia, Jonathan Flax, Victor Kucherov, Aisha Siebert, Thomas Osinski, Alex Rosenberg, Christopher Fucile, Samuel Richheimer, and Carla J. Beckham. 2016. "Expression of the Long Non-Coding RNA HOTAIR Correlates with Disease Progression in Bladder Cancer and Is Contained in Bladder Cancer Patient Urinary Exosomes." *PLOS ONE* 11 (1): e0147236. doi:10.1371/journal.pone.0147236.

Bissig, Christin, and Jean Gruenberg. 2014. "ALIX and the Multivesicular Endosome: ALIX in Wonderland." *Trends in Cell Biology* 24 (1): 19–25. doi:10.1016/j.tcb.2013.10.009.

Bitarte, Nerea, Eva Bandres, Valentina Boni, Ruth Zarate, Javier Rodriguez, Marisol Gonzalez-Huarriz, Ines Lopez, et al. 2011. "MicroRNA-451 Is Involved in the Self-Renewal, Tumorigenicity, and Chemoresistance of Colorectal Cancer Stem Cells." *STEM CELLS* 29 (11): 1661–71. doi:10.1002/stem.741.

Black, Douglas L. 2003. "Mechanisms of Alternative Pre-Messenger RNA Splicing." Review-article. *Http://Dx.doi.org/10.1146/annurev.biochem.72.121801.161720*. November 28. http://www.annualreviews.org/doi/10.1146/annurev.biochem.72.121801.161720.

Bobrie, Angélique, Sophie Krumeich, Fabien Reyal, Chiara Recchi, Luis F. Moita, Miguel C. Seabra, Matias Ostrowski, and Clotilde Théry. 2012. "Rab27a Supports Exosome-Dependent and -Independent Mechanisms That Modify the Tumor Microenvironment and Can Promote Tumor Progression." *Cancer Research* 72 (19): 4920–30. doi:10.1158/0008-5472.CAN-12-0925.

Boelens, Mirjam C., Tony J. Wu, Barzin Y. Nabet, Bihui Xu, Yu Qiu, Taewon Yoon, Diana J. Azzam, et al. 2014. "Exosome Transfer from Stromal to Breast Cancer Cells Regulates Therapy Resistance Pathways." *Cell* 159 (3): 499–513. doi:10.1016/j.cell.2014.09.051.

Bolukbasi, Mehmet Fatih, Arda Mizrak, Gokhan Baris Ozdener, Sibylle Madlener, Thomas Ströbel, Erdogan Pekcan Erkan, Jian-Bing Fan, Xandra O Breakefield, and Okay Saydam. 2012. "miR-1289 and 'Zipcode'-like Sequence Enrich mRNAs in Microvesicles." *Molecular Therapy. Nucleic Acids* 1 (2): e10. doi:10.1038/mtna.2011.2.

Brosnan, Christopher Andrew, and Olivier Voinnet. 2011. "Cell-to-Cell and Long-Distance siRNA Movement in Plants: Mechanisms and Biological Implications." *Current Opinion in Plant Biology*, Cell signalling and gene regulation, 14 (5): 580–87. doi:10.1016/j.pbi.2011.07.011.

Burger, Koert N.J. 2000. "Greasing Membrane Fusion and Fission Machineries." *Traffic* 1 (8): 605–13. doi:10.1034/j.1600-0854.2000.010804.x.

Burroughs, A. M., Y. Ando, M. J. L. de Hoon, Y. Tomaru, T. Nishibu, R. Ukekawa, T. Funakoshi, et al. 2010. "A Comprehensive Survey of 3' Animal miRNA Modification Events and a Possible Role for 3' Adenylation in Modulating miRNA Targeting Effectiveness." *Genome Research* 20 (10): 1398–1410. doi:10.1101/gr.106054.110.

Calin, George A., and Carlo M. Croce. 2006. "MicroRNA Signatures in Human Cancers." *Nature Reviews Cancer* 6 (11): 857–66. doi:10.1038/nrc1997.

Capel, Blanche, Amanda Swain, Silvia Nicolis, Adam Hacker, Michael Walter, Peter Koopman, Peter Goodfellow, and Robin Lovell-Badge. 1993. "Circular Transcripts of the Testis-Determining Gene< I> Sry</i> in Adult Mouse Testis." *Cell* 73 (5): 1019–1030.

Cha, Diana J., Jeffrey L. Franklin, Yongchao Dou, Qi Liu, James N. Higginbotham, Michelle Demory Beckler, Alissa M. Weaver, et al. 2015. "KRAS-Dependent Sorting of miRNA to Exosomes." *eLife* 4 (July): e07197. doi:10.7554/eLife.07197.

Chakrabortty, Sudipto K., Ashwin Prakash, Gal Nechooshtan, Stephen Hearn, and Thomas R. Gingeras. 2015. "Extracellular Vesicle-Mediated Transfer of Processed and Functional RNY5 RNA." *RNA* 21 (11): 1966–79. doi:10.1261/rna.053629.115.

Chen, Dahu, Yutong Sun, Yuan Yuan, Zhenbo Han, Peijing Zhang, Jinsong Zhang, M. James You, et al. 2014. "miR-100 Induces Epithelial-Mesenchymal Transition but Suppresses Tumorigenesis, Migration and Invasion." *PLoS Genet* 10 (2): e1004177. doi:10.1371/journal.pgen.1004177.

Chen, X., H. Liang, J. Zhang, K. Zen, and C.-Y. Zhang. 2013. "microRNAs Are Ligands of Toll-like Receptors." *RNA* 19 (6): 737–39. doi:10.1261/rna.036319.112.

Chen, Xi, Yi Ba, Lijia Ma, Xing Cai, Yuan Yin, Kehui Wang, Jigang Guo, et al. 2008. "Characterization of microRNAs in Serum: A Novel Class of Biomarkers for Diagnosis of Cancer and Other Diseases." *Cell Research* 18 (10): 997–1006. doi:10.1038/cr.2008.282.

Cheng, Zhuan-Fen, and Murray P. Deutscher. 2005. "An Important Role for RNase R in mRNA Decay." *Molecular Cell* 17 (2): 313–18. doi:10.1016/j.molcel.2004.11.048.

Chevillet, John R., Qing Kang, Ingrid K. Ruf, Hilary A. Briggs, Lucia N. Vojtech, Sean M. Hughes, Heather H. Cheng, et al. 2014. "Quantitative and Stoichiometric Analysis of the microRNA Content of Exosomes." *Proceedings of the National Academy of Sciences* 111 (41): 14888–93. doi:10.1073/pnas.1408301111.

Chiba, Mitsuru. 2012. "Exosomes Secreted from Human Colorectal Cancer Cell Lines Contain mRNAs, microRNAs and Natural Antisense RNAs, That Can Transfer into the Human Hepatoma HepG2 and Lung Cancer A549 Cell Lines." *Oncology Reports*, August. doi:10.3892/or.2012.1967.

Chong, Mark M. W., Guoan Zhang, Sihem Cheloufi, Thomas A. Neubert, Gregory J. Hannon, and Dan R. Littman. 2010. "Canonical and Alternate Functions of the microRNA Biogenesis Machinery." *Genes & Development* 24 (17): 1951–60. doi:10.1101/gad.1953310.

Christov, C. P., E. Trivier, and T. Krude. 2008. "Noncoding Human Y RNAs Are Overexpressed in Tumours and Required for Cell Proliferation." *British Journal of Cancer* 98 (5): 981–88. doi:10.1038/sj.bjc.6604254.

Christov, Christo P., Timothy J. Gardiner, Dávid Szüts, and Torsten Krude. 2006. "Functional Requirement of Noncoding Y RNAs for Human Chromosomal DNA Replication." *Molecular and Cellular Biology* 26 (18): 6993–7004. doi:10.1128/MCB.01060-06.

Chugani, D. C., L. H. Rome, and N. L. Kedersha. 1993. "Evidence That Vault Ribonucleoprotein Particles Localize to the Nuclear Pore Complex." *Journal of Cell Science* 106 (1): 23–29.

Cocquerelle, Claude, Benedicte Mascrez, D. Hetuin, and Bernard Bailleul. 1993. "Mis-Splicing Yields Circular RNA Molecules." *The FASEB Journal* 7 (1): 155–160.

Cocucci, Emanuele, and Jacopo Meldolesi. 2015. "Ectosomes and Exosomes: Shedding the Confusion between Extracellular Vesicles." *Trends in Cell Biology* 25 (6): 364–72. doi:10.1016/j.tcb.2015.01.004.

Colombo, Marina, Catarina Moita, Guillaume van Niel, Joanna Kowal, James Vigneron, Philippe Benaroch, Nicolas Manel, Luis F. Moita, Clotilde Théry, and Gra\cca Raposo. 2013. "Analysis of ESCRT Functions in Exosome Biogenesis, Composition and Secretion Highlights the Heterogeneity of Extracellular Vesicles." *Journal of Cell Science*, jcs–128868.

Colombo, Marina, Graça Raposo, and Clotilde Théry. 2014. "Biogenesis, Secretion, and Intercellular Interactions of Exosomes and Other Extracellular Vesicles." *Annual Review of Cell and Developmental Biology* 30 (1): 255–89. doi:10.1146/annurev-cellbio-101512-122326.

Conley, Andrew, Valentina R. Minciacchi, Dhong Hyun Lee, Beatrice S. Knudsen, Beth Y. Karlan, Luigi Citrigno, Giuseppe Viglietto, et al. 2016. "High-Throughput Sequencing of Two Populations of Extracellular Vesicles Provides an mRNA Signature That Can Be Detected in the Circulation of Breast Cancer Patients." *RNA Biology*, November, 1–12. doi:10.1080/15476286.2016.1259061.

Conn, Simon J., Katherine A. Pillman, John Toubia, Vanessa M. Conn, Marika Salmanidis, Caroline A.

Phillips, Suraya Roslan, Andreas W. Schreiber, Philip A. Gregory, and Gregory J. Goodall. 2015. "The RNA Binding Protein Quaking Regulates Formation of circRNAs." *Cell* 160 (6): 1125–34. doi:10.1016/j.cell.2015.02.014.

Consortium, The ENCODE Project. 2004. "The ENCODE (ENCyclopedia Of DNA Elements) Project." *Science* 306 (5696): 636–40. doi:10.1126/science.1105136.

Cook, Kate B., Hilal Kazan, Khalid Zuberi, Quaid Morris, and Timothy R. Hughes. 2011. "RBPDB: A Database of RNA-Binding Specificities." *Nucleic Acids Research* 39 (suppl_1): D301–8. doi:10.1093/nar/gkq1069.

Cortez, Maria Angelica, Carlos Bueso-Ramos, Jana Ferdin, Gabriel Lopez-Berestein, Anil K. Sood, and George A. Calin. 2011. "MicroRNAs in Body Fluids—the Mix of Hormones and Biomarkers." *Nature Reviews Clinical Oncology* 8 (8): 467–77. doi:10.1038/nrclinonc.2011.76.

Creemers, Esther E., Anke J. Tijsen, and Yigal M. Pinto. 2012. "Circulating MicroRNAs Novel Biomarkers and Extracellular Communicators in Cardiovascular Disease?" *Circulation Research* 110 (3): 483–95. doi:10.1161/CIRCRESAHA.111.247452.

Demory Beckler, M., J. N. Higginbotham, J. L. Franklin, A.-J. Ham, P. J. Halvey, I. E. Imasuen, C. Whitwell, M. Li, D. C. Liebler, and R. J. Coffey. 2012. "Proteomic Analysis of Exosomes from Mutant KRAS Colon Cancer Cells Identifies Intercellular Transfer of Mutant KRAS." *Molecular & Cellular Proteomics* 12 (2): 343–55. doi:10.1074/mcp.M112.022806.

Deng, Zhongbin, Jingyao Mu, Michael Tseng, Binks Wattenberg, Xiaoying Zhuang, Nejat K. Egilmez, Qilong Wang, et al. 2015. "Enterobacteria-Secreted Particles Induce Production of Exosome-like S1P-Containing Particles by Intestinal Epithelium to Drive Th17-Mediated Tumorigenesis." *Nature Communications* 6 (April): 6956. doi:10.1038/ncomms7956.

Dhahbi, Joseph M., Stephen R. Spindler, Hani Atamna, Dario Boffelli, Patricia Mote, and David I. K. Martin. 2013. "5′-YRNA Fragments Derived by Processing of Transcripts from Specific YRNA Genes and Pseudogenes Are Abundant in Human Serum and Plasma." *Physiological Genomics* 45 (21): 990–98. doi:10.1152/physiolgenomics.00129.2013.

Dhahbi, Joseph M., Stephen R. Spindler, Hani Atamna, Amy Yamakawa, Dario Boffelli, Patricia Mote, and David IK Martin. 2013. "5′ tRNA Halves Are Present as Abundant Complexes in Serum, Concentrated in Blood Cells, and Modulated by Aging and Calorie Restriction." *BMC Genomics* 14: 298. doi:10.1186/1471-2164-14-298.

Di Vizio, Dolores, Matteo Morello, Andrew C. Dudley, Peter W. Schow, Rosalyn M. Adam, Samantha Morley, David Mulholland, et al. 2012. "Large Oncosomes in Human Prostate Cancer Tissues and in the Circulation of Mice with Metastatic Disease." *The American Journal of Pathology* 181 (5): 1573–84. doi:10.1016/j.ajpath.2012.07.030.

Dieci, Giorgio, Anastasia Conti, Aldo Pagano, and Davide Carnevali. 2013. "Identification of RNA Polymerase III-Transcribed Genes in Eukaryotic Genomes." *Biochimica et Biophysica Acta (BBA) - Gene Regulatory Mechanisms*, Transcription by Odd Pols, 1829 (3–4): 296–305. doi:10.1016/j.bbagrm.2012.09.010.

Djebali, Sarah, Carrie A. Davis, Angelika Merkel, Alex Dobin, Timo Lassmann, Ali Mortazavi, Andrea Tanzer, et al. 2012. "Landscape of Transcription in Human Cells." *Nature* 489 (7414): 101–8. doi:10.1038/nature11233.

Dou, Yongchao, Diana J. Cha, Jeffrey L. Franklin, James N. Higginbotham, Dennis K. Jeppesen, Alissa M. Weaver, Nripesh Prasad, et al. 2016. "Circular RNAs Are down-Regulated in KRAS Mutant Colon Cancer Cells and Can Be Transferred to Exosomes." *Scientific Reports* 6 (November): 37982. doi:10.1038/srep37982.

D'Souza-Schorey, Crislyn, and James W. Clancy. 2012. "Tumor-Derived Microvesicles: Shedding Light on Novel Microenvironment Modulators and Prospective Cancer Biomarkers." *Genes & Development* 26 (12): 1287–99. doi:10.1101/gad.192351.112.

Elsik, Christine G., Deepak R. Unni, Colin M. Diesh, Aditi Tayal, Marianne L. Emery, Hung N. Nguyen, and Darren E. Hagen. 2016. "Bovine Genome Database: New Tools for Gleaning Function from the Bos Taurus Genome." *Nucleic Acids Research* 44 (D1): D834–39. doi:10.1093/nar/gkv1077.

Emmrich, Stephan, Mareike Rasche, Jennifer Schöning, Christina Reimer, Sarva Keihani, Aliaksandra Maroz, Ying Xie, et al. 2014. "miR-99a/100~125b Tricistrons Regulate Hematopoietic Stem and Progenitor Cell Homeostasis by Shifting the Balance between TGFβ and Wnt Signaling." *Genes & Development* 28 (8): 858–74. doi:10.1101/gad.233791.113.

Escrevente, Cristina, Sascha Keller, Peter Altevogt, and Júlia Costa. 2011. "Interaction and Uptake of Exosomes by Ovarian Cancer Cells." *BMC Cancer* 11 (March): 108. doi:10.1186/1471-2407-11-108.

Eulalio, Ana, Felix Tritschler, and Elisa Izaurralde. 2009. "The GW182 Protein Family in Animal Cells: New Insights into Domains Required for miRNA-Mediated Gene Silencing." *RNA* 15 (8): 1433–42. doi:10.1261/rna.1703809.

Fabbri, M., A. Paone, F. Calore, R. Galli, E. Gaudio, R. Santhanam, F. Lovat, et al. 2012. "PNAS Plus: MicroRNAs Bind to Toll-like Receptors to Induce Prometastatic Inflammatory Response." *Proceedings of the National Academy of Sciences* 109 (31): E2110–16. doi:10.1073/pnas.1209414109.

Faller, William J., Thomas J. Jackson, John R. P. Knight, Rachel A. Ridgway, Thomas Jamieson, Saadia A. Karim, Carolyn Jones, et al. 2015. "mTORC1-Mediated Translational Elongation Limits Intestinal Tumour Initiation and Growth." *Nature* 517 (7535): 497–500. doi:10.1038/nature13896.

Fatica, Alessandro, and Irene Bozzoni. 2014. "Long Non-Coding RNAs: New Players in Cell Differentiation and Development." *Nature Reviews Genetics* 15 (1): 7–21. doi:10.1038/nrg3606.

Feng, Du, Wen-Long Zhao, Yun-Ying Ye, Xiao-Chen Bai, Rui-Qin Liu, Lei-Fu Chang, Qiang Zhou, and Sen-Fang Sui. 2010. "Cellular Internalization of Exosomes Occurs Through Phagocytosis." *Traffic* 11 (5): 675–87. doi:10.1111/j.1600-0854.2010.01041.x.

Fischer, Stefanie, Kerstin Cornils, Thomas Speiseder, Anita Badbaran, Rudolph Reimer, Daniela Indenbirken, Adam Grundhoff, Bärbel Brunswig-Spickenheier, Malik Alawi, and Claudia Lange. 2016. "Indication of Horizontal DNA Gene Transfer by Extracellular Vesicles." *PLOS ONE* 11 (9): e0163665. doi:10.1371/journal.pone.0163665.

Fitzner, Dirk, Mareike Schnaars, Denise van Rossum, Gurumoorthy Krishnamoorthy, Payam Dibaj, Mostafa Bakhti, Tommy Regen, Uwe-Karsten Hanisch, and Mikael Simons. 2011. "Selective Transfer of Exosomes from Oligodendrocytes to Microglia by Macropinocytosis." *Journal of Cell Science* 124 (3): 447–58. doi:10.1242/jcs.074088.

Freedman, Jane E., Mark Gerstein, Eric Mick, Joel Rozowsky, Daniel Levy, Robert Kitchen, Saumya Das, et al. 2016. "Diverse Human Extracellular RNAs Are Widely Detected in Human Plasma." *Nature Communications* 7 (April): 11106. doi:10.1038/ncomms11106.

Garcia, Eric L., Adewunmi Onafuwa-Nuga, Soyeong Sim, Steven R. King, Sandra L. Wolin, and Alice Telesnitsky. 2009. "Packaging of Host mY RNAs by Murine Leukemia Virus May Occur Early in Y RNA Biogenesis." *Journal of Virology* 83 (23): 12526–34. doi:10.1128/JVI.01219-09.

Ge, Yi-Yuan, Qing Shi, Zhi-Yuan Zheng, Jiao Gong, Chunxian Zeng, Jine Yang, and Shi-Mei Zhuang. 2014. "MicroRNA-100 Promotes the Autophagy of Hepatocellular Carcinoma Cells by Inhibiting the Expression of mTOR and IGF-1R." *Oncotarget* 5 (14): 6218–28.

Gebeshuber, C. A., and J. Martinez. 2013. "miR-100 Suppresses IGF2 and Inhibits Breast Tumorigenesis by Interfering with Proliferation and Survival Signaling." *Oncogene* 32 (27): 3306–10. doi:10.1038/onc.2012.372.

Gibbings, Derrick J., Constance Ciaudo, Mathieu Erhardt, and Olivier Voinnet. 2009. "Multivesicular Bodies Associate with Components of miRNA Effector Complexes and Modulate miRNA Activity." *Nature Cell Biology* 11 (9): 1143–49. doi:10.1038/ncb1929.

Glažar, Petar, Panagiotis Papavasileiou, and Nikolaus Rajewsky. 2014. "circBase: A Database for Circular RNAs." *RNA* 20 (11): 1666–70. doi:10.1261/rna.043687.113.

Goodarzi, Hani, Xuhang Liu, Hoang C. B. Nguyen, Steven Zhang, Lisa Fish, and Sohail F. Tavazoie. 2015. "Endogenous tRNA-Derived Fragments Suppress Breast Cancer Progression via YBX1 Displacement." *Cell* 161 (4): 790–802. doi:10.1016/j.cell.2015.02.053.

Gopinath, Subash C. B., Akimasa Matsugami, Masato Katahira, and Penmetcha K. R. Kumar. 2005. "Human Vault-Associated Non-Coding RNAs Bind to Mitoxantrone, a Chemotherapeutic Compound." *Nucleic Acids Research* 33 (15): 4874–81. doi:10.1093/nar/gki809.

Gould, Stephen J., and Graça Raposo. 2013. "As We Wait: Coping with an Imperfect Nomenclature for Extracellular Vesicles." *Journal of Extracellular Vesicles* 2 (February). doi:10.3402/jev.v2i0.20389.

Gregory, Richard I., Kai-ping Yan, Govindasamy Amuthan, Thimmaiah Chendrimada, Behzad Doratotaj, Neil Cooch, and Ramin Shiekhattar. 2004. "The Microprocessor Complex Mediates the Genesis of microRNAs." *Nature* 432 (7014): 235–40. doi:10.1038/nature03120.

Griffiths-Jones, Sam, Russell J. Grocock, Stijn van Dongen, Alex Bateman, and Anton J. Enright. 2006. "miRBase: microRNA Sequences, Targets and Gene Nomenclature." *Nucleic Acids Research* 34 (suppl 1): D140–44. doi:10.1093/nar/gkj112.

Grundmann, Sebastian, Felix P. Hans, Sheena Kinniry, Jennifer Heinke, Thomas Helbing, Franziska Bluhm, Joost P. G. Sluijter, et al. 2011. "MicroRNA-100 Regulates Neovascularization by Suppression of Mammalian Target of Rapamycin in Endothelial and Vascular Smooth Muscle Cells." *Circulation* 123 (9): 999–1009. doi:10.1161/CIRCULATIONAHA.110.000323.

Guduric-Fuchs, Jasenka, Anna O'Connor, Bailey Camp, Christina L O'Neill, Reinhold J Medina, and David A Simpson. 2012. "Selective Extracellular Vesicle-Mediated Export of an Overlapping Set of microRNAs from Multiple Cell Types." *BMC Genomics* 13 (1): 357. doi:10.1186/1471-2164-13-357.

Guo, Junjie U., Vikram Agarwal, Huili Guo, and David P. Bartel. 2014. "Expanded Identification and Characterization of Mammalian Circular RNAs." *Genome Biology* 15 (7): 409. doi:10.1186/s13059-014-0409-z.

Hager, Martin H., Samantha Morley, Diane R. Bielenberg, Sizhen Gao, Matteo Morello, Ilona N. Holcomb, Wennuan Liu, et al. 2012. "DIAPH3 Governs the Cellular Transition to the Amoeboid Tumour Phenotype." *EMBO Molecular Medicine* 4 (8): 743. doi:10.1002/emmm.201200242.

Hammond, Scott M., Emily Bernstein, David Beach, and Gregory J. Hannon. 2000. "An RNA-Directed Nuclease Mediates Post-Transcriptional Gene Silencing in Drosophila Cells." *Nature* 404 (6775): 293–96. doi:10.1038/35005107.

Hannun, Yusuf A., and Lina M. Obeid. 2002. "The Ceramide-Centric Universe of Lipid-Mediated Cell Regulation: Stress Encounters of the Lipid Kind." *Journal of Biological Chemistry* 277 (29): 25847–50. doi:10.1074/jbc.R200008200.

Hansen, Thomas B., Trine I. Jensen, Bettina H. Clausen, Jesper B. Bramsen, Bente Finsen, Christian K. Damgaard, and Jørgen Kjems. 2013. "Natural RNA Circles Function as Efficient microRNA Sponges." *Nature*. doi:10.1038/nature11993.

Hansen, Thomas B., Jørgen Kjems, and Christian K. Damgaard. 2013. "Circular RNA and miR-7 in Cancer." *Cancer Research* 73 (18): 5609–12. doi:10.1158/0008-5472.CAN-13-1568.

Haussecker, Dirk, Yong Huang, Ashley Lau, Poornima Parameswaran, Andrew Z. Fire, and Mark A. Kay. 2010. "Human tRNA-Derived Small RNAs in the Global Regulation of RNA Silencing." *RNA* 16 (4): 673–95. doi:10.1261/rna.2000810.

Heo, Inha, Minju Ha, Jaechul Lim, Mi-Jeong Yoon, Jong-Eun Park, S. Chul Kwon, Hyeshik Chang, and V. Narry Kim. 2012. "Mono-Uridylation of Pre-MicroRNA as a Key Step in the Biogenesis of Group II Let-7 MicroRNAs." *Cell* 151 (3): 521–32. doi:10.1016/j.cell.2012.09.022.

Herrmann, Christine, Elaheh Golkaramnay, Elisabeth Inman, Leonard Rome, and Walter Volknandt. 1999. "Recombinant Major Vault Protein Is Targeted to Neuritic Tips of PC12 Cells." *The Journal of Cell Biology* 144 (6): 1163–72. doi:10.1083/jcb.144.6.1163.

Higginbotham, James N., Michelle Demory Beckler, Jonathan D. Gephart, Jeffrey L. Franklin, Galina Bogatcheva, Gert-Jan Kremers, David W. Piston, et al. 2011a. "Amphiregulin Exosomes Increase Cancer Cell Invasion." *Current Biology* 21 (9): 779–86. doi:10.1016/j.cub.2011.03.043.

———. 2011b. "Amphiregulin Exosomes Increase Cancer Cell Invasion." *Current Biology* 21 (9): 779–86. doi:10.1016/j.cub.2011.03.043.

Hizir, Zoheir, Silvia Bottini, Valerie Grandjean, Michele Trabucchi, and Emanuela Repetto. 2017. "RNY (YRNA)-Derived Small RNAs Regulate Cell Death and Inflammation in Monocytes/Macrophages." *Cell Death & Disease* 8 (1): e2530. doi:10.1038/cddis.2016.429.

Hoen, Esther N. M. Nolte-'t, Henk P. J. Buermans, Maaike Waasdorp, Willem Stoorvogel, Marca H. M. Wauben, and Peter A. C. 't Hoen. 2012. "Deep Sequencing of RNA from Immune Cell-Derived Vesicles Uncovers the Selective Incorporation of Small Non-Coding RNA Biotypes with Potential Regulatory Functions." *Nucleic Acids Research* 40 (18): 9272–85. doi:10.1093/nar/gks658.

Hoen, Esther N. M. Nolte-'t, Sonja I. Buschow, Stephen M. Anderton, Willem Stoorvogel, and Marca H. M. Wauben. 2009. "Activated T Cells Recruit Exosomes Secreted by Dendritic Cells via LFA-1." *Blood* 113 (9): 1977–81. doi:10.1182/blood-2008-08-174094.

Hollox, Edward J., and Boon-Peng Hoh. 2014. "Human Gene Copy Number Variation and Infectious Disease." *Human Genetics* 133 (10): 1217–33. doi:10.1007/s00439-014-1457-x.

Hong, Bok Sil, Ji-Hoon Cho, Hyunjung Kim, Eun-Jeong Choi, Sangchul Rho, Jongmin Kim, Ji Hyun Kim, et al. 2009. "Colorectal Cancer Cell-Derived Microvesicles Are Enriched in Cell Cycle-Related mRNAs That Promote Proliferation of Endothelial Cells." *BMC Genomics* 10: 556. doi:10.1186/1471-2164-10-556.

Horman, Shane R., Maja M. Janas, Claudia Litterst, Bingbing Wang, Ian J. MacRae, Mary J. Sever, David V. Morrissey, et al. 2013. "Akt-Mediated Phosphorylation of Argonaute 2 Downregulates Cleavage and Upregulates Translational Repression of MicroRNA Targets." *Molecular Cell* 50 (3): 356–67. doi:10.1016/j.molcel.2013.03.015.

Hoshino, Daisuke, Kellye C. Kirkbride, Kaitlin Costello, Emily S. Clark, Seema Sinha, Nathan Grega-Larson, Matthew J. Tyska, and Alissa M. Weaver. 2013. "Exosome Secretion Is Enhanced by Invadopodia and Drives Invasive Behavior." *Cell Reports*. doi:10.1016/j.celrep.2013.10.050.

Hsieh, I.-Shan, Kung-Chao Chang, Yao-Tsung Tsai, Jhen-Yu Ke, Pei-Jung Lu, Kuen-Haur Lee, Shauh-Der Yeh, Tse-Ming Hong, and Yuh-Ling Chen. 2013. "MicroRNA-320 Suppresses the Stem Cell-like Characteristics of Prostate Cancer Cells by Downregulating the Wnt/Beta-Catenin Signaling Pathway." *Carcinogenesis* 34 (3): 530–38. doi:10.1093/carcin/bgs371.

Huang, Xiaoyi, Tiezheng Yuan, Michael Tschannen, Zhifu Sun, Howard Jacob, Meijun Du, Meihua Liang, et al. 2013. "Characterization of Human Plasma-Derived Exosomal RNAs by Deep Sequencing." *BMC Genomics* 14 (1): 319. doi:10.1186/1471-2164-14-319.

Hussain, Shobbir, Abdulrahim A. Sajini, Sandra Blanco, Sabine Dietmann, Patrick Lombard, Yoichiro Sugimoto, Maike Paramor, et al. 2013. "NSun2-Mediated Cytosine-5 Methylation of Vault Noncoding RNA Determines Its Processing into Regulatory Small RNAs." *Cell Reports* 4 (2): 255–61. doi:10.1016/j.celrep.2013.06.029.

Ince-Dunn, Gulayse, Hirotaka J. Okano, Kirk B. Jensen, Woong-Yang Park, Ru Zhong, Jernej Ule, Aldo Mele, et al. 2012. "Neuronal Elav-like (Hu) Proteins Regulate RNA Splicing and Abundance to Control Glutamate Levels and Neuronal Excitability." *Neuron* 75 (6): 1067–80. doi:10.1016/j.neuron.2012.07.009.

Ivanov, Andranik, Sebastian Memczak, Emanuel Wyler, Francesca Torti, Hagit T. Porath, Marta R. Orejuela, Michael Piechotta, et al. 2015. "Analysis of Intron Sequences Reveals Hallmarks of Circular RNA Biogenesis in Animals." *Cell Reports* 10 (2): 170–77. doi:10.1016/j.celrep.2014.12.019.

Ivanov, Pavel, Mohamed M. Emara, Judit Villen, Steven P. Gygi, and Paul Anderson. 2011. "Angiogenin-Induced tRNA Fragments Inhibit Translation Initiation." *Molecular Cell* 43 (4): 613–23. doi:10.1016/j.molcel.2011.06.022.

Iwasaki, Yuka, Mikiko Siomi, and Haruhiko Siomi. 2015. "PIWI-Interacting RNA: Its Biogenesis and Functions." *Annual Review of Biochemistry* 84 (1): 405–33. doi:10.1146/annurev-biochem-060614-034258.

Izquierdo, José M. 2008. "Hu Antigen R (HuR) Functions as an Alternative Pre-mRNA Splicing Regulator of Fas Apoptosis-Promoting Receptor on Exon Definition." *Journal of Biological*

Chemistry 283 (27): 19077–84. doi:10.1074/jbc.M800017200.
Izquierdo, M. A., G. L. Scheffer, M. J. Flens, G. Giaccone, H. J. Broxterman, C. J. Meijer, P. van der Valk, and R. J. Scheper. 1996. "Broad Distribution of the Multidrug Resistance-Related Vault Lung Resistance Protein in Normal Human Tissues and Tumors." *The American Journal of Pathology* 148 (3): 877.
Jacob, François, and Jacques Monod. 1961. "Genetic Regulatory Mechanisms in the Synthesis of Proteins." *Journal of Molecular Biology* 3 (3): 318–56. doi:10.1016/S0022-2836(61)80072-7.
Jahn, Reinhard, and Thomas C. Südhof. 1999. "Membrane Fusion and Exocytosis." *Annual Review of Biochemistry* 68 (1): 863–911. doi:10.1146/annurev.biochem.68.1.863.
Jakobsen, Kristine Raaby, Emilie Sørensen, Karin Kathrine Brøndum, Tina Fuglsang Daugaard, Rune Thomsen, and Anders Lade Nielsen. 2013. "Direct RNA Sequencing Mediated Identification of mRNA Localized in Protrusions of Human MDA-MB-231 Metastatic Breast Cancer Cells." *Journal of Molecular Signaling* 8: 9. doi:10.1186/1750-2187-8-9.
Jambhekar, Ashwini, and Joseph L. DeRisi. 2007. "Cis-Acting Determinants of Asymmetric, Cytoplasmic RNA Transport." *RNA* 13 (5): 625–42. doi:10.1261/rna.262607.
Janas, Tadeusz, Teresa Janas, and Michael Yarus. 2006. "Specific RNA Binding to Ordered Phospholipid Bilayers." *Nucleic Acids Research* 34 (7): 2128–36. doi:10.1093/nar/gkl220.
Jeck, William R., and Norman E. Sharpless. 2014. "Detecting and Characterizing Circular RNAs." *Nature Biotechnology* 32 (5): 453–61. doi:10.1038/nbt.2890.
Jeck, William R., Jessica A. Sorrentino, Kai Wang, Michael K. Slevin, Christin E. Burd, Jinze Liu, William F. Marzluff, and Norman E. Sharpless. 2013. "Circular RNAs Are Abundant, Conserved, and Associated with ALU Repeats." *RNA* 19 (2): 141–57. doi:10.1261/rna.035667.112.
Ji, Hong, Maoshan Chen, David W. Greening, Weifeng He, Alin Rai, Wenwei Zhang, and Richard J. Simpson. 2014. "Deep Sequencing of RNA from Three Different Extracellular Vesicle (EV) Subtypes Released from the Human LIM1863 Colon Cancer Cell Line Uncovers Distinct Mirna-Enrichment Signatures." *PLoS ONE* 9 (10): e110314. doi:10.1371/journal.pone.0110314.
Ji, Q., L. Zhang, X. Liu, L. Zhou, W. Wang, Z. Han, H. Sui, et al. 2014. "Long Non-Coding RNA MALAT1 Promotes Tumour Growth and Metastasis in Colorectal Cancer through Binding to SFPQ and Releasing Oncogene PTBP2 from SFPQ/PTBP2 Complex." *British Journal of Cancer* 111 (4): 736–48. doi:10.1038/bjc.2014.383.
Jose, Antony M., Giancarlo A. Garcia, and Craig P. Hunter. 2011. "Two Classes of Silencing RNAs Move between Caenorhabditis Elegans Tissues." *Nature Structural & Molecular Biology* 18 (11): 1184–88. doi:10.1038/nsmb.2134.
Kahlert, Christoph, and Raghu Kalluri. 2013. "Exosomes in Tumor Microenvironment Influence Cancer Progression and Metastasis." *Journal of Molecular Medicine* 91 (4): 431–37. doi:10.1007/s00109-013-1020-6.
Kajimoto, Taketoshi, Taro Okada, Satoshi Miya, Lifang Zhang, and Shun-ichi Nakamura. 2013. "Ongoing Activation of Sphingosine 1-Phosphate Receptors Mediates Maturation of Exosomal Multivesicular Endosomes." *Nature Communications* 4 (November). doi:10.1038/ncomms3712.
Kalra, Hina, Richard J. Simpson, Hong Ji, Elena Aikawa, Peter Altevogt, Philip Askenase, Vincent C. Bond, et al. 2012. "Vesiclepedia: A Compendium for Extracellular Vesicles with Continuous Community Annotation." *PLoS Biology* 10 (12). doi:10.1371/journal.pbio.1001450.
Katz, Yarden, Feifei Li, Nicole J. Lambert, Ethan S. Sokol, Wai-Leong Tam, Albert W. Cheng, Edoardo M. Airoldi, et al. 2014. "Musashi Proteins Are Post-Transcriptional Regulators of the Epithelial-Luminal Cell State." *eLife* 3 (November): e03915. doi:10.7554/eLife.03915.
Kedersha, N. L., and L. H. Rome. 1986. "Isolation and Characterization of a Novel Ribonucleoprotein Particle: Large Structures Contain a Single Species of Small RNA." *The Journal of Cell Biology* 103 (3): 699–709. doi:10.1083/jcb.103.3.699.
Ketting, R F, S E Fischer, E Bernstein, T Sijen, G J Hannon, and R H Plasterk. 2001. "Dicer Functions in RNA Interference and in Synthesis of Small RNA Involved in Developmental Timing in C. Elegans." *Genes & Development* 15 (20): 2654–59. doi:10.1101/gad.927801.

Khvorova, Anastasia, Yong-Geun Kwak, Michael Tamkun, Irene Majerfeld, and Michael Yarus. 1999. "RNAs That Bind and Change the Permeability of Phospholipid Membranes." *Proceedings of the National Academy of Sciences* 96 (19): 10649–54. doi:10.1073/pnas.96.19.10649.

Kim, Jayoung, Samantha Morley, Minh Le, Denis Bedoret, Dale T. Umetsu, Dolores Di Vizio, and Michael R. Freeman. 2014. "Enhanced Shedding of Extracellular Vesicles from Amoeboid Prostate Cancer Cells: Potential Effects on the Tumor Microenvironment." *Cancer Biology & Therapy* 15 (4): 409. doi:10.4161/cbt.27627.

Koppers-Lalic, Danijela, Michael Hackenberg, Irene V. Bijnsdorp, Monique A. J. van Eijndhoven, Payman Sadek, Daud Sie, Nicoletta Zini, et al. 2014. "Nontemplated Nucleotide Additions Distinguish the Small RNA Composition in Cells from Exosomes." *Cell Reports* 8 (6): 1649–58. doi:10.1016/j.celrep.2014.08.027.

Kosaka, N., H. Iguchi, Y. Yoshioka, F. Takeshita, Y. Matsuki, and T. Ochiya. 2010. "Secretory Mechanisms and Intercellular Transfer of MicroRNAs in Living Cells." *Journal of Biological Chemistry* 285 (23): 17442–52. doi:10.1074/jbc.M110.107821.

Kosaka, Nobuyoshi, Hirohisa Izumi, Kazunori Sekine, and Takahiro Ochiya. 2010. "microRNA as a New Immune-Regulatory Agent in Breast Milk." *Silence* 1 (March): 7. doi:10.1186/1758-907X-1-7.

Kowalski, Madzia P., and Torsten Krude. 2015. "Functional Roles of Non-Coding Y RNAs." *The International Journal of Biochemistry & Cell Biology* 66 (September): 20–29. doi:10.1016/j.biocel.2015.07.003.

Kozomara, Ana, and Sam Griffiths-Jones. 2011. "miRBase: Integrating microRNA Annotation and Deep-Sequencing Data." *Nucleic Acids Research* 39 (suppl 1): D152–57. doi:10.1093/nar/gkq1027.

Krol, Jacek, Inga Loedige, and Witold Filipowicz. 2010. "The Widespread Regulation of microRNA Biogenesis, Function and Decay." *Nature Reviews Genetics* 11 (9): 597–610. doi:10.1038/nrg2843.

LaConti, Joseph J., Narayan Shivapurkar, Anju Preet, Anne Deslattes Mays, Ivana Peran, Sung Eun Kim, John L. Marshall, Anna T. Riegel, and Anton Wellstein. 2011. "Tissue and Serum microRNAs in the KrasG12D Transgenic Animal Model and in Patients with Pancreatic Cancer." Edited by Janine Santos. *PLoS ONE* 6 (6): e20687. doi:10.1371/journal.pone.0020687.

Lander, Eric S., Lauren M. Linton, Bruce Birren, Chad Nusbaum, Michael C. Zody, Jennifer Baldwin, Keri Devon, et al. 2001. "Initial Sequencing and Analysis of the Human Genome." *Nature* 409 (6822): 860–921. doi:10.1038/35057062.

Larson, Michael C., Jeffrey E. Woodliff, Cheryl A. Hillery, Tyce J. Kearl, and Ming Zhao. 2012. "Phosphatidylethanolamine Is Externalized at the Surface of Microparticles." *Biochimica et Biophysica Acta* 1821 (12). doi:10.1016/j.bbalip.2012.08.017.

Lawrie, Charles H., Shira Gal, Heather M. Dunlop, Beena Pushkaran, Amanda P. Liggins, Karen Pulford, Alison H. Banham, et al. 2008. "Detection of Elevated Levels of Tumour-Associated microRNAs in Serum of Patients with Diffuse Large B-Cell Lymphoma." *British Journal of Haematology* 141 (5): 672–75. doi:10.1111/j.1365-2141.2008.07077.x.

Lázaro-Ibáñez, Elisa, Taral R. Lunavat, Su Chul Jang, Carmen Escobedo-Lucea, Jorge Oliver-De La Cruz, Pia Siljander, Jan Lötvall, and Marjo Yliperttula. 2017. "Distinct Prostate Cancer-Related mRNA Cargo in Extracellular Vesicle Subsets from Prostate Cell Lines." *BMC Cancer* 17. doi:10.1186/s12885-017-3087-x.

Lee, George Leighton, Albert Dobi, and Shiv Srivastava. 2011. "Prostate Cancer: Diagnostic Performance of the PCA3 Urine Test." *Nature Reviews Urology* 8 (3): 123–24. doi:10.1038/nrurol.2011.10.

Lee, Rosalind C., Rhonda L. Feinbaum, and Victor Ambros. 1993. "The C. Elegans Heterochronic Gene< I> Lin-4</i> Encodes Small RNAs with Antisense Complementarity To< I> Lin-14</i>." *Cell* 75 (5): 843–854.

Lee, Yong Sun, Yoshiyuki Shibata, Ankit Malhotra, and Anindya Dutta. 2009. "A Novel Class of Small RNAs: tRNA-Derived RNA Fragments (tRFs)." *Genes & Development* 23 (22): 2639–49. doi:10.1101/gad.1837609.

Lee, Yoontae, Chiyoung Ahn, Jinju Han, Hyounjeong Choi, Jaekwang Kim, Jeongbin Yim, Junho Lee, et

al. 2003. “The Nuclear RNase III Drosha Initiates microRNA Processing.” *Nature* 425 (6956): 415–19. doi:10.1038/nature01957.

Lefebvre, Fabio Alexis, Louis Philip Benoit Bouvrette, Lilyanne Perras, Alexis Blanchet-Cohen, Delphine Garnier, Janusz Rak, and Éric Lécuyer. 2016. “Comparative Transcriptomic Analysis of Human and Drosophila Extracellular Vesicles.” *Scientific Reports* 6 (June): 27680. doi:10.1038/srep27680.

Lehmann, Sabrina M., Christina Krüger, Boyoun Park, Katja Derkow, Karen Rosenberger, Jan Baumgart, Thorsten Trimbuch, et al. 2012. “An Unconventional Role for miRNA: Let-7 Activates Toll-like Receptor 7 and Causes Neurodegeneration.” *Nature Neuroscience* 15 (6): 827–35. doi:10.1038/nn.3113.

Lerner, M. R., J. A. Boyle, J. A. Hardin, and J. A. Steitz. 1981. “Two Novel Classes of Small Ribonucleoproteins Detected by Antibodies Associated with Lupus Erythematosus.” *Science* 211 (4480): 400–402. doi:10.1126/science.6164096.

Li, Hong. 2007. “Complexes of tRNA and Maturation Enzymes: Shaping up for Translation.” *Current Opinion in Structural Biology*, Nucleic acids / Sequences and topology, 17 (3): 293–301. doi:10.1016/j.sbi.2007.05.002.

Li, J. -Y., W. Volknandt, A. Dahlstrom, C. Herrmann, J. Blasi, B. Das, and H. Zimmermann. 1999. “Axonal Transport of Ribonucleoprotein Particles (Vaults).” *Neuroscience* 91 (3): 1055–65. doi:10.1016/S0306-4522(98)00622-8.

Li, Mu, Emily Zeringer, Timothy Barta, Jeoffrey Schageman, Angie Cheng, and Alexander V. Vlassov. 2014. “Analysis of the RNA Content of the Exosomes Derived from Blood Serum and Urine and Its Potential as Biomarkers.” *Philosophical Transactions of the Royal Society B: Biological Sciences* 369 (1652). doi:10.1098/rstb.2013.0502.

Li, Yan, Qiupeng Zheng, Chunyang Bao, Shuyi Li, Weijie Guo, Jiang Zhao, Di Chen, Jianren Gu, Xianghuo He, and Shenglin Huang. 2015. “Circular RNA Is Enriched and Stable in Exosomes: A Promising Biomarker for Cancer Diagnosis.” *Cell Research* 25 (8): 981–84. doi:10.1038/cr.2015.82.

Li, Zhaoyong, Chuan Huang, Chun Bao, Liang Chen, Mei Lin, Xiaolin Wang, Guolin Zhong, et al. 2015. “Exon-Intron Circular RNAs Regulate Transcription in the Nucleus.” *Nature Structural & Molecular Biology* 22 (3): 256–64. doi:10.1038/nsmb.2959.

Liang, Dongming, and Jeremy E. Wilusz. 2014. “Short Intronic Repeat Sequences Facilitate Circular RNA Production.” *Genes & Development* 28 (20): 2233–47. doi:10.1101/gad.251926.114.

Liang, Hongwei, Suyang Zhang, Zheng Fu, Yanbo Wang, Nan Wang, Yanqing Liu, Chihao Zhao, et al. 2015. “Effective Detection and Quantification of Dietetically Absorbed Plant microRNAs in Human Plasma.” *The Journal of Nutritional Biochemistry* 26 (5): 505–12. doi:10.1016/j.jnutbio.2014.12.002.

Lima, Luize G., Roger Chammas, Robson Q. Monteiro, Maria Elisabete C. Moreira, and Marcello A. Barcinski. 2009. “Tumor-Derived Microvesicles Modulate the Establishment of Metastatic Melanoma in a Phosphatidylserine-Dependent Manner.” *Cancer Letters* 283 (2): 168–75. doi:10.1016/j.canlet.2009.03.041.

Liu, Teresa T., Gustavo Arango-Argoty, Zhihua Li, Yuefeng Lin, Sang Woo Kim, Anne Dueck, Fatih Ozsolak, et al. 2015. “Noncoding RNAs That Associate with YB-1 Alter Proliferation in Prostate Cancer Cells.” *RNA* 21 (6): 1159–72. doi:10.1261/rna.045559.114.

Lu, Albert, Francesc Tebar, Blanca Alvarez-Moya, Cristina López-Alcalá, Maria Calvo, Carlos Enrich, Neus Agell, Takeshi Nakamura, Michiyuki Matsuda, and Oriol Bachs. 2009. “A Clathrin-Dependent Pathway Leads to KRas Signaling on Late Endosomes En Route to Lysosomes.” *The Journal of Cell Biology* 184 (6): 863–79. doi:10.1083/jcb.200807186.

Lu, Jun, Gad Getz, Eric A. Miska, Ezequiel Alvarez-Saavedra, Justin Lamb, David Peck, Alejandro Sweet-Cordero, et al. 2005. “MicroRNA Expression Profiles Classify Human Cancers.” *Nature* 435 (7043): 834–38. doi:10.1038/nature03702.

Luga, Valbona, Liang Zhang, Alicia M. Viloria-Petit, Abiodun A. Ogunjimi, Mohammad R. Inanlou,

Elaine Chiu, Marguerite Buchanan, Abdel Nasser Hosein, Mark Basik, and Jeffrey L. Wrana. 2012. “Exosomes Mediate Stromal Mobilization of Autocrine Wnt-PCP Signaling in Breast Cancer Cell Migration.” *Cell* 151 (7): 1542–56. doi:10.1016/j.cell.2012.11.024.

Lund, Elsebet, Stephan Güttinger, Angelo Calado, James E. Dahlberg, and Ulrike Kutay. 2004. “Nuclear Export of MicroRNA Precursors.” *Science* 303 (5654): 95–98. doi:10.1126/science.1090599.

Ma, Li, Ferenc Reinhardt, Elizabeth Pan, Jürgen Soutschek, Balkrishen Bhat, Eric G. Marcusson, Julie Teruya-Feldstein, George W. Bell, and Robert A. Weinberg. 2010. “Therapeutic Silencing of miR-10b Inhibits Metastasis in a Mouse Mammary Tumor Model.” *Nature Biotechnology* 28 (4): 341–47. doi:10.1038/nbt.1618.

Maas, Sybren L. N., Xandra O. Breakefield, and Alissa M. Weaver. 2016. “Extracellular Vesicles: Unique Intercellular Delivery Vehicles.” *Trends in Cell Biology*. doi:10.1016/j.tcb.2016.11.003.

Maraia, R J, N Sasaki-Tozawa, C T Driscoll, E D Green, and G J Darlington. 1994. “The Human Y4 Small Cytoplasmic RNA Gene Is Controlled by Upstream Elements and Resides on Chromosome 7 with All Other hY scRNA Genes.” *Nucleic Acids Research* 22 (15): 3045–52.

Matera, A. Gregory, Rebecca M. Terns, and Michael P. Terns. 2007. “Non-Coding RNAs: Lessons from the Small Nuclear and Small Nucleolar RNAs.” *Nature Reviews Molecular Cell Biology* 8 (3): 209–20. doi:10.1038/nrm2124.

McKenzie, Andrew J., Daisuke Hoshino, Nan Hyung Hong, Diana J. Cha, Jeffrey L. Franklin, Robert J. Coffey, James G. Patton, and Alissa M. Weaver. 2016. “KRAS-MEK Signaling Controls Ago2 Sorting into Exosomes.” *Cell Reports* 15 (5): 978–87. doi:10.1016/j.celrep.2016.03.085.

Meiri, Eti, Asaf Levy, Hila Benjamin, Miriam Ben-David, Lahav Cohen, Avital Dov, Nir Dromi, et al. 2010. “Discovery of microRNAs and Other Small RNAs in Solid Tumors.” *Nucleic Acids Research* 38 (18): 6234–46. doi:10.1093/nar/gkq376.

Meller, Victoria, Sonal Joshi, and Nikita Deshpande. 2015. “Modulation of Chromatin by Noncoding RNA.” *Annual Review of Genetics* 49 (1): 673–95. doi:10.1146/annurev-genet-112414-055205.

Melo, Sonia A., Hikaru Sugimoto, Joyce T. O’Connell, Noritoshi Kato, Alberto Villanueva, August Vidal, Le Qiu, et al. 2014. “Cancer Exosomes Perform Cell-Independent MicroRNA Biogenesis and Promote Tumorigenesis.” *Cancer Cell* 0 (0). doi:10.1016/j.ccell.2014.09.005.

Memczak, Sebastian, Marvin Jens, Antigoni Elefsinioti, Francesca Torti, Janna Krueger, Agnieszka Rybak, Luisa Maier, et al. 2013. “Circular RNAs Are a Large Class of Animal RNAs with Regulatory Potency.” *Nature*. doi:10.1038/nature11928.

Mercer, Tim R., Marcel E. Dinger, Cameron P. Bracken, Gabriel Kolle, Jan M. Szubert, Darren J. Korbie, Marjan E. Askarian-Amiri, et al. 2010. “Regulated Post-Transcriptional RNA Cleavage Diversifies the Eukaryotic Transcriptome.” *Genome Research* 20 (12): 1639–50. doi:10.1101/gr.112128.110.

Mercer, Tim R., Dagmar Wilhelm, Marcel E. Dinger, Giulia Soldà, Darren J. Korbie, Evgeny A. Glazov, Vy Truong, et al. 2011. “Expression of Distinct RNAs from 3′ Untranslated Regions.” *Nucleic Acids Research* 39 (6): 2393–2403. doi:10.1093/nar/gkq1158.

Merola, Roberta, Luigi Tomao, Anna Antenucci, Isabella Sperduti, Steno Sentinelli, Serena Masi, Chiara Mandoj, et al. 2015. “PCA3 in Prostate Cancer and Tumor Aggressiveness Detection on 407 High-Risk Patients: A National Cancer Institute Experience.” *Journal of Experimental & Clinical Cancer Research : CR* 34 (1). doi:10.1186/s13046-015-0127-8.

Milani, Gloria, Tobia Lana, Silvia Bresolin, Sanja Aveic, Anna Pasto, Chiara Frasson, and Geertruy te Kronnie. 2017. “Expression Profiling of Circulating Microvesicles Reveals Intercellular Transmission of Oncogenic Pathways.” *Molecular Cancer Research*, January, molcanres.0307.2016. doi:10.1158/1541-7786.MCR-16-0307.

Mills, Jason C., Nicole L. Stone, Joseph Erhardt, and Randall N. Pittman. 1998. “Apoptotic Membrane Blebbing Is Regulated by Myosin Light Chain Phosphorylation.” *The Journal of Cell Biology* 140 (3): 627.

Minciacchi, Valentina R., Sungyong You, Cristiana Spinelli, Samantha Morley, Mandana Zandian, Paul-Joseph Aspuria, Lorenzo Cavallini, et al. 2015. “Large Oncosomes Contain Distinct Protein

Cargo and Represent a Separate Functional Class of Tumor-Derived Extracellular Vesicles." *Oncotarget* 6 (13): 11327. doi:10.18632/oncotarget.3598.

Mitchell, Patrick S., Rachael K. Parkin, Evan M. Kroh, Brian R. Fritz, Stacia K. Wyman, Era L. Pogosova-Agadjanyan, Amelia Peterson, et al. 2008. "Circulating microRNAs as Stable Blood-Based Markers for Cancer Detection." *Proceedings of the National Academy of Sciences* 105 (30): 10513–18. doi:10.1073/pnas.0804549105.

Mittelbrunn, María, Cristina Gutiérrez-Vázquez, Carolina Villarroya-Beltri, Susana González, Fátima Sánchez-Cabo, Manuel Ángel González, Antonio Bernad, and Francisco Sánchez-Madrid. 2011. "Unidirectional Transfer of microRNA-Loaded Exosomes from T Cells to Antigen-Presenting Cells." *Nature Communications* 2 (April): 282. doi:10.1038/ncomms1285.

Montecalvo, Angela, Adriana T. Larregina, William J. Shufesky, Donna Beer Stolz, Mara L. G. Sullivan, Jenny M. Karlsson, Catherine J. Baty, et al. 2012. "Mechanism of Transfer of Functional microRNAs between Mouse Dendritic Cells via Exosomes." *Blood* 119 (3): 756–66. doi:10.1182/blood-2011-02-338004.

Morelli, Adrian E., Adriana T. Larregina, William J. Shufesky, Mara L. G. Sullivan, Donna Beer Stolz, Glenn D. Papworth, Alan F. Zahorchak, et al. 2004. "Endocytosis, Intracellular Sorting, and Processing of Exosomes by Dendritic Cells." *Blood* 104 (10): 3257–66. doi:10.1182/blood-2004-03-0824.

Morello, Matteo, Valentina R. Minciacchi, Paola de Candia, Julie Yang, Edwin Posadas, Hyung Kim, Duncan Griffiths, et al. 2013. "Large Oncosomes Mediate Intercellular Transfer of Functional microRNA." *Cell Cycle* 12 (22): 3526. doi:10.4161/cc.26539.

Mulcahy, Laura Ann, Ryan Charles Pink, and David Raul Francisco Carter. 2014. "Routes and Mechanisms of Extracellular Vesicle Uptake." *Journal of Extracellular Vesicles* 3 (August). doi:10.3402/jev.v3.24641.

Muralidharan-Chari, Vandhana, James Clancy, Carolyn Plou, Maryse Romao, Philippe Chavrier, Graca Raposo, and Crislyn D'Souza-Schorey. 2009. "ARF6-Regulated Shedding of Tumor Cell-Derived Plasma Membrane Microvesicles." *Current Biology* 19 (22): 1875–85. doi:10.1016/j.cub.2009.09.059.

Nabhan, Joseph F., Ruoxi Hu, Raymond S. Oh, Stanley N. Cohen, and Quan Lu. 2012. "Formation and Release of Arrestin Domain-Containing Protein 1-Mediated Microvesicles (ARMMs) at Plasma Membrane by Recruitment of TSG101 Protein." *Proceedings of the National Academy of Sciences* 109 (11): 4146–51. doi:10.1073/pnas.1200448109.

Nagaraja, Ankur K., Chad J. Creighton, Zhifeng Yu, Huifeng Zhu, Preethi H. Gunaratne, Jeffrey G. Reid, Emuejevoke Olokpa, et al. 2010. "A Link between Mir-100 and FRAP1/mTOR in Clear Cell Ovarian Cancer." *Molecular Endocrinology* 24 (2): 447–63. doi:10.1210/me.2009-0295.

Nakase, Ikuhiko, Nahoko Bailey Kobayashi, Tomoka Takatani-Nakase, and Tetsuhiko Yoshida. 2015. "Active Macropinocytosis Induction by Stimulation of Epidermal Growth Factor Receptor and Oncogenic Ras Expression Potentiates Cellular Uptake Efficacy of Exosomes." *Scientific Reports* 5 (June): 10300. doi:10.1038/srep10300.

Nan, Yang, Lei Han, Anling Zhang, Guangxiu Wang, Zhifan Jia, Yang Yang, Xiao Yue, Peiyu Pu, Yue Zhong, and Chunsheng Kang. 2010. "MiRNA-451 Plays a Role as Tumor Suppressor in Human Glioma Cells." *Brain Research* 1359 (November): 14–21. doi:10.1016/j.brainres.2010.08.074.

Nanbo, Asuka, Eri Kawanishi, Ryuji Yoshida, and Hironori Yoshiyama. 2013. "Exosomes Derived from Epstein-Barr Virus-Infected Cells Are Internalized via Caveola-Dependent Endocytosis and Promote Phenotypic Modulation in Target Cells." *Journal of Virology* 87 (18): 10334–47. doi:10.1128/JVI.01310-13.

Neilsen, Corine T., Gregory J. Goodall, and Cameron P. Bracken. 2012. "IsomiRs – the Overlooked Repertoire in the Dynamic microRNAome." *Trends in Genetics* 28 (11): 544–49. doi:10.1016/j.tig.2012.07.005.

Newman, Martin A., Vidya Mani, and Scott M. Hammond. 2011. "Deep Sequencing of microRNA Precursors Reveals Extensive 3? End Modification." *RNA* 17 (10): 1795–1803.

doi:10.1261/rna.2713611.
Nicolas, Francisco Esteban, Adam E. Hall, Tibor Csorba, Carly Turnbull, and Tamas Dalmay. 2012. "Biogenesis of Y RNA-Derived Small RNAs Is Independent of the microRNA Pathway." *FEBS Letters* 586 (8): 1226–30. doi:10.1016/j.febslet.2012.03.026.
Nigro, Janice M., Kathleen R. Cho, Eric R. Fearon, Scott E. Kern, J. Michael Ruppert, Jonathan D. Oliner, Kenneth W. Kinzler, and Bert Vogelstein. 1991. "Scrambled Exons." *Cell* 64 (3): 607–13. doi:10.1016/0092-8674(91)90244-S.
Noerholm, Mikkel, Leonora Balaj, Tobias Limperg, Afshin Salehi, Lin Dan Zhu, Fred H. Hochberg, Xandra O. Breakefield, Bob S. Carter, and Johan Skog. 2012. "RNA Expression Patterns in Serum Microvesicles from Patients with Glioblastoma Multiforme and Controls." *BMC Cancer* 12: 22. doi:10.1186/1471-2407-12-22.
Ohshima, Keiichi, Kanako Inoue, Akemi Fujiwara, Keiichi Hatakeyama, Kaori Kanto, Yuko Watanabe, Koji Muramatsu, et al. 2010. "Let-7 MicroRNA Family Is Selectively Secreted into the Extracellular Environment via Exosomes in a Metastatic Gastric Cancer Cell Line." *PLoS ONE* 5 (10): e13247. doi:10.1371/journal.pone.0013247.
Palma, Jaime, Sree C. Yaddanapudi, Lucy Pigati, Mallory A. Havens, Sarah Jeong, Geoffrey A. Weiner, Kristina Mary Ellen Weimer, Brittany Stern, Michelle L. Hastings, and Dominik M. Duelli. 2012. "MicroRNAs Are Exported from Malignant Cells in Customized Particles." *Nucleic Acids Research* 40 (18): 9125–38. doi:10.1093/nar/gks656.
Parolini, Isabella, Cristina Federici, Carla Raggi, Luana Lugini, Simonetta Palleschi, Angelo De Milito, Carolina Coscia, et al. 2009. "Microenvironmental pH Is a Key Factor for Exosome Traffic in Tumor Cells." *Journal of Biological Chemistry* 284 (49): 34211–22. doi:10.1074/jbc.M109.041152.
Pasquinelli, Amy E., Brenda J. Reinhart, Frank Slack, Mark Q. Martindale, Mitzi I. Kuroda, Betsy Maller, David C. Hayward, et al. 2000. "Conservation of the Sequence and Temporal Expression of Let-7 Heterochronic Regulatory RNA." *Nature* 408 (6808): 86–89. doi:10.1038/35040556.
Patton, James G., Jeffrey L. Franklin, Alissa M. Weaver, Kasey Vickers, Bing Zhang, Robert J. Coffey, K. Mark Ansel, et al. 2015. "Biogenesis, Delivery, and Function of Extracellular RNA." *Journal of Extracellular Vesicles* 4 (August). doi:10.3402/jev.v4.27494.
Pegtel, D. Michiel, Katherine Cosmopoulos, David A. Thorley-Lawson, Monique A. J. van Eijndhoven, Erik S. Hopmans, Jelle L. Lindenberg, Tanja D. de Gruijl, Thomas Würdinger, and Jaap M. Middeldorp. 2010. "Functional Delivery of Viral miRNAs via Exosomes." *Proceedings of the National Academy of Sciences* 107 (14): 6328–33. doi:10.1073/pnas.0914843107.
Perreault, Jonathan, Jean-François Noël, Francis Brière, Benoit Cousineau, Jean-François Lucier, Jean-Pierre Perreault, and Gilles Boire. 2005. "Retropseudogenes Derived from the Human Ro/SS-A Autoantigen-Associated hY RNAs." *Nucleic Acids Research* 33 (6): 2032–41. doi:10.1093/nar/gki504.
Perry, David K, and Yusuf A Hannun. 1998. "The Role of Ceramide in Cell Signaling." *Biochimica et Biophysica Acta (BBA) - Molecular and Cell Biology of Lipids* 1436 (1–2): 233–43. doi:10.1016/S0005-2760(98)00145-3.
Persson, Helena, Anders Kvist, Johan Vallon-Christersson, Patrik Medstrand, Åke Borg, and Carlos Rovira. 2009. "The Non-Coding RNA of the Multidrug Resistance-Linked Vault Particle Encodes Multiple Regulatory Small RNAs." *Nature Cell Biology* 11 (10): 1268–71. doi:10.1038/ncb1972.
Petrelli, A., A. Perra, K. Schernhuber, M. Cargnelutti, A. Salvi, C. Migliore, E. Ghiso, et al. 2012. "Sequential Analysis of Multistage Hepatocarcinogenesis Reveals That miR-100 and PLK1 Dysregulation Is an Early Event Maintained along Tumor Progression." *Oncogene* 31 (42): 4517–26. doi:10.1038/onc.2011.631.
Pigati, Lucy, Sree C. S. Yaddanapudi, Ravi Iyengar, Dong-Ja Kim, Steven A. Hearn, David Danforth, Michelle L. Hastings, and Dominik M. Duelli. 2010. "Selective Release of MicroRNA Species from Normal and Malignant Mammary Epithelial Cells." *PLoS ONE* 5 (10): e13515.

doi:10.1371/journal.pone.0013515.
Pink, Ryan Charles, Kate Wicks, Daniel Paul Caley, Emma Kathleen Punch, Laura Jacobs, and David Raul Francisco Carter. 2011. “Pseudogenes: Pseudo-Functional or Key Regulators in Health and Disease?” *RNA* 17 (5): 792–98. doi:10.1261/rna.2658311.
Poliseno, Laura, Leonardo Salmena, Jiangwen Zhang, Brett Carver, William J. Haveman, and Pier Paolo Pandolfi. 2010. “A Coding-Independent Function of Gene and Pseudogene mRNAs Regulates Tumour Biology.” *Nature* 465 (7301): 1033–38. doi:10.1038/nature09144.
Poon, Ivan K. H., Yu-Hsin Chiu, Allison J. Armstrong, Jason M. Kinchen, Ignacio J. Juncadella, Douglas A. Bayliss, and Kodi S. Ravichandran. 2014. “Unexpected Link between an Antibiotic, Pannexin Channels and Apoptosis.” *Nature* 507 (7492): 329–34. doi:10.1038/nature13147.
Raposo, Graca, Hans W. Nijman, Willem Stoorvogel, R. Liejendekker, Clifford V. Harding, C. J. Melief, and Hans J. Geuze. 1996. “B Lymphocytes Secrete Antigen-Presenting Vesicles.” *The Journal of Experimental Medicine* 183 (3): 1161–1172.
Raposo, Graça, and Willem Stoorvogel. 2013. “Extracellular Vesicles: Exosomes, Microvesicles, and Friends.” *The Journal of Cell Biology* 200 (4): 373–83. doi:10.1083/jcb.201211138.
Ratti, Antonia, Claudia Fallini, Claudia Colombrita, Alessia Pascale, Umberto Laforenza, Alessandro Quattrone, and Vincenzo Silani. 2008. “Post-Transcriptional Regulation of Neuro-Oncological Ventral Antigen 1 by the Neuronal RNA-Binding Proteins ELAV.” *Journal of Biological Chemistry* 283 (12): 7531–41. doi:10.1074/jbc.M706082200.
Reinhart, Brenda J., Frank J. Slack, Michael Basson, Amy E. Pasquinelli, Jill C. Bettinger, Ann E. Rougvie, H. Robert Horvitz, and Gary Ruvkun. 2000. “The 21-Nucleotide Let-7 RNA Regulates Developmental Timing in Caenorhabditis Elegans.” *Nature* 403 (6772): 901–6. doi:10.1038/35002607.
Ridder, Kirsten, Alexandra Sevko, Janina Heide, Maria Dams, Anne-Kathleen Rupp, Jadranka Macas, Julia Starmann, et al. 2015. “Extracellular Vesicle-Mediated Transfer of Functional RNA in the Tumor Microenvironment.” *OncoImmunology* 4 (6): e1008371. doi:10.1080/2162402X.2015.1008371.
Rubartelli, Anna, Alessandro Poggi, and M. Raffaella Zocchi. 1997. “The Selective Engulfment of Apoptotic Bodies by Dendritic Cells Is Mediated by the αvβ3 Integrin and Requires Intracellular and Extracellular Calcium.” *European Journal of Immunology* 27 (8): 1893–1900. doi:10.1002/eji.1830270812.
Rutjes, Saskia A., Annemarie van der Heijden, Paul J. Utz, Walther J. van Venrooij, and Ger J. M. Pruijn. 1999. “Rapid Nucleolytic Degradation of the Small Cytoplasmic Y RNAs during Apoptosis.” *Journal of Biological Chemistry* 274 (35): 24799–807. doi:10.1074/jbc.274.35.24799.
Rybak-Wolf, Agnieszka, Christin Stottmeister, Petar Glažar, Marvin Jens, Natalia Pino, Sebastian Giusti, Mor Hanan, et al. 2015. “Circular RNAs in the Mammalian Brain Are Highly Abundant, Conserved, and Dynamically Expressed.” *Molecular Cell* 58 (5): 870–85. doi:10.1016/j.molcel.2015.03.027.
Saad, Fawzy A., Libero Vitiello, Luciano Merlini, Maria L. Mostacciuolo, Salvatore Oliviero, and Gian A. Danieli. 1992. “A 3′ Consensus Splice Mutation in the Human Dystrophin Gene Detected by a Screening for Intra-Exonic Deletions.” *Human Molecular Genetics* 1 (5): 345–46. doi:10.1093/hmg/1.5.345.
Salzman, Julia, Raymond E. Chen, Mari N. Olsen, Peter L. Wang, and Patrick O. Brown. 2013. “Cell-Type Specific Features of Circular RNA Expression.” *PLOS Genetics* 9 (9): e1003777. doi:10.1371/journal.pgen.1003777.
Schepeler, Troels, Jørgen T. Reinert, Marie S. Ostenfeld, Lise L. Christensen, Asli N. Silahtaroglu, Lars Dyrskjøt, Carsten Wiuf, et al. 2008. “Diagnostic and Prognostic MicroRNAs in Stage II Colon Cancer.” *Cancer Research* 68 (15): 6416–24. doi:10.1158/0008-5472.CAN-07-6110.
Schwarz, Dianne S., György Hutvágner, Tingting Du, Zuoshang Xu, Neil Aronin, and Phillip D. Zamore. 2003. “Asymmetry in the Assembly of the RNAi Enzyme Complex.” *Cell* 115 (2): 199–208. doi:10.1016/S0092-8674(03)00759-1.

Segura, Elodie, Carole Nicco, Bérangère Lombard, Philippe Véron, Graça Raposo, Frédéric Batteux, Sebastian Amigorena, and Clotilde Théry. 2005. "ICAM-1 on Exosomes from Mature Dendritic Cells Is Critical for Efficient Naive T-Cell Priming." *Blood* 106 (1): 216–23. doi:10.1182/blood-2005-01-0220.

Senji Shirasawa, Masanori Furuse, Nobuhiko Yokoyama, and Takehiko Sasazuki. 1993. "Altered Growth of Human Colon Cancer Cell Lines Disrupted at Activated Ki-Ras." *Science* 260 (5104): 85–88.

Shechner, David M., Ezgi Hacisuleyman, Scott T. Younger, and John L. Rinn. 2015. "Multiplexable, Locus-Specific Targeting of Long RNAs with CRISPR-Display." *Nature Methods* 12 (7): 664–70. doi:10.1038/nmeth.3433.

Shen, Beiyi, Ning Wu, Jr-Ming Yang, and Stephen J. Gould. 2011. "Protein Targeting to Exosomes/Microvesicles by Plasma Membrane Anchors." *Journal of Biological Chemistry* 286 (16): 14383–95. doi:10.1074/jbc.M110.208660.

Shurtleff, Matthew J., Morayma M. Temoche-Diaz, Kate V. Karfilis, Sayaka Ri, and Randy Schekman. 2016. "Y-Box Protein 1 Is Required to Sort microRNAs into Exosomes in Cells and in a Cell-Free Reaction." *eLife* 5 (August): e19276. doi:10.7554/eLife.19276.

Silva, Roberta Peres da, Rosana Puccia, Marcio L. Rodrigues, Débora L. Oliveira, Luna S. Joffe, Gabriele V. César, Leonardo Nimrichter, Samuel Goldenberg, and Lysangela R. Alves. 2015. "Extracellular Vesicle-Mediated Export of Fungal RNA." *Scientific Reports* 5 (January): 7763. doi:10.1038/srep07763.

Sim, Soyeong, and Sandra L. Wolin. 2011. "Emerging Roles for the Ro 60-kDa Autoantigen in Noncoding RNA Metabolism." *Wiley Interdisciplinary Reviews: RNA* 2 (5): 686–99. doi:10.1002/wrna.85.

Simpson, Richard J., Hina Kalra, and Suresh Mathivanan. 2012. "ExoCarta as a Resource for Exosomal Research." *Journal of Extracellular Vesicles* 1. doi:10.3402/jev.v1i0.18374.

Skog, Johan, Tom Wurdinger, Sjoerd van Rijn, Dimphna Meijer, Laura Gainche, Miguel Sena-Esteves, William T. Curry, Robert S. Carter, Anna M. Krichevsky, and Xandra O. Breakefield. 2008. "Glioblastoma Microvesicles Transport RNA and Protein That Promote Tumor Growth and Provide Diagnostic Biomarkers." *Nature Cell Biology* 10 (12): 1470–76. doi:10.1038/ncb1800.

Squadrito, Mario Leonardo, Caroline Baer, Frédéric Burdet, Claudio Maderna, Gregor D. Gilfillan, Robert Lyle, Mark Ibberson, and Michele De Palma. 2014. "Endogenous RNAs Modulate MicroRNA Sorting to Exosomes and Transfer to Acceptor Cells." *Cell Reports* 8 (5): 1432–46. doi:10.1016/j.celrep.2014.07.035.

Steinman, R. M., S. E. Brodie, and Z. A. Cohn. 1976. "Membrane Flow during Pinocytosis. A Stereologic Analysis." *The Journal of Cell Biology* 68 (3): 665–87. doi:10.1083/jcb.68.3.665.

Tabet, Fatiha, Kasey C. Vickers, Luisa F. Cuesta Torres, Carrie B. Wiese, Bassem M. Shoucri, Gilles Lambert, Claire Catherinet, et al. 2014. "HDL-Transferred microRNA-223 Regulates ICAM-1 Expression in Endothelial Cells." *Nature Communications* 5 (February). doi:10.1038/ncomms4292.

Tachibana, Isao, and Martin E. Hemler. 1999. "Role of Transmembrane 4 Superfamily (Tm4sf) Proteins Cd9 and Cd81 in Muscle Cell Fusion and Myotube Maintenance." *The Journal of Cell Biology* 146 (4): 893–904. doi:10.1083/jcb.146.4.893.

Taille, Alexandre de la, Min-Wei Chen, Martin Burchardt, Dominique K. Chopin, and Ralph Buttyan. 1999. "Apoptotic Conversion." *Cancer Research* 59 (21): 5461–63.

Tarasov, V. A., D. G. Matishov, E. F. Shin, N. V. Boyko, N. N. Timoshkina, M. A. Makhotkin, A. M. Lomonosov, A. A. Kirpiy, O. I. Kit, and A. Yu. Maximov. 2014. "Coordinated Aberrant Expression of miRNAs in Colon Cancer." *Russian Journal of Genetics* 50 (10): 1090–1101. doi:10.1134/S1022795414080109.

Taylor, Rebecca C., Sean P. Cullen, and Seamus J. Martin. 2008. "Apoptosis: Controlled Demolition at the Cellular Level." *Nature Reviews Molecular Cell Biology* 9 (3): 231–41. doi:10.1038/nrm2312.

Tehler, Disa, Nina Molin Høyland-Kroghsbo, and Anders H. Lund. 2011. "The miR-10 microRNA

Precursor Family." *RNA Biology* 8 (5): 728–34. doi:10.4161/rna.8.5.16324.
Teissier, Élodie, and Eve-Isabelle Pécheur. 2007. "Lipids as Modulators of Membrane Fusion Mediated by Viral Fusion Proteins." *European Biophysics Journal* 36 (8): 887–99. doi:10.1007/s00249-007-0201-z.
Teunissen, Sander W. M., Martijn J. M. Kruithof, A. Darise Farris, John B. Harley, Walther J. van Venrooij, and Ger J. M. Pruijn. 2000. "Conserved Features of Y RNAs: A Comparison of Experimentally Derived Secondary Structures." *Nucleic Acids Research* 28 (2): 610–19.
Thayanithy, Venugopal, Victor Babatunde, Elizabeth L. Dickson, Phillip Wong, Sanghoon Oh, Xu Ke, Afsar Barlas, et al. 2014. "Tumor Exosomes Induce Tunneling Nanotubes in Lipid Raft-Enriched Regions of Human Mesothelioma Cells." *Experimental Cell Research* 323 (1): 178–88. doi:10.1016/j.yexcr.2014.01.014.
Thompson, Debrah M., and Roy Parker. 2009. "The RNase Rny1p Cleaves tRNAs and Promotes Cell Death during Oxidative Stress in Saccharomyces Cerevisiae." *The Journal of Cell Biology* 185 (1): 43–50. doi:10.1083/jcb.200811119.
Thomson, Daniel W., Katherine A. Pillman, Matthew L. Anderson, David M. Lawrence, John Toubia, Gregory J. Goodall, and Cameron P. Bracken. 2015. "Assessing the Gene Regulatory Properties of Argonaute-Bound Small RNAs of Diverse Genomic Origin." *Nucleic Acids Research* 43 (1): 470. doi:10.1093/nar/gku1242.
Thornton, James E., Peng Du, Lili Jing, Ljiljana Sjekloca, Shuibin Lin, Elena Grossi, Piotr Sliz, Leonard I. Zon, and Richard I. Gregory. 2014. "Selective microRNA Uridylation by Zcchc6 (TUT7) and Zcchc11 (TUT4)." *Nucleic Acids Research*, September, gku805. doi:10.1093/nar/gku805.
Tian, Tian, Yuanyuan Wang, Haitao Wang, Zhaoqi Zhu, and Zhongdang Xiao. 2010. "Visualizing of the Cellular Uptake and Intracellular Trafficking of Exosomes by Live-Cell Microscopy." *Journal of Cellular Biochemistry* 111 (2): 488–96. doi:10.1002/jcb.22733.
Tian, Tian, Yan-Liang Zhu, Yue-Yuan Zhou, Gao-Feng Liang, Yuan-Yuan Wang, Fei-Hu Hu, and Zhong-Dang Xiao. 2014. "Exosome Uptake through Clathrin-Mediated Endocytosis and Macropinocytosis and Mediating miR-21 Delivery." *Journal of Biological Chemistry* 289 (32): 22258–67. doi:10.1074/jbc.M114.588046.
Trajkovic, Katarina, Chieh Hsu, Salvatore Chiantia, Lawrence Rajendran, Dirk Wenzel, Felix Wieland, Petra Schwille, Britta Brügger, and Mikael Simons. 2008. "Ceramide Triggers Budding of Exosome Vesicles into Multivesicular Endosomes." *Science* 319 (5867): 1244–47. doi:10.1126/science.1153124.
Turchinovich, A., T. R. Samatov, and B. Burwinkel. 2013. "Circulating miRNAs: Cell–cell Communication Function?" *Frontiers in Non-Coding RNA* 4: 119. doi:10.3389/fgene.2013.00119.
Turchinovich, Andrey, Ludmila Weiz, Anne Langheinz, and Barbara Burwinkel. 2011. "Characterization of Extracellular Circulating microRNA." *Nucleic Acids Research* 39 (16): 7223–33. doi:10.1093/nar/gkr254.
Valadi, Hadi, Karin Ekström, Apostolos Bossios, Margareta Sjöstrand, James J Lee, and Jan O Lötvall. 2007. "Exosome-Mediated Transfer of mRNAs and microRNAs Is a Novel Mechanism of Genetic Exchange between Cells." *Nature Cell Biology* 9 (6): 654–59. doi:10.1038/ncb1596.
Velho, Sergia, and Kevin M. Haigis. 2011. "Regulation of Homeostasis and Oncogenesis in the Intestinal Epithelium by Ras." *Experimental Cell Research*, Special Issue - Gastroenterology, 317 (19): 2732–39. doi:10.1016/j.yexcr.2011.06.002.
Vickers, Kasey C., Brian T. Palmisano, Bassem M. Shoucri, Robert D. Shamburek, and Alan T. Remaley. 2011. "MicroRNAs Are Transported in Plasma and Delivered to Recipient Cells by High-Density Lipoproteins." *Nature Cell Biology* 13 (4): 423–33. doi:10.1038/ncb2210.
Vickers, Kasey C., Leslie A. Roteta, Holli Hucheson-Dilks, Leng Han, and Yan Guo. 2015. "Mining Diverse Small RNA Species in the Deep Transcriptome." *Trends in Biochemical Sciences* 40 (1): 4–7. doi:10.1016/j.tibs.2014.10.009.
Villarroya-Beltri, Carolina, Cristina Gutiérrez-Vázquez, Fátima Sánchez-Cabo, Daniel Pérez-Hernández,

Jesús Vázquez, Noa Martin-Cofreces, Dannys Jorge Martinez-Herrera, Alberto Pascual-Montano, María Mittelbrunn, and Francisco Sánchez-Madrid. 2013a. “Sumoylated hnRNPA2B1 Controls the Sorting of miRNAs into Exosomes through Binding to Specific Motifs.” *Nature Communications* 4 (December). doi:10.1038/ncomms3980.

———. 2013b. “Sumoylated hnRNPA2B1 Controls the Sorting of miRNAs into Exosomes through Binding to Specific Motifs.” *Nature Communications* 4 (December). doi:10.1038/ncomms3980.

Vizio, Dolores Di, Jayoung Kim, Martin H. Hager, Matteo Morello, Wei Yang, Christopher J. Lafargue, Lawrence True, et al. 2009. “Oncosome Formation in Prostate Cancer: Association with a Region of Frequent Chromosomal Deletion in Metastatic Disease.” *Cancer Research* 69 (13): 5601. doi:10.1158/0008-5472.CAN-08-3860.

Vogelstein, Bert, Eric R. Fearon, Stanley R. Hamilton, Scott E. Kern, Ann C. Preisinger, Mark Leppert, Alida M.M. Smits, and Johannes L. Bos. 1988. “Genetic Alterations during Colorectal-Tumor Development.” *New England Journal of Medicine* 319 (9): 525–32. doi:10.1056/NEJM198809013190901.

Vojtech, Lucia, Sangsoon Woo, Sean Hughes, Claire Levy, Lamar Ballweber, Renan P. Sauteraud, Johanna Strobl, et al. 2014. “Exosomes in Human Semen Carry a Distinctive Repertoire of Small Non-Coding RNAs with Potential Regulatory Functions.” *Nucleic Acids Research* 42 (11): 7290–7304. doi:10.1093/nar/gku347.

Volinia, Stefano, George A. Calin, Chang-Gong Liu, Stefan Ambs, Amelia Cimmino, Fabio Petrocca, Rosa Visone, et al. 2006. “A microRNA Expression Signature of Human Solid Tumors Defines Cancer Gene Targets.” *Proceedings of the National Academy of Sciences of the United States of America* 103 (7): 2257–61. doi:10.1073/pnas.0510565103.

Voss, N. R., and M. Gerstein. 2005. “Calculation of Standard Atomic Volumes for RNA and Comparison with Proteins: RNA Is Packed More Tightly.” *Journal of Molecular Biology* 346 (2): 477–92. doi:10.1016/j.jmb.2004.11.072.

Wagner, Jasmin, Meliana Riwanto, Christian Besler, Andrea Knau, Stephan Fichtlscherer, Tino Röxe, Andreas M. Zeiher, Ulf Landmesser, and Stefanie Dimmeler. 2013. “Characterization of Levels and Cellular Transfer of Circulating Lipoprotein-Bound MicroRNAsSignificance.” *Arteriosclerosis, Thrombosis, and Vascular Biology* 33 (6): 1392–1400. doi:10.1161/ATVBAHA.112.300741.

Wang, Min, Dong Ren, Wei Guo, Zeyu Wang, Shuai Huang, Hong Du, Libing Song, and Xinsheng Peng. 2014. “Loss of miR-100 Enhances Migration, Invasion, Epithelial-Mesenchymal Transition and Stemness Properties in Prostate Cancer Cells through Targeting Argonauteï¿½2.” *International Journal of Oncology*, April. doi:10.3892/ijo.2014.2413.

Wang, Peter L., Yun Bao, Muh-Ching Yee, Steven P. Barrett, Gregory J. Hogan, Mari N. Olsen, José R. Dinneny, Patrick O. Brown, and Julia Salzman. 2014. “Circular RNA Is Expressed across the Eukaryotic Tree of Life.” *PLOS ONE* 9 (3): e90859. doi:10.1371/journal.pone.0090859.

Warburton, Peter E., Dan Hasson, Flavia Guillem, Chloe Lescale, Xiaoping Jin, and Gyorgy Abrusan. 2008. “Analysis of the Largest Tandemly Repeated DNA Families in the Human Genome.” *BMC Genomics* 9: 533. doi:10.1186/1471-2164-9-533.

Wei, Chunyao, Leonidas Salichos, Carli M. Wittgrove, Antonis Rokas, and James G. Patton. 2012. “Transcriptome-Wide Analysis of Small RNA Expression in Early Zebrafish Development.” *RNA* 18 (5): 915–29. doi:10.1261/rna.029090.111.

Welton, Joanne L., Sanjay Khanna, Peter J. Giles, Paul Brennan, Ian A. Brewis, John Staffurth, Malcolm D. Mason, and Aled Clayton. 2010. “Proteomics Analysis of Bladder Cancer Exosomes.” *Molecular & Cellular Proteomics* 9 (6): 1324–38. doi:10.1074/mcp.M000063-MCP201.

Westcott, Peter M. K., Kyle D. Halliwill, Minh D. To, Mamunur Rashid, Alistair G. Rust, Thomas M. Keane, Reyno Delrosario, et al. 2014. “The Mutational Landscapes of Genetic and Chemical Models of Kras-Driven Lung Cancer.” *Nature*. doi:10.1038/nature13898.

Westholm, Jakub O., Pedro Miura, Sara Olson, Sol Shenker, Brian Joseph, Piero Sanfilippo, Susan E. Celniker, Brenton R. Graveley, and Eric C. Lai. 2014. “Genome-Wide Analysis of Drosophila

Circular RNAs Reveals Their Structural and Sequence Properties and Age-Dependent Neural Accumulation." *Cell Reports* 9 (5): 1966–80. doi:10.1016/j.celrep.2014.10.062.
Wienholds, E. 2005. "MicroRNA Expression in Zebrafish Embryonic Development." *Science* 309 (5732): 310–11. doi:10.1126/science.1114519.
Wilczynska, A., and M. Bushell. 2015. "The Complexity of miRNA-Mediated Repression." *Cell Death & Differentiation* 22 (1): 22–33. doi:10.1038/cdd.2014.112.
Wilusz, Jeremy E., Hongjae Sunwoo, and David L. Spector. 2009. "Long Noncoding RNAs: Functional Surprises from the RNA World." *Genes & Development* 23 (13): 1494–1504. doi:10.1101/gad.1800909.
Wong, Rachel, and David Cunningham. 2008. "Using Predictive Biomarkers to Select Patients With Advanced Colorectal Cancer for Treatment With Epidermal Growth Factor Receptor Antibodies." *Journal of Clinical Oncology* 26 (35): 5668–70. doi:10.1200/JCO.2008.19.5024.
Xie, Mingyi, Mingfeng Li, Anna Vilborg, Nara Lee, Mei-Di Shu, Valeria Yartseva, Nenad Šestan, and Joan A. Steitz. 2013. "Mammalian 5′-Capped MicroRNA Precursors That Generate a Single MicroRNA." *Cell* 155 (7): 1568–80. doi:10.1016/j.cell.2013.11.027.
Yamasaki, Satoshi, Pavel Ivanov, Guo-fu Hu, and Paul Anderson. 2009. "Angiogenin Cleaves tRNA and Promotes Stress-Induced Translational Repression." *The Journal of Cell Biology* 185 (1): 35–42. doi:10.1083/jcb.200811106.
Yang, Jr-Ming, and Stephen J. Gould. 2013. "The Cis-Acting Signals That Target Proteins to Exosomes and Microvesicles." *Biochemical Society Transactions* 41 (1): 277–82. doi:10.1042/BST20120275.
Yao, Bing, Lan B La, Ying-Chi Chen, Lung-Ji Chang, and Edward K L Chan. 2012. "Defining a New Role of GW182 in Maintaining miRNA Stability." *EMBO Reports* 13 (12): 1102–8. doi:10.1038/embor.2012.160.
Yi, Rui, Yi Qin, Ian G. Macara, and Bryan R. Cullen. 2003. "Exportin-5 Mediates the Nuclear Export of Pre-microRNAs and Short Hairpin RNAs." *Genes & Development* 17 (24): 3011–16. doi:10.1101/gad.1158803.
Zeng, Yan, Heidi Sankala, Xiaoxiao Zhang, and Paul R. Graves. 2008. "Phosphorylation of Argonaute 2 at Serine-387 Facilitates Its Localization to Processing Bodies." *Biochemical Journal* 413 (3): 429. doi:10.1042/BJ20080599.
Zernecke, Alma, Kiril Bidzhekov, Heidi Noels, Erdenechimeg Shagdarsuren, Lin Gan, Bernd Denecke, Mihail Hristov, et al. 2009. "Delivery of MicroRNA-126 by Apoptotic Bodies Induces CXCL12-Dependent Vascular Protection." *Science Signaling* 2 (100): ra81. doi:10.1126/scisignal.2000610.
Zhang, Bing, Jing Wang, Xiaojing Wang, Jing Zhu, Qi Liu, Zhiao Shi, Matthew C. Chambers, et al. 2014. "Proteogenomic Characterization of Human Colon and Rectal Cancer." *Nature* 513 (7518): 382–87. doi:10.1038/nature13438.
Zhang, Xiao-Ou, Hai-Bin Wang, Yang Zhang, Xuhua Lu, Ling-Ling Chen, and Li Yang. 2014. "Complementary Sequence-Mediated Exon Circularization." *Cell* 159 (1): 134–47. doi:10.1016/j.cell.2014.09.001.
Zhang, Yujing, Danqing Liu, Xi Chen, Jing Li, Limin Li, Zhen Bian, Fei Sun, et al. 2010. "Secreted Monocytic miR-150 Enhances Targeted Endothelial Cell Migration." *Molecular Cell* 39 (1): 133–44. doi:10.1016/j.molcel.2010.06.010.
Zhou, Ming-Kai, Xiao-Jun Liu, Zhi-Guo Zhao, and Yi-Meng Cheng. 2014. "MicroRNA-100 Functions as a Tumor Suppressor by Inhibiting Lgr5 Expression in Colon Cancer Cells." *Molecular Medicine Reports*, December. doi:10.3892/mmr.2014.3052.
Zon, Arend van, Marieke H. Mossink, Martijn Schoester, George L. Scheffer, Rik J. Scheper, Pieter Sonneveld, and Erik A. C. Wiemer. 2001. "Multiple Human Vault RNAs EXPRESSION AND ASSOCIATION WITH THE VAULT COMPLEX." *Journal of Biological Chemistry* 276 (40): 37715–21. doi:10.1074/jbc.M106055200.